CHALMERS
UNIVERSITY OF TECHNOLOGY

Data-driven Modelling and Optimized Management of the District Cooling System and Thermal Energy Storage in Gothenburg

Master's thesis in Sustainable Energy System

OMAR ZABIAN

CHI TAT CHAN

DEPARTMENT OF ARCHITECTURE AND CIVIL ENGINEERING
Division of Building Services Engineering

CHALMERS UNIVERSITY OF TECHNOLOGY
Gothenburg, Sweden 2022
www.chalmers.se

Master's thesis 2022

Data-driven Modelling and Optimized Management of the District Cooling System and Thermal Energy Storage in Gothenburg

OMAR ZABIAN

CHI TAT CHAN

CHALMERS
UNIVERSITY OF TECHNOLOGY

Department of Architecture and Civil Engineering
Division of Building Services Engineering
Chalmers University of Technology
Gothenburg, Sweden 2022

Data-driven Modelling and Optimized Management of the District Cooling System and Thermal Energy Storage in Gothenburg
OMAR ZABIAN & CHI TAT CHAN

Supervisor: Maria Jangsten, Chalmers Department of Architecture and Civil Engineering
Supervisor: Anders Strand, Göteborg Energi
Examiner: Anders Trüschel, Chalmers Department of Architecture and Civil Engineering

Master's Thesis 2022
Department of Architecture and Civil Engineering
Division of Building Services Engineering
Chalmers University of Technology
SE-412 96 Gothenburg, Sweden
Telephone: +46 31-772 1000

Typeset in LaTeX
Printed by Chalmers Reproservice
Gothenburg, Sweden 2022

Data-driven Modelling and Optimized Management of the District Cooling System and Thermal Energy Storage in Gothenburg

OMAR ZABAIN & CHI TAT CHAN
Department of Architecture and Civil Engineering
Division of Building Services Engineering
Chalmers University of Technology

Abstract

District cooling system (DCS) is a sustainable and cost-effective way to provide cooling energy in urban areas[1]. DCS is growing in Sweden due to the increase in cooling energy demand. In Gothenburg, an expansion of DCS will be done by installing more cooling units and a cold-water thermal energy storage unit (TES). This paper first models the potential operation of the TES of low loading temperature below 4 °C by using computational fluid dynamics model Ansys Fluent. Then, it formulates an investment model by using linear programming (LP) to investigate the optimal size of the units, potential benefits and drawbacks to the system, in 2040.

The research results in this study demonstrate that the operation of discharging temperature of water of 1 °C is unlikely in the operational point of view due to the intensive mixing in the low-temperature zone. The thermocline layer is only established between the warm return water zone and the cold zone. The thickness of the thermocline layer grows with time with the conduction and diffusion due to temperature difference within the medium.

The balance between the investment and the operational cost decides the optimum size for the TES and the new production plant. TES has an investment priority advantage as it has a cheaper investment cost compared with the use of mechanical chillers, and a lower operational cost because it can be charged during the off-peak hours with low electricity prices. However, one of the limiting factors for the size of TES is the available chiller's capacity for charging the TES, and another factor is the peak cooling demand. TES is optimized with the lowest total cost by running on a daily cycle. It saves operational costs by charging during off-peak hours and discharging during peak hours.

In addition, the absorption chiller is a cost-effective choice to invest in to charge the TES over the compressor chillers. This is due to the availability of free waste heat, which has given an operational cost advantage for the absorption chillers, even though they have higher investment costs.

The optimal size of the investment of cooling units has some uncertainties due to the unavailability of assured data on the electricity price and cooling demand, which greatly affect the operation of the overall DCS in the future.

Keywords: Cooling Thermal Energy Storage, District Cooling Network, CFD, cost optimization

Acknowledgements

We would like to extend our sincere thanks to our supervisor at Chalmers University of Technology, Maria Jangsten for all the support, and encouragement. This study would not have been possible without her. We are very grateful for her. We wish also to thank our supervisor Anders Strand at Göteborg Energi for his overall insight in the field, which has made this an inspiring and practical experience for us. We want to thank our examiner, Anders Trüschel at Chalmers University of Technology, for his continuous feedback and review of our work.

We also want to thank professor Jan-Olof Dalenbäck and Torbjörn Lindholm for their valuable comments, guidance, continuous assistance and unwavering support on the thesis.

Our thanks also go to our family for their unconditional support during this period. We take this opportunity to thank everyone at the division of building services engineering and energy technology for dedicating time to answer our questions and help whenever needed. They were always willing and enthusiastic to assist in any way they could throughout the research project.

It has been a pleasure working with everyone; we had many great memories during the process that will be remembered forever. And by this acknowledgment, we want to express our gratitude and appreciation.

This publication was produced at Chalmers University of Technology, during a scholarship period funded by the Swedish Institute for Omar Zabian.

Omar Zabian & Chi Tat Chan, Gothenburg, May 2022

Contents

List of Figures **ix**

List of Tables **xiii**

1 Introduction **1**
1.1 Background & Motivation . . . 1
1.2 Aim . . . 1
1.3 Research Questions . . . 2
1.4 Specific Tasks . . . 2
1.4.1 Modelling of Cooling Thermal Storage Tank . . . 3
1.4.2 Modelling of Cooling Energy Dispatch . . . 3
1.5 Scope and Boundaries . . . 3
1.6 Limitations and Delimitations . . . 3
1.7 Thesis Outline . . . 4

2 Technical Background **5**
2.1 District Cooling System . . . 5
2.2 Cooling Technologies . . . 6
2.3 Cooling Thermal Energy Storage . . . 8
2.3.1 Overview . . . 8
2.3.2 Why TES . . . 8
2.3.3 TES Types . . . 9
2.3.4 Comparing different types of thermal energy storages . . . 11
2.4 District Cooling System in Gothenburg . . . 15
2.5 Future Development of District Cooling System in Gothenburg . . . 19

3 Literature Review **21**
3.1 Thermocline in Stratified Cooling TES . . . 21
3.2 Energy Dispatch Modelling of District Cooling System . . . 27

4 Methodology **29**
4.1 Introduction . . . 29
4.2 Modelling of Cooling Thermal Energy Storage Tank . . . 29
4.2.1 Tank configuration . . . 30
4.2.2 Assumptions . . . 32
4.2.3 Initial and Boundary Conditions . . . 32
4.2.4 Input Data . . . 33

4.2.5 Governing Equations . . . 33
4.2.6 Scenarios . . . 33
4.3 Energy Dispatch Investment Modelling . . . 37
4.3.1 Assumptions . . . 37
4.3.2 Generation and storage . . . 37
4.3.3 Cooling Loads . . . 40
4.3.4 Loading temperature . . . 42
4.3.5 Energy costs . . . 43
4.3.6 Thermal Efficiency and Coefficient of Performance . . . 43
4.3.7 Modelling Scenarios . . . 45
4.3.8 Investment Dispatch Model Formulation . . . 48
4.4 Sensitivity Analysis Scenarios . . . 51
4.4.1 Electricity price . . . 51
4.4.2 Cooling Demand Profile . . . 52

5 Results **55**
5.1 Computational Fluid Dynamics Modelling . . . 55
5.1.1 Summary . . . 55
5.1.2 Scenario 1 . . . 55
5.1.3 Scenario 2 . . . 58
5.1.4 Temperature Gradient . . . 59
5.1.5 Thermocline Thickness . . . 63
5.1.6 Discussion . . . 67
5.2 Optimization Modelling . . . 69
5.2.1 Summary . . . 69
5.2.2 Scenario 2-a . . . 70
5.2.3 Scenarios outcomes . . . 109
5.2.4 Sensitivity Analysis Results . . . 114
5.2.5 Discussion . . . 119

6 Conclusion and Future work **123**
6.1 Conclusion . . . 123
6.2 Future Work . . . 124

Bibliography **127**

List of Figures

1.1 Schematic of Research tasks 3

2.1 Schematic of District Cooling System 6
2.2 Classification of Thermal Energy Storage System [2] 10
2.3 District Cooling System in Gothenburg 2021 15
2.4 Distribution of Cooling Technologies' Usage 16
2.5 Outdoor Temperature in 2020 Gothenburg, Sweden 17
2.6 Cooling Demand in 2020 Gothenburg, Sweden 18
2.7 Cooling Demand from 1st-7th August in 2020 Gothenburg, Sweden . 18

3.1 Typical stratification temperature profile [3] 22
3.2 TES parameters for optimum thermal performance [4] 23
3.3 Common performance indicators used to assess the thermocline TES tank [5] 24

4.1 Schematic of CFD Modelling 30
4.2 Schematic of Stratified thermal storage tank with radial parallel plate diffusers 31
4.3 Tank Configuration 31
4.4 Meshing of Tank 31
4.5 Freshwater density against temperature 34
4.6 Modelling Scenario 1 35
4.7 Modelling Scenario 2 35
4.8 Relation between Specific cost against storage capacity of tank 39
4.9 Predicted Cooling Load Profile in 2040. 41
4.10 Cooling Load Profile in 2020. 41
4.11 Daily Load Profile. 42
4.12 Electricity Price Profile in 2040. 43
4.13 Coefficient of performance against cooling load of centrifugal compressor chiller 44
4.14 New cooling production plant scenarios in year 2040 45
4.15 Historical electricity prices data *[6]* 52
4.16 Historical cooling demand data 53

5.1 Cross-section graphical illustration during charging of 4 °C chilled water at different time steps 56

5.2 Cross-section graphical illustration during charging of 1 °C chilled water and charging of 13 °C return water at different time steps . . . 57
5.3 Cross-section graphical illustration of charging of water of 1 °C and discharging of Scenario B at different time steps 58
5.4 Temperature Profile during charging of water of 4 °C of Scenario A . 59
5.5 Temperature Profile during charging of water of 1 °C of Scenario A . 60
5.6 Temperature Profile during charging of water of 13 °C of Scenario A . 61
5.7 Temperature Profile during charging of water of 1 °C of Scenario B . 62
5.8 Temperature Profile during charging of water of 13 °C of Scenario B . 63
5.9 Thermocline thickness by time during charging of water of 4 °C of Scenario A 64
5.10 Thermocline thickness by time during charging of water of 13 °C of Scenario A 65
5.11 Thermocline thickness by time during charging of water of 13 °C of Scenario B 65
5.12 Yearly Cooling Demand Profile 71
5.13 Yearly Electricity Price Profile 72
5.14 Yearly TES State Of Charge Profile 73
5.15 Yearly TES Charge and Discharge Profile 74
5.16 Yearly Existing Cooling Production Profile 75
5.17 Yearly New Cooling Production Profile 76
5.18 Yearly TES Discharge Profile 77
5.19 Week 33 Cooling Demand Profile 78
5.20 Week 33 Electricity Price Profile 79
5.21 Week 33 TES State Of Charge Profile 79
5.22 Week 33 TES Charge and Discharge Profile 80
5.23 Week 33 Existing Cooling Production Profile 80
5.24 Week 33 New Cooling Production Profile 81
5.25 Week 33 TES Discharge Profile 81
5.26 Week 33 Cooling Demand and Production Profile 82
5.27 Week 25 Cooling Demand Profile 82
5.28 Week 25 Electricity Price Profile 83
5.29 Week 25 TES State Of Charge Profile 83
5.30 Week 25 TES Charge and Discharge Profile 84
5.31 Week 25 Existing Cooling Production Profile 84
5.32 Week 25 New Cooling Production Profile 85
5.33 Week 25 TES Discharge Profile 85
5.34 Week 25 Cooling Demand and Production Profile 86
5.35 DUT 100% Daily Cooling Demand Profile 86
5.36 DUT 100% Daily Electricity Price Profile 87
5.37 DUT 100% Daily TES State Of Charge Profile 88
5.38 DUT 100% Daily TES Charge and Discharge Profile 89
5.39 DUT 100% Daily Existing Cooling Production Profile 90
5.40 DUT 100% Daily New Cooling Production Profile 91
5.41 DUT 100% Daily TES Discharge Profile 91
5.42 DUT 100% Daily Cooling Demand and Production Profile 92

5.43 DUT 75% Daily Cooling Demand Profile 93
5.44 DUT 75% Daily Electricity Price Profile 94
5.45 DUT 75% Daily TES State Of Charge Profile 95
5.46 DUT 75% Daily TES Charge and Discharge Profile 96
5.47 DUT 75% Daily Existing Cooling Production Profile 97
5.48 DUT 75% Daily New Cooling Production Profile 98
5.49 DUT 75% Daily TES Discharge Profile 99
5.50 DUT 75% Daily Cooling Demand and Production Profile 100
5.51 DUT 50% Daily Cooling Demand Profile 101
5.52 DUT 50% Daily Electricity Price Profile 102
5.53 DUT 50% Daily TES State Of Charge Profile 103
5.54 DUT 50% Daily TES Charge and Discharge Profile 104
5.55 DUT 50% Daily Existing Cooling Production Profile 105
5.56 DUT 50% Daily New Cooling Production Profile 106
5.57 DUT 50% Daily TES Discharge Profile 107
5.58 DUT 50% Daily Cooling Demand and Production Profile 108
5.59 Scenario 1 - Sub-scenarios TES capacity and New Cooling Plant Capacity comparison 111
5.60 Scenario 2 - Sub-scenarios TES capacity and New Cooling Plant Capacity comparison 113
5.61 Scenario 2 - Sub-scenarios total annualized cost 113
5.62 Scenario 2a - TES capacity and New Cooling Plant Capacity as per different historical electricity prices data 115
5.63 Scenario 2a - Total annualized cost as per different historical electricity prices data 116
5.64 Scenario 2a - TES capacity and New Cooling Plant Capacity as per different historical cooling demand data 118
5.65 Scenario 2a - Total annualized cost as per different historical cooling demand data 119

List of Tables

2.1 DC TES main characteristics[7] 11
2.2 Generalized comparison between different cooling TES technologies [8] 13
2.3 Capacity of cooling units 15
2.4 Capacity of cooling units 20

4.1 Dimensions of the tank 32
4.2 Operating parameters of the tank 33
4.3 Operating details of scenario A 35
4.4 Operating details of scenario B 35
4.5 Capacity of cooling units 38
4.6 Scenario 1: general data input 47
4.7 Scenario 2: general data input 48
4.8 Yearly average electricity prices as per Nordpool. [6] 51

5.1 Optimization Modeling Scenarios 69
5.2 Scenario 1 results 110
5.3 Scenario 2 results 112
5.4 Scenario 2-a - historical electricity prices data results 114
5.5 Scenario 2-a - historical cooling demand data results 116

Nomenclature

Abbreviations

BTU	British thermal unit
CHW	Chilled water
COP	Coefficient of performance
DCS	District cooling system
DH	District heating
DHS	District heating system
$DUT100\%$	Maximum cooling load at outside design temperature of 25°C
$DUT50\%$	50% of the Maximum cooling load at outside design temperature of 25°C
$DUT75\%$	75% of the maximum cooling load at outside design temperature of 25°C
HP	Heat pump
LTF	Low temperature fluid
$MSEK$	Million Swedish Krona
sf	annuity factor
SOC	State of Charge
TES	Thermal energy storage

Symbols

$\dot{q}$	heat transfer rate [J/s]
η_{ch}	Charging efficiency [%]
η_{dis}	Discharging efficiency [%]
η_{st}	Storage efficiency [%]
μ	Molecular viscosity[Pas]
∇	Gradient operator
$\overline{\overline{\tau}}$	Deviatoric stress tensor
ρ	Fluid density [kg/m3]
υ	Fluid velocity [m/s]
$C_{TES_{new}}$	Invested capacity of thermal energy storage tank [MW]
COP_{ac}	Coefficient of performance of absorption chiller [kWh]
COP_{com}	Coefficient of performance of compressor chiller [kWh]
COP_{new}	Coefficient of performance of the new chiller [kWh]
e	Energy Content[J]
E_{In}	Energy Input [kWh]
E_{Out}	Energy Output [kWh]
e_{price}	Electricity price [SEK/hour]
E_{St}	Energy stored [kWh]

f	External body force[N]
I	Unit tensor
$inv_{Q_{new}}$	Specific Investment cost of new chiller [SEK/MW/h]
$inv_{TES_{new}}$	Specific Investment cost of thermal energy storage tank [SEK/MWh/h]
p	Fluid pressure [pa]
P_{ac}	Power rating of absorption chiller[MW]
P_{com}	Power rating of compressor chiller[MW]
P_{new}	Power rating of new chiller[MW]
$P_{Q_{new}}$	Invested capacity of the new chiller [MW]
Q_{ac}	Cooling energy generated by absorption chillers [kWh]
Q_{charge}	Charge from TES [MWh]
Q_{com}	Cooling energy generated by compressor chillers [kWh]
Q_{demand}	Cooling demand [MWh]
$Q_{discharge}$	Discharge from TES [MWh]
Q_{new}	Cooling energy generated by the new chilling plant [kWh]
Q_{tes}	Power rating of TES [MW]
$SOC_{tes,min}$	Minimum state of charge of battery energy storage
SOC_{TES}	State of charge of TES
t	time
W	Work Input [kWh]

1
Introduction

1.1 Background & Motivation

Mitigating climate change is the major challenge in the world now. A more efficient and sustainable energy system is part of the solution to reduce greenhouse gas emissions. Space cooling accounts for roughly 20% of the total electricity demand in the buildings in the world today [9]. The space cooling demand has increased 4% annually on average since 2000 and increasing trending is expected to continue in the future [10].

In Sweden, district cooling system was first introduced in 1992 in Västerås. Currently, more than 40 urban areas have a district cooling system, with the aim of offering an efficient, cost effective, reliable and sustainable way to provide energy [11]. In Gothenburg, the cooling demand is growing alongside with the expansion of infrastructures and economic development. Moreover, the ambient temperature is expected to increase in the future due to climate change. With these factors, it is predicted that the cooling demand will increase significantly from around 40MW in 2020 to around 160 MW in 2040 during peak hours, a fourfold increase. And thus, the interest of expanding district cooling system is increasing in Gothenburg.

Along with increasing energy demand, intermittency of electricity generation in the future electric system and the change in energy system paradigm, energy storage technologies are regarded as an important component contributing to a reliable and robust system, which can help by reducing the peak consumption and use the intermittent energy more efficiently[12]. However, currently there are only a few district cooling systems in Sweden possessing a thermal storage system and the benefits of integrating it into the systems are not fully understood. Moreover, there are still many practical challenges regarding the use of a stratified thermal energy storage for cooling, including during charging and discharging operation. Therefore, this thesis is conducted to investigate the operation of future district cooling system with thermal energy storage in Gothenburg in a cost effective way.

1.2 Aim

The thesis studies the district cooling system in Gothenburg owned by Göteborg Energi. The objective is to investigate the optimal operation in the district cooling system with thermal energy storage and to assess the potential system impacts,

challenges and benefits of having thermal storage system within Gothenburg. In addition, how different futuristic scenarios with the involvement of this energy storage would impact the economic benefits and the technical boundaries. The master thesis should produce the following preliminary deliverables:

1. Answering the research questions.
2. A prototype of a model that can capture the behaviour of the thermal energy storage within the district cooling network.
3. Results of the model in providing system insights.

1.3 Research Questions

The thesis aims at answering the following research questions:

1. Investigating how the charging and discharging will occur to and from the district cooling network using water as a medium and what are the sequence of operation by lowering the temperature of water below 4 °C in thermal energy storage?

2. What would be the optimal lowest temperature for the thermal energy storage operation?

3. What are the advantages and disadvantages of using low temperature water thermal energy storage in comparison with other type of thermal energy storages?

4. What is the optimal control of the thermocline in the storage tank?

5. What are the advantages and disadvantages of investing in thermal energy storage within the district cooling system taking into consideration the impact in the district cooling network, the production plant, the customer usage and the energy prices.

1.4 Specific Tasks

A preliminary technical background review and literature review will be done to deepen the knowledge of district cooling system and network, cooling technology and cooling thermal storage technology. A further look at the district cooling system in the context of Gothenburg thus can be conducted to understand the future application of thermal storage tank and development of network. Thus, a research focus can be obtained accordingly. Based on the information obtained, a computational fluid dynamics model can be thus done by using Workbench Ansys Fluent to investigate the future operation scenarios of thermal storage tank. After the operation of thermal storage tank is fulled understood, a investment model can be done by using linear programming problem solver via Python. The optimal size of the new thermal storage tank and chiller can be found with the feedback from the CFD model. The operation of the new system can also be investigated and system

insight can be given. A sensitivity analysis will be conducted to study the impacts of important parameters to the system. A overall analysis and discussion will be done subsequently.

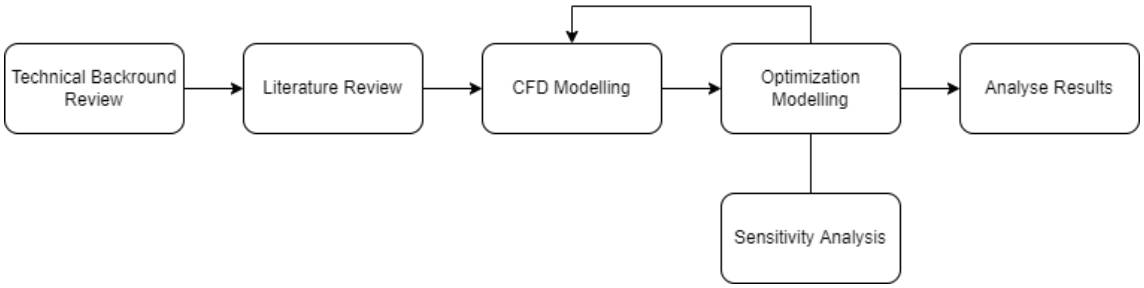

Figure 1.1: Schematic of Research tasks

1.4.1 Modelling of Cooling Thermal Storage Tank

The temperature gradient and thermocline phenomenon inside the thermal storage tank will be studied by:

- Construct a thermal storage tank in the Ansys fluent Software
- Design charging and discharging scenarios at different loading temperatures
- Simulate different scenarios

1.4.2 Modelling of Cooling Energy Dispatch

This part will develop an investment model for thermal energy storage tank and the new chiller. An energy dispatch model will be done to assess the optimal operation of the district cooling system. This will be accomplished by:

- Determining the objective function, constant, variables and parameters of the system
- Formulate linear equations of the system
- Program the equations in Python
- Run the program and simulate different scenarios

1.5 Scope and Boundaries

The scope includes the study of district cooling system in Gothenburg, operated by Göteborg Energi. The data used in this study will be obtained from Göteborg Energi and external sources. The main aim of the computational fluid dynamics model and the energy dispatch modelling is to simulate the operation of district cooling network of future scenario in 2040.

1.6 Limitations and Delimitations

The network configuration affecting the distribution of chilled water can be significant. However, in this thesis, the network effects will be neglected to reduce

complexity. It is assumed that all the pipelines in the network have enough capacity to provide cooling services needed.

The energy prices of heat and electricity in the future are uncertain and it can affect the results of the model significantly. The electricity prices data are assumed in the thesis.

The investment cost in the optimization model will be considered as SEK/MW, which the cost is assumed to be linearly proportional to capacity installed.

The constraints for ramping up and ramping down of the cooling units are neglected. Therefore, the operation of cooling units is not affected by the previous hour.

The operation between the district cooling system and district heating system are decoupled. Therefore, the effects of district heating system on the district cooling system is neglected.

1.7 Thesis Outline

The thesis consists of six chapters, including the introduction. These chapters are summarized below:

Technical Background: This chapter describes the background knowledge of district cooling system and in the context of Gothenburg.

Literature Review: This chapter reviews literature about the technical issues for designing thermal storage tanks and methods for modelling energy systems.

Methodology: This chapter describes the methodology of conducting the study.

Results: This chapter illustrates the results obtained from both computational fluid dynamics modelling, and cost optimization model.

Discussion: This chapter raises up the discussion based on the results obtained from the study.

Conclusion: This chapter emphasizes the main conclusions of the study and the future work.

2

Technical Background

This chapter embodies the research and literature review of district cooling system and its associated technologies. Section 2.1 will illustrate the concept and fundamentals of district cooling system, including its benefits and motivation. Section 2.2 and 2.3 describe cooling and thermal energy storage technologies in the existing district cooling system respectively. Section 2.4 will look into the existing district cooling system managed by Göteborg Energi. Section 2.5 will look into the future development of district cooling system in Gothenburg.

2.1 District Cooling System

District cooling system is a central cooling production system with distribution network to provide cooling services to the end users. The main component in the system includes a district cooling plant, a chilled water distribution network and a heat exchange substation and the connected buildings[1]. Cooling energy is produced centrally in the plant. And the cooled medium such as chilled water is delivered through the distribution networks to the end users by a direct heat exchange with the cooling load or a secondary heat exchange and further to the load. The benefits of DCS are the capability to provide cooling services in a more efficient, reliable and environmentally friendly way compared to using individual chillers. There are also additional benefits of reducing noise pollution, improving city skyline, improving space utilization etc...[13]. A combination of cooling technologies in the central plant are usually operated to attain optimal operation. High investment cost and low operating cost are the characteristics of DCS. Installation of chilling plants and distribution networks are major investments for DCS. Low operating cost can be achieved by utilizing available cheap resources nearby such as river cooling and waste heat from industries. Due to its high investment cost of distribution network, it is only economically beneficial to provide energy in areas with high energy demand, where the cooling density is high enough to level its high investment cost due to economic of scale[1]. Thermal energy storage is an additional component for DCS. It stores cooling energy during the off-peak hours and provides energy during peak hours or when the energy cost is high. It can help reduce amplitude and duration of peak loads and increase the value of energy during off-peak hours, stabilizing energy cost. It can also reduce the number of chillers needed to be stored for fulfilling peak demand, which can lower investment cost. TES can also be used as an emergency cooling source if there is any failure in the system, which can supply cooling services for short duration.

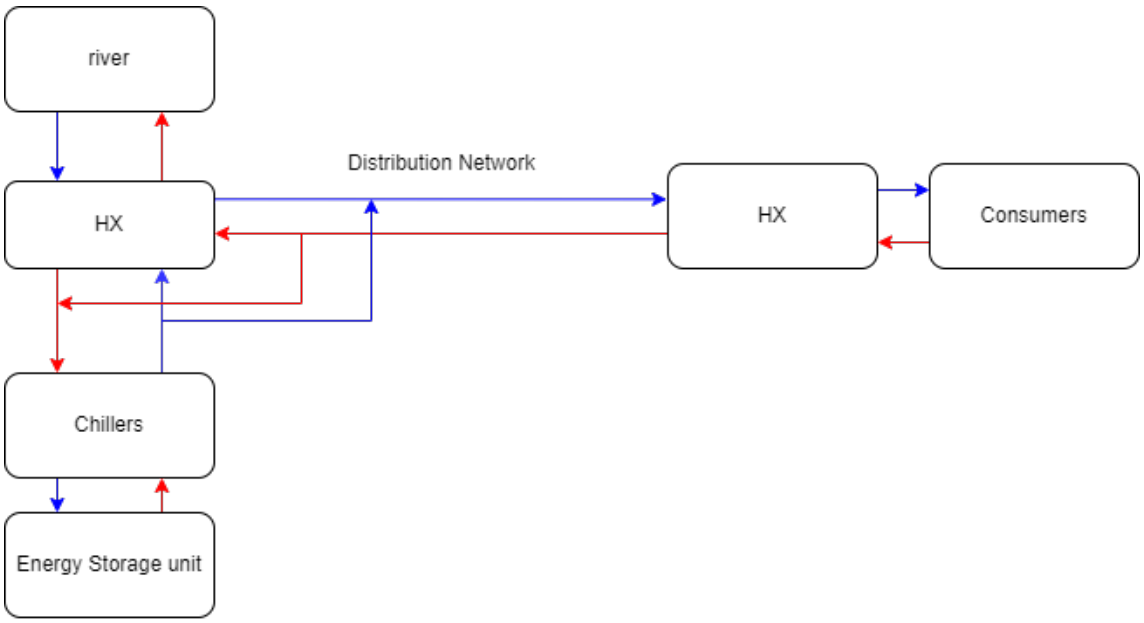

Figure 2.1: Schematic of District Cooling System

2.2 Cooling Technologies

This part describes cooling technologies used in district cooling system.

1. **Centrifugal Liquid Compressor Chiller**
   Centrifugal compressor chiller is a common type of chiller used in district cooling system with a coefficient of performance of above 7. It makes use of vapor compression cycle and is common to use R-123 or R-134a as the refrigerant. The main components are condenser, compressor, throttle and evaporator. Heat exchange is done between the evaporator and the chiller water side, which provide cooling services. The refrigerant then is compressed to high pressure level and passes through the condenser to reject heat. Cooling tower is usually used for heat rejection to the ambient environment. The refrigerant passes through the expansion valve and the cycle repeats[14].

2. **Absorption Chiller**
   The major components of an absorption chiller contain an evaporator, a condenser and an expansion valve, similar to a conventional compressor. But instead of having a compressor in compressor chiller, it is replaced by a generator and an absorber. Two different fluids are utilized in an absorption chiller, namely the absorbent and the refrigerant. The absorbent, which is usually lithium bromide or ammonia, is circulated between the generator and the absorber. The refrigerant, which is usually water, is circulated between condenser, evaporator and expansion valve, generator and absorber. The main characteristic of this chiller is the utilization of heat as the main driving force

for the cooling process instead of electricity. Low grade heat can be used as an input to drive the chiller such as waste heat from industry. Condenser and generator are in the high-pressure zone, whereas evaporator and absorber are in the low-pressure zone. Generator takes waste heat from the industry to heat up the absorbent in high pressure environment. Water is then evaporated as vapor and the absorbent becomes more concentrated. The water vapor then goes to the condenser for condensation to reject heat to the environment. The concentrated absorbent is transferred to the absorber through the throttle to the absorber. The absorbent in the absorber absorbs water vapor from the evaporator and dilute the solution. Then, the absorbent is pumped to the generator through a small pump. The cycle repeats.

There are three types of absorption chillers, namely single-effect absorption chillers, double-effect absorption chillers and direct-fired absorption chillers. Single-effect chillers and double-effect chillers have similar composition, but the double-effect chillers have one more generator and heat exchanger to recover the heat from the condenser, so that less heating demand is needed. Therefore, it is more efficient than the single-effect chillers. Direct-fired chiller is similar to single-effect chillers. But instead of using hot water, heat is provided to generator by a direct gas flame. Thus, the temperature in the generator is much higher and allows better refrigerating effect in the evaporator. But on the other hand, it can be more costly due to the use of higher grade heat.

3. **Free Cooling**
   There are two kinds of free cooling sources that can be used in the system, including cooling from natural water resources and from cooling towers.

   (a) From lake, sea water or river: If the natural water resource is cold enough to use for cooling and the resource is accessible by the district cooling plant, free cooling energy can be harnessed to offer low-cost and sustainable energy. Free cooling is used for pre-cooling and is complemented with additional chillers to fulfill the cooling requirement when the water temperature is not low enough in warmer seasons.

   (b) By cooling tower: Cooling towers that connected to the cooling system during normal operation can be utilized to provide free cooling at time when the ambient air is cold and dry. During operation, the chiller is shut down and is isolated from the cooling tower. The cold ambient air enters the cooling tower and cools down inlet hot water. A heat exchanger is connected between the primary side of the cooling tower and the secondary side where cooling energy is distributed to the load. However, the utilization of this type of cooling largely depends on the difference between the ambient wet bulb temperature and the loading temperature.[15]

2.3 Cooling Thermal Energy Storage

2.3.1 Overview

Thermal energy storage can be used in different applications, from the individual process, building, multiuser-building, district, town, or region, it permits excess thermal energy to be stored and then later to be utilised even by hours, days, or months. It helps in creating a balance for the energy demand usage between day and night, or for Seasonal thermal energy storage (storing winter cold for summer cooling, or summer heat for winter heating). Several applications and technologies are used to store this energy such as water or ice tanks, boreholes with heat exchangers with an access to masses of native earth or bedrock, deep aquifers contained between impermeable strata; shallow, lined pits filled with gravel and water and insulated at the top, mixture solutions or phase change materials (PCM) [16].

For district cooling TES application, the norm is usually to go with the decision of choosing an insulated tank of water that can store the energy for a certain period of time in a form of cooled or frozen medium, usually the cooling/ freezing of the medium in the storage happens at night and weekends when low cooling demand is need by the DCS (off-peak hours), and then the stored medium warmed or melted during the daytime releasing the stored energy when high cooling demand is required by the DCS (on-peak hours). The main reason to use the TES technology is to reduce the number of the used chillers or use smaller chillers capacity to operate during the on-peak hours. Where some of the chillers which are unrequired during the off-peak hours will remain operating during the off-peak hours to recharge the TES with cooled or frozen medium [3].

2.3.2 Why TES

Several advantages and benefits drive the use of TES in the DCS, some are direct and others indirect advantages, taking into account that the type of TES plays a role in which the benefits can be given for the DCS.

The primary benefits are multifaceted. Firstly, it can reduce the operating cost by lowering peak electric power demand by shifting the cooling demand from on-peak hours to off-peak hours, which means reducing the running cost of using high, on-peak-hour electricity costs, and instead, using more of the low, off-peak-hour cost. Secondly, reducing or avoiding the investment of cooling production units (chillers), which will reduce the production plant's capacity, will slightly increase the net capital cost.

Additionally, it has a fast pay-back time and even an immediate net-investment cost for installing chilled water (CWH) or low temperature fluid (LTF) TES versus not using the TES option within the DCS. Thirdly, in some cases, the TES investment can be further reduced if electricity providers offer an incentive scheme for reducing the peak electricity demand in the system [17].

In addition to the primary benefits, there is a potential for other benefits of having the TES with DCS which might depend on the situation of the DCS and the storage type. Such as firstly, TES can provide support for flattening and balancing the profile of the electricity and the thermal demand, which can lead to a further possibility of economically deploying the CHP within the energy system (improving the fuel consumption and the system energy efficiency). Secondly, considering the use of the electricity demand at off-peak hours to charge the TES will reduce the electrical energy consumption, which leads to less use of fuel energy sources and eventually reduces emissions. Thirdly, it provides flexibility to do maintenance for the chiller plants during daytime hours and it can work as emergency standby cooling if standby cooling is required.

Moreover, the advantage of having CHW and LTF TES is that can be located independently from the production plant while still connected to the distribution network, and ice and LFT TES tanks have the advantage of reducing the investment cost of piping and the equipment, and the cost of energy and pumping through using low-temperature supply. Moreover, the LTF TES uses the aqueous fluid which can protect the system from corrosion and microbiological activity [17].

2.3.3 TES Types

Several TES technologies are available today, each one has different characteristics. Firstly, Latent TES such as ice TES is used when changing of phase between solid and liquid states and is considered to store and release thermal energy.

The benefits of ice TES that it is compact, the technology available, and it can be used to provide low CHW supply temperature which can reduce the capital and the operation cost, from the other side the drawbacks are that it requires the chillers to operate at low temperatures and it consumes high energy per unit. Secondly, sensible TES such as CHW TES and LTF TES, where both use the change in temperature of the medium to store and release the thermal energy.

The benefit of using the sensible TES is the lower capital cost compared to ice storage and only-chiller plants, sensible TES are simpler to control, operate, and even use to retrofit the only-chillers plant[2].

Figure 2.2 represents different classification methods for TES, in this and the next chapters, we will discuss the TES classification based on the storage medium (Sensible or latent) and specifically the CHW TES, LFT TES, and the ice TES.

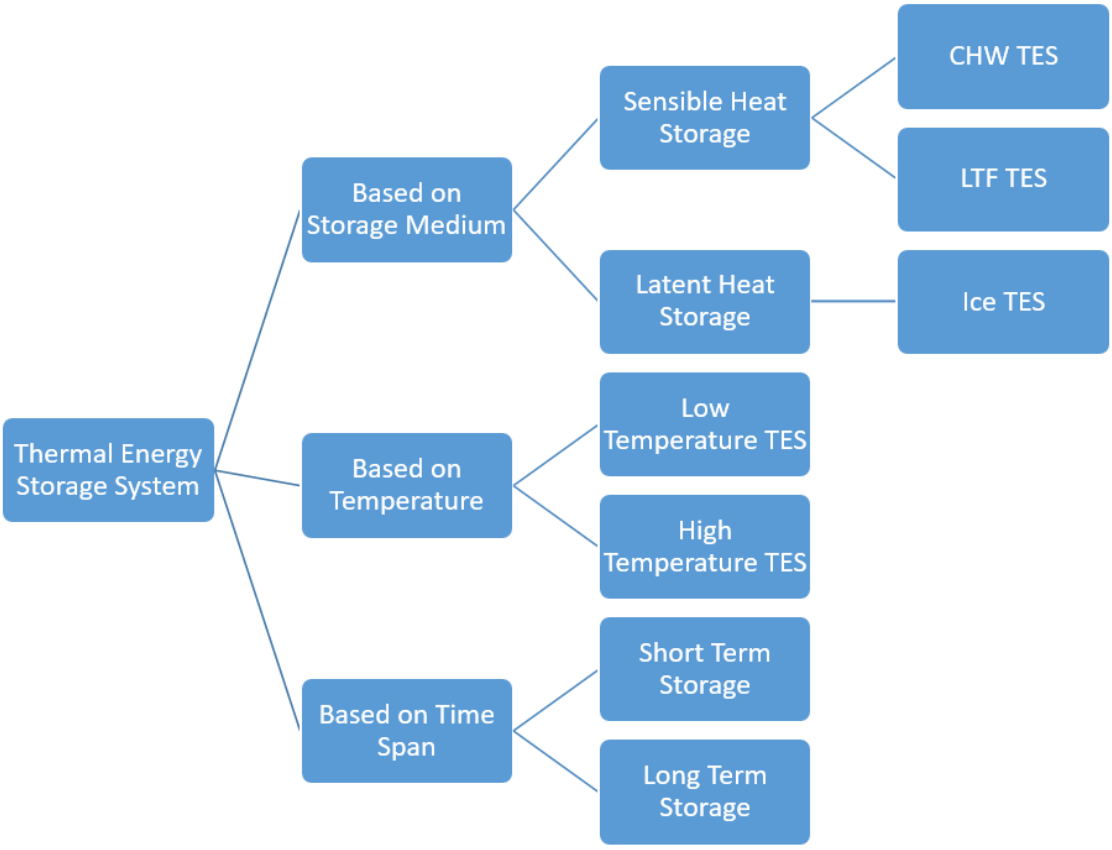

Figure 2.2: Classification of Thermal Energy Storage System [2]

Table 2.1 present summarize the main characteristics of different types of DC TES.

Table 2.1: DC TES main characteristics[7]

	Ice TES	CHW TES	LTF TES
Chiller type	Note 1	Standard water	Standard water (slightly cooler refrigeration plant)
Cooling is stored as	Latent heat (Change in phase)	Sensible heat (change in temp)	Sensible heat (change in temp)
Typical TES specific volume	0.08 to 0.11 m3/ton-h	0.3 to 0.5 m3/ton-h	0.2 to 0.3 m3/ton-h
Discharge temp from TES	(1°C to 2°C)	(0°C to 2°C) above charging temperature	(1°C to 2°C) above charging temperature
Charge temp to TES	(-9°C to –4°C)	(4°C to 7°C)	(-2 C to +2°C)
Recharge chiller plant power (electricity in/ thermal out)	0.8 to 1.1 KW/ton	0.6 to 0.7 KW/ton	0.7 to 0.8 KW/ton
Discharge fluid	Note 2	Water	LTF

Note1: Ice Harvester uses prepackaged of built-up ice making equipment, and external melt, internal melt and encapsulated ice use low-temperature refrigeration plant.
Note 2: Ice harvester and external melt ice use water, and internal melt and encapsulated ice use secondary coolant. Note3: Ton-h refer to ton per cooling (defined as delivering 12,000 BTU/hour of cooling)[7].

2.3.4 Comparing different types of thermal energy storages

(A) **Ice TES**

The energy in Ice TES is stored as latent heat, changing the phase of water between solid and liquid, where during off-peak hours the ice is formed to be melted later on when needed during the on-peak hours. The TES recharges with a range of -8°C to -2°C, with a possibility to discharge and supply at a temperature between 1°C to 7°C as needed. The ice TES is very compact and has a low specific volume compared to other types of TES with a specific volume between 0.08 to 0.11 m3/ton-h. It is also worth mentioning that even though the ice storage is more compact due to the use of ice water as a medium and requires less space, but still it has a less economy-of-scale advantage compared with the other types of TES.

There are several available technologies for Ice TES such as ice-on-coil, encapsulated ice, ice harvesters, and ice slurry. They differentiate by the installation and operation point of view [3].

When it comes to operation of the most common type of ICE TES, ice-on-coil technology, the principle is to use the heat transfer between a tank filled with water and water-glycol or refrigerant running inside coils submerged inside the tank. One of two methods even an internal or external melt ice-on-coil

system, where either the warm fluid is the water in the tank or the water-glycol/refrigerant is used to melt the formed ice, can do discharging the tank. Talking more in detail about the external system, charging the tank happens at night when ice is formed on the exterior surface of the pipes, the glycol-water temperature starts making the ice at –4.4 to –3.3 °C and then it lowered to –9.4 to –7.2 °C to manage the thermal resistance of the formed ice layer. During the day, the water will discharge from the tank and warmer water will be returned to the tank, and due to the warm return temperature, the ice will start melting. At the same time, the glycol-water chiller will be in operation, and the supply temperature of the chillers will be warmer than the discharge from the tank, then the mixed temperature will head to the heat exchanger to supply the desired temperature for the system[3].

(B) **CHW TES**
The energy in CHW TES is stored as sensible heat by changing the temperature of the medium in the storage (usual water). During off-peak hours, the tank is charged with cold water, and later is discharged during on-peak hours. The TES recharges with a range of 4°C to 6°C, with the possibility to discharge and supply water with the temperature again between the same temperature of 4°C to 6°C as needed. The CHW TES is less compact and has a higher specific volume compared to other types of TES (Ice and LTF TES) with a specific volume between 0.3 to 0.5 m3/ton-h. The height of CHW TES can reach from 30 to 46 meters. The higher the tank the less footprint is required. It is also worth mentioning that CHW TES is beneficial when it comes to economy-of-scale compared to the other types of TES [3].

When it comes to operation of the CHW TES. CHW TES work on the stratification principle where the return water from DCS to the tank is warmer than the water temperature discharged from the tank and as its density is less it will be floating on the top of the tank. The cooler water in the tank has a higher density and remains in the bottom, to ensure these internal flow diffusers are used, the cooler water will be supplied at low velocity from the lowest point of the tank to the DCS, the supply occurs at 4.0°C where the pure water has it highest density [3].

(C) **LTF TES**
Similar to the CHW TES, the energy in LTF TES is stored as sensible heat by changing the temperature of the medium in the storage. During off-peak hours the tank is charged with cold water and is discharged during on-peak hours. The TES recharges with a range of -1°C to 2°C, with a possibility to discharge and supply the temperature again between the same temperature -1°C to 2°C as needed (below 4°C). The CHW TES is less compact and has a higher specific volume compared with Ice TES with a specific volume between 0.2 to 0.3 m3/ton-h. Similar to CHW TES, taller tanks are used so area footprint can be minimized. Where LFT TES has better economy-of-scale compared to Ice TES but less benefit compared to the CHW TES [3].

When it comes to operation of the LTF TES. Similar to the CHW TES, the LTF works on the stratification principle but uses lower supply and discharge temperatures from the tank. To make sure this is applicable, as the water's highest density occurs at 4.0°C, the water is mixed with various admixtures/ additives to achieve a lower temperature than 4°C while ensuring the coldest fluid remains in the bottom [3].
In conclusion, each TES technology has some limitations and advantages compared to each other. These limitations and advantages can be generalized. However, when selecting a specific TES technology, these generalizations should be reviewed with attention and caution about where they will be considered. Table 2.2 presents a generalized comparison between different cooling TES technologies.Noting that in Case of Gothenburg DCS, several factors were in the advantage for selecting CHW TES such as the economic aspect of large scale of TES, energy efficiency, ease retrofit of the DCS, simplicity and reliability, and the possibility to install the TES remotely from the existing chillers.

Table 2.2: Generalized comparison between different cooling TES technologies [8]

	ICE TES	CHW TES	LTF TES
Unit volume (volume/ton-h)	Good	Poor	Fair
Footprint (plan area/ton-h)	Good	Fair	Good
Modularity	Excellent	Poor	Good
Economy-of-scale	Poor	Excellent	Good
Energy efficiency	Fair	Excellent	Good
Low temperature capability	Good	Poor	Excellent
Ease of retrofit	Fair	Excellent	Good
Rapid discharge capability	Fair	Good	Good
Simplicity and reliability	Fair	Excellent	Good
Site remotely from chillers	Poor	Excellent	Excellent
Dual-use as fire protection	Poor	Excellent	Poor
Storage material cost	Low	Low	High

CHW TES uses standard water chillers with a supply temperature between 4 and 7°C, the same water chillers technology can be used for LFT TES but with lower supply temperatures of -2 and 2°C. Ice storage (external-melt) may use packaged chillers to cool a secondary medium for the ice forming temperature or may have a built-up refrigeration plant. The volume for the CHW TES varies depending on the temperature difference range between the supply and the return temperature and it can be between 0.088 to 0.169 m3/kWh. The volume of ice storage also varies between 0.013 to 0.027 m3/kWh depending

on the technology used. LFT TES has a better economy-of-scale compared to Ice TES but less benefit compared to the CHW TES. The CHW TES can be beneficial when it comes to economy-of-scale compared to the other types of TES. Ice storage can slightly benefit when it comes to economy-of-scale even though its benefits from the change of the medium phase [3].

The vertical cylinder is the preferred tank shape for CHW TES. A cylindrical tank has a lower surface-to-volume ratio than a rectangular tank of the same volume, more evenly distributes stresses, and has a lower likelihood of leakage.

This helps to have less insulation to meet design objectives for ambient heat gain, and thus costs less to build each ton-hour (kWh t) of stored cooling. Tanks that are square or rectangular are easier to integrate into building designs. However, when it comes to the heat gain, these tanks are not ideal, but if the tank is integrated into the building structure, this disadvantage may be mitigated by lower construction costs. When it comes to spherical tanks, have the smallest surface-to-volume ratio, however, they don't stratify properly and aren't recommended. Also, the horizontal cylindrical tanks are not suggested for stratified chilled-water storage. On the other side, the Ice TES can be designed in different shapes without impacting the performance such as in rectangular or spherical, cylindrical shape [3].

2.4 District Cooling System in Gothenburg

Göteborg Energi is the sole district cooling supplier in Gothenburg. The existing system has eight cooling plants located around the city centre and a distribution network connecting between the plants and the end users with total distance of around 30 km. Currently a total cooling capacity of 75.9 MW is installed. The location of the cooling plants and the network layout are shown in Figure 2.3 below. The capacity of cooling units are shown in table 4.2.

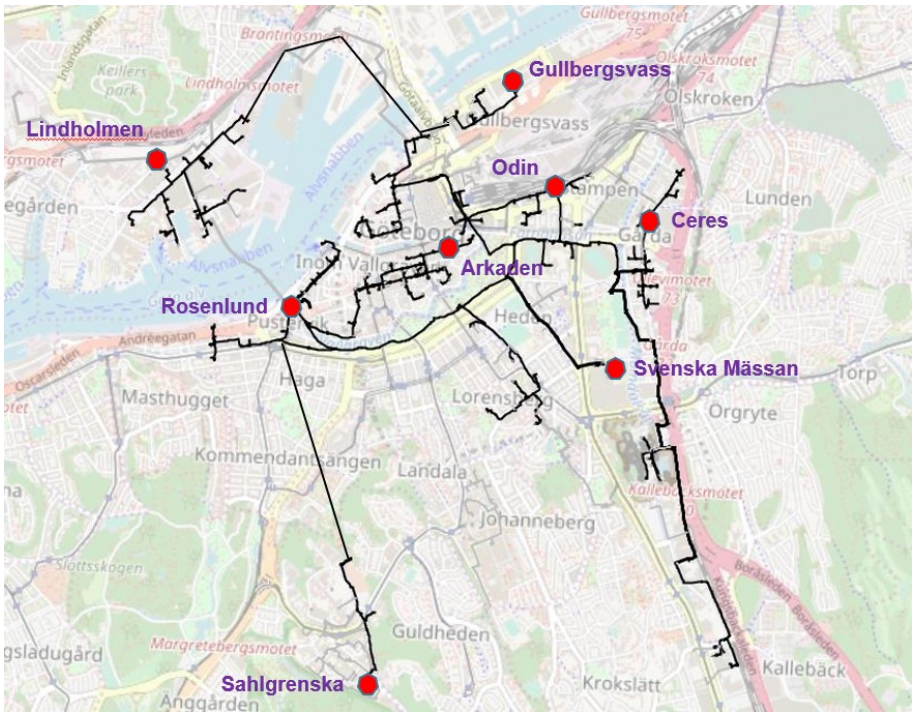

Figure 2.3: District Cooling System in Gothenburg 2021

Table 2.3: Capacity of cooling units

Location	Total Capacity (MW)	Absorption Chiller(MW)	Compressor(MW)
Rosenlund	32	22	10
Gullbergsvass	11.15	3	8.15
Arkaden	4.75	1.1	3.65
Odin	4.65	2	2.65
Ceres	1.87	1.2	0.67
Svenska Massan	4.65	3.4	1.25
Sahlgrenska	3.06	0	3.06
Lindholmen	15.55	3	12.55

The distribution network is scaled for a temperature difference of 10 °C between the feeding and return flow of chilled water temperature. Typically, the feeding water

temperature from the chilling plants is between 4 °C to 6 °C, and the return temperature is around 13 °C. The pressure difference at the customer's control valve is between 100 to 600 kPa. The connections between the district cooling networks and the end users are indirect, which means there are heat exchangers in between to separate the district cooling system side and the end users' load side. The cooling plants produce energy in three ways, which are free cooling from river, absorption chillers and compressor chillers. The plants harness cheap and sustainable energy from the river and waste heat from the industries. The plant in Rosenlund is located next to the river Göta älv where the water temperature varies between 0.5 to 22 °C throughout the year. In winter time, when the sea water is below 5 °C, free cooling is available to fulfill all the cooling demand needed, as shown in figure 2.4 below. In summer time, pre-cooling by river water is also done before further cooling by chillers, which correspond to the period from April to June and from September and November in figure 2.4 below. Absorption chillers utilize waste heat from industries, which otherwise needed to be rejected, as an input for providing cooling energy. It is available in summer time when the district heating demand is low. Therefore, absorption chillers are running only in the summer time as shown in figure 2.4 below. This is a more cost-effective and energy-efficient option with lower carbon emission compared with conventional air conditioning. Compressor chiller is mainly used during high-demand hours to fulfill the peak demand due to its high operating cost which depends on the electricity prices. They mainly operate in summer time when the cooling demand is high, as shown in figure 2.4 below.

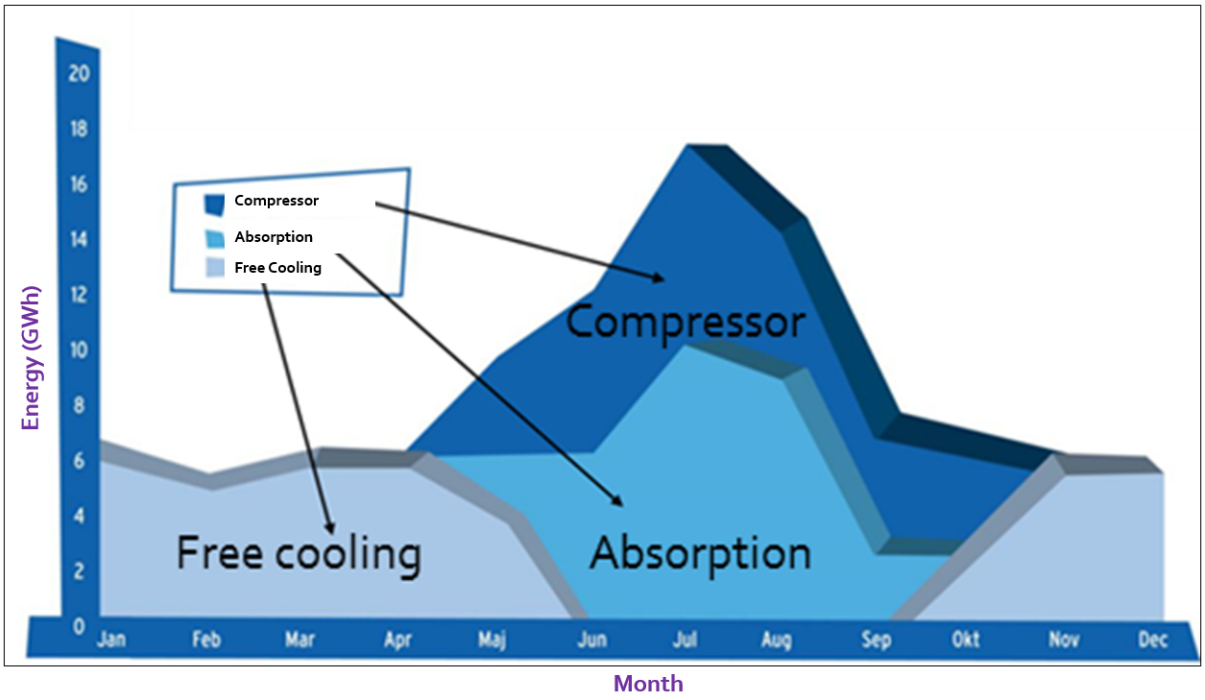

Figure 2.4: Distribution of Cooling Technologies' Usage.

The main customers in Gothenburg are offices, malls, hotels, data centres and hospitals, mainly for space cooling. Currently, as the main cooling application is space

cooling, the cooling demand is closely related to the outdoor ambient temperature. A higher outdoor temperature induces higher cooling demand. Figure 2.5 and 2.6 show the outdoor temperature and cooling demand in Gothenburg throughout the whole year of 2020. The outdoor temperature and cooling demand generally varies accordingly. It can be seen that the total cooling demand is generally below 10MW when the outdoor temperature is below 15 °C. When the temperature is above 15 °C, the cooling demand increase significantly. In 2020, there are some hours that the outdoor temperature reached almost 30 °C and cooling demand was almost 57MW, which is multiple times of the normal cooling demand. Figure 2.7 shows the cooling demand in the first week of August in 2020. The variation of cooling demand follows the change in outdoor temperatures in similar manner.

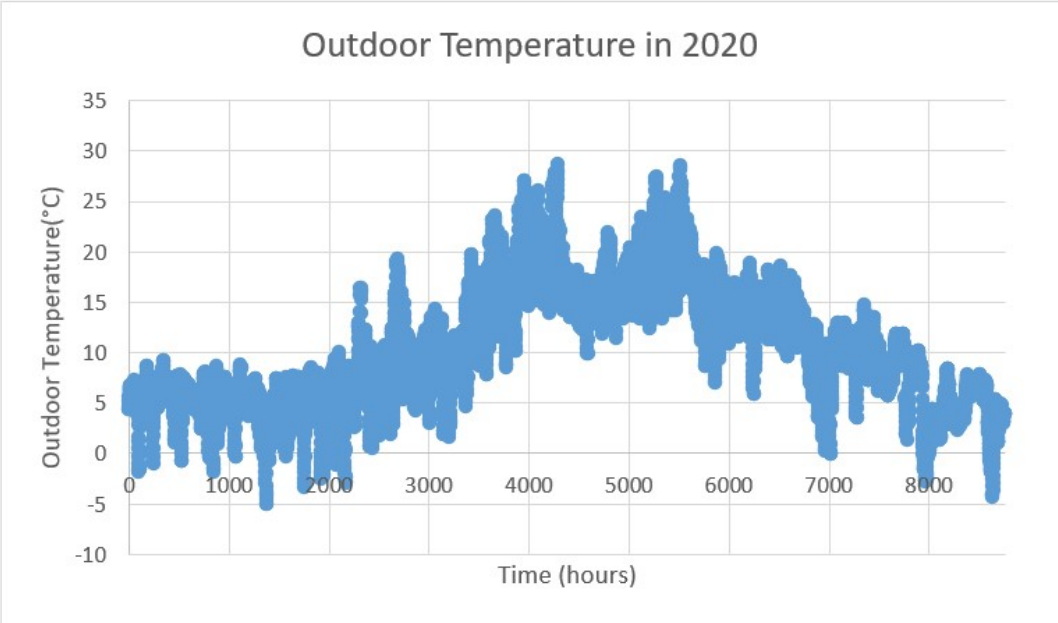

Figure 2.5: Outdoor Temperature in 2020 Gothenburg, Sweden

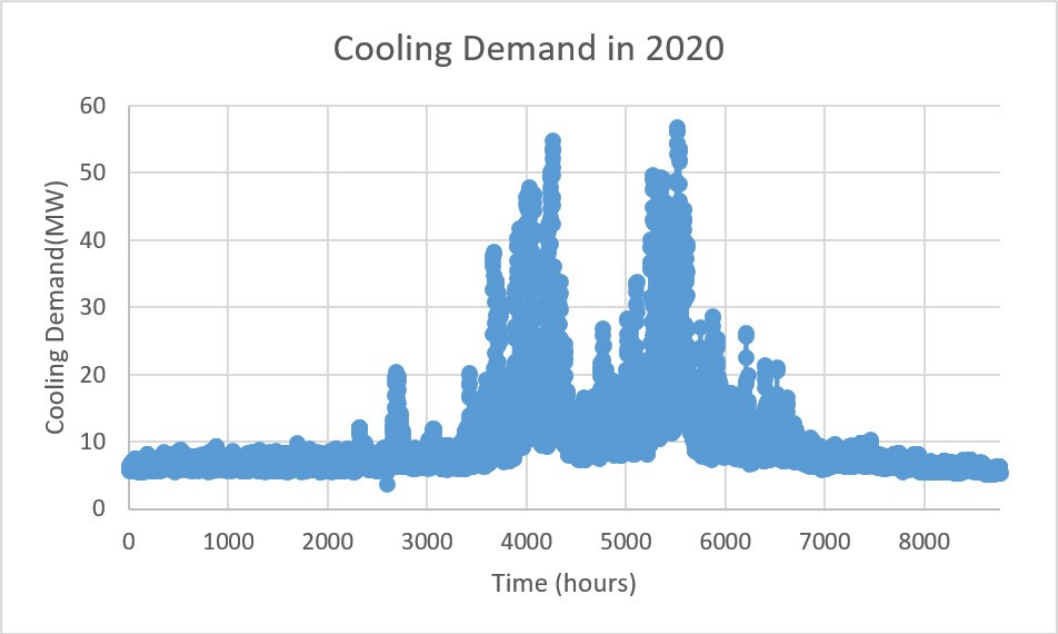

Figure 2.6: Cooling Demand in 2020 Gothenburg, Sweden

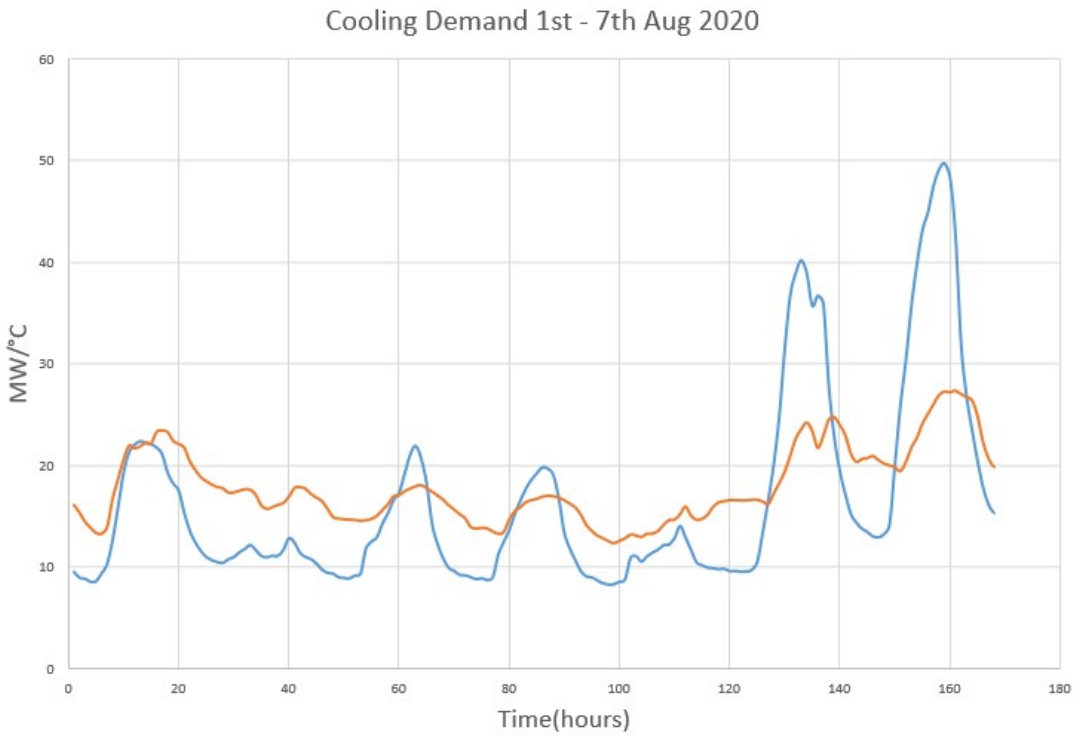

Figure 2.7: Cooling Demand from 1st-7th August in 2020 Gothenburg, Sweden

2.5 Future Development of District Cooling System in Gothenburg

The peak cooling demand is expected to reach 160MW in 2040 due to the expansion of commercial and industrial infrastructures and the expected increase in ambient temperature. Five more chilling plants are expected to be built from 2024-2032 to reach a total capacity of 131 MW.

There is also a plan to construct a thermal storage tank in 2028 to improve the operation and decrease the operational cost. The volume of the tank will be between 22000-33000 m^3 and power rating between 30-40MW, with a loading temperature between 1-7°C. The tank will be built next to Spårvagnsdepån and the tank will be charged mainly by that chiller during off-peak hours. The expected installed capacity is around 171MW.

As mentioned before, the current peak demand is mainly met by compressor, which has a high operating cost due to the high price of electricity during peak hours. Therefore, the aim of the storage tank is to replace the need of compressors during these hours and shift the load from peak hours to off peak hours by the storage capacity. So that less chillers are needed to be installed while they are just running a few hours of a day, and it can also lower operational cost by purchasing electricity at lower price.

Moreover, except the new chiller in Spårvagnsdepån, there is a plan to replace all existing absorption chillers to compressor chillers in the future. This is because if multiple absorption chillers are used in district cooling system, the return temperature from the absorption chillers to the district heating system will not be low enough and the desire temperature in the district heating system cannot be achieved. This will adversely affect the district heating system because of more distribution pump work and less efficient energy recovery for the condensation process in the central heating plant. The efficiency in the district heating system thus will be lower. Therefore, in year 2040, it is expected that there will be at least 116MW of compressor chillers installed. The following table 2.4 illustrates the expected capacities of cooling plants in year 2040.

Table 2.4: Capacity of cooling units

Location	Total Capacity (MW)
Skeppsbron	20
Gullbergsvass	11.2
Gasklockan	30
Odin	4.7
Ceres	5.6
Medicinareberget	10
Almedal	11
Spårvagnsdepan	15
Lindholmen	15.6
Nya Mässan	5
Sahlgrenska	3
Thermal Storage Tank	40
Total	171.1

3

Literature Review

This section reviews the literature about technical issues in a cold-water TES tank and the important aspects when designing a cooling thermal storage tank, including thermocline layer development and mixing phenomenon during charging and discharging of water, and the loading temperature of the tank. It is followed by looking at the modelling method about optimization of investment in the energy system.

3.1 Thermocline in Stratified Cooling TES

By producing and maintaining a thermocline between the warm upper zone and the cold bottom zone, the stratified storage tanks will achieve the required essential separation between cold and warm water, where the cold water below the thermocline is separated from the warm water above by a stable, well-defined thermocline layer. At different temperatures, the density of the stored medium also changes, where the temperature and density of the medium play a role in deciding the bottom and the upper zone of the thermocline layer.

During the charging cycle, chilled water from the cooling equipment enters the tank from the bottom diffusers and warm water escapes through the top diffusers. The thermocline rises as the volume of chilled water increases and warm water is displaced with colder water. The overall amount of water in the tank does not change. During discharge, the water flow is reversed and the mechanism is reversed by pulling the chilled supply water from the tank's bottom and sending warm return water to the tank's top. The flow into and out of the tank is distributed using a diffuser. Water flows smoothly into the tank with a well-designed diffuser, limiting turbulence and leaving the thermocline undisturbed. The greater temperature difference between the warm return and cold supply water from the storage increases the storage capacity of the stratified tank and the density difference, making stratification much easier.

The thermocline layer gets thickened due to the conduction of heat via the thermocline through and along the tank's walls. As a result, the volume of usable chilled water decreases as the thermocline degrades. If a charged storage tank is left inactive, the thermocline will eventually deteriorate over time to the point where all of the water in the tank is no longer useful, requiring the tank to be refilled with cold water. Depending on the design of the diffuser and the thermocline aging time, the

thickness of the thermocline varies [3].

Figure 3.1 demonstrates the thermocline layer to separate the discharge water at 4°C from the charging water at 14°C (typical DC CHW TES), in a temperature versus height profile.

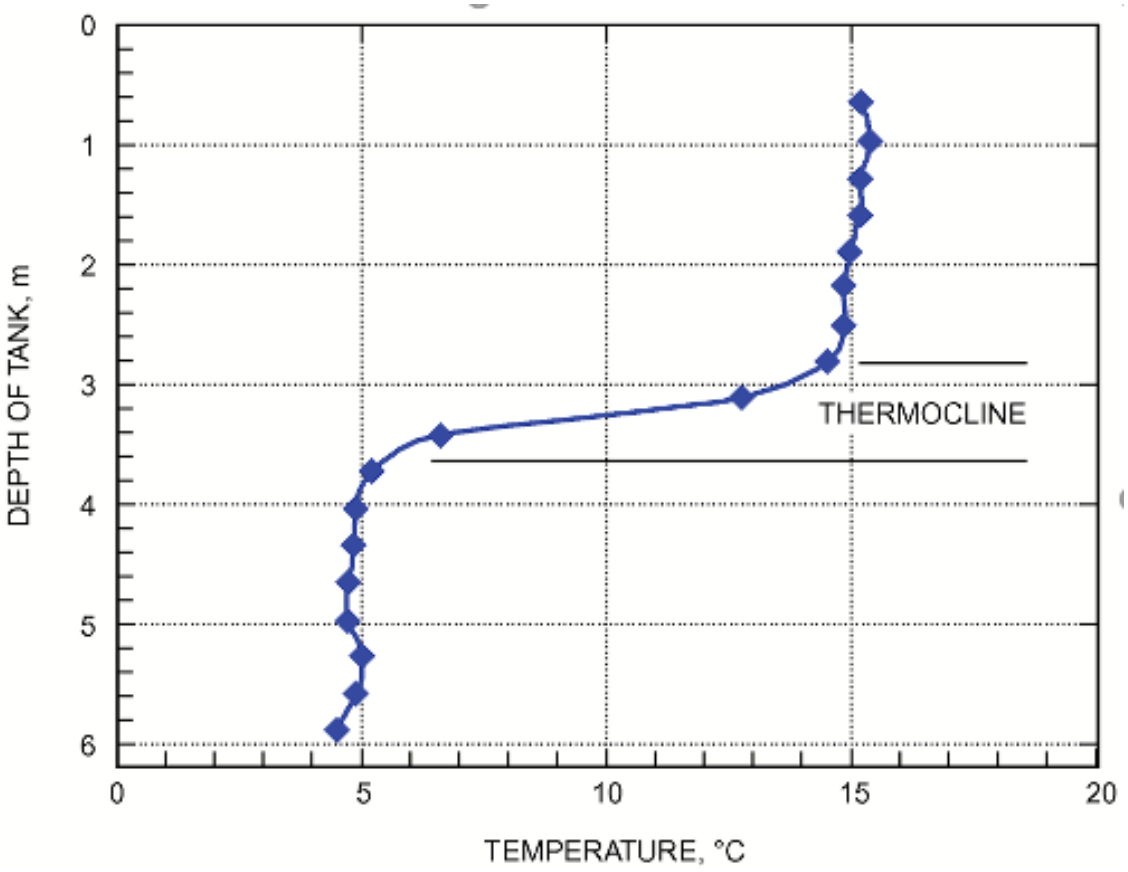

Figure 3.1: Typical stratification temperature profile [3]

When correctly constructed diffusers are utilized, the thermocline thickness will be independent of tank dimensions. By increasing the height-to-diameter ratio of the storage cylindrical tank, the portion that the thermocline occupied from the tank volume will also reduce. As a result, the thermocline has less of an impact on total usable capacity with a taller tank. In addition, if the diffuser system is constructed with a higher inlet Reynolds number such as because of space constraints within the tank as a reason. The effect of this method is usually a thicker thermocline and thus less usable volume within the tank [3].

In case the discharge rate happened at a high velocity, this will lead to creating a thicker thermocline layer and increase the percentage of the unused volume inside the storage tank [18]. Therefore, the velocity of the flow in the dis/charge distri-cution pipes from/to TES should not exceed 0.3 m/s in order to not interrupt or degrade the thermocline layer and keep it thin as possible to create a separation

between the cold and hot fluid [7].

Mentioning the above, it is important to indicate the impacting parameters in a thermocline TES system and serve them as the design variables that can be tweaked to optimize and enhance the performance of the TES system. These parameters can be divided into categories as follows [18]:

- The conditions of operation such as the flow rate, heat transfer fluid media, the cycle of operation, the operational temperature, and cut-off temperature.
- The tank geometry such as the flow inlet/outlet dimension and location, flow distributor characteristics, tank height to the diameter aspect ratio, tank form, and insulation.
- The packing conditions; the packed media and packing configuration.

The most influential factor on the level of thermal stratification and the performance of thermocline TES systems is first, the flow rate, which the tank geometry and temperature differential play a big role in determining the best flow rate value. Secondly, the working temperature for the dis/charge of the storage, including the cut-off, the operational, and the initial thermal condition for the storage. Thirdly, the inlet/outlet location which is recommended to be placed near the storage tank's upper and lower wall, and lastly the type of the flow distributor used can be categorized into three types based on their major functions: multi-branch, inversed flux, and radial flux [4]. Figure 3.2 represents the thermal performance parameters that need to be taken into consideration to achieve the optimum operation of the TES.

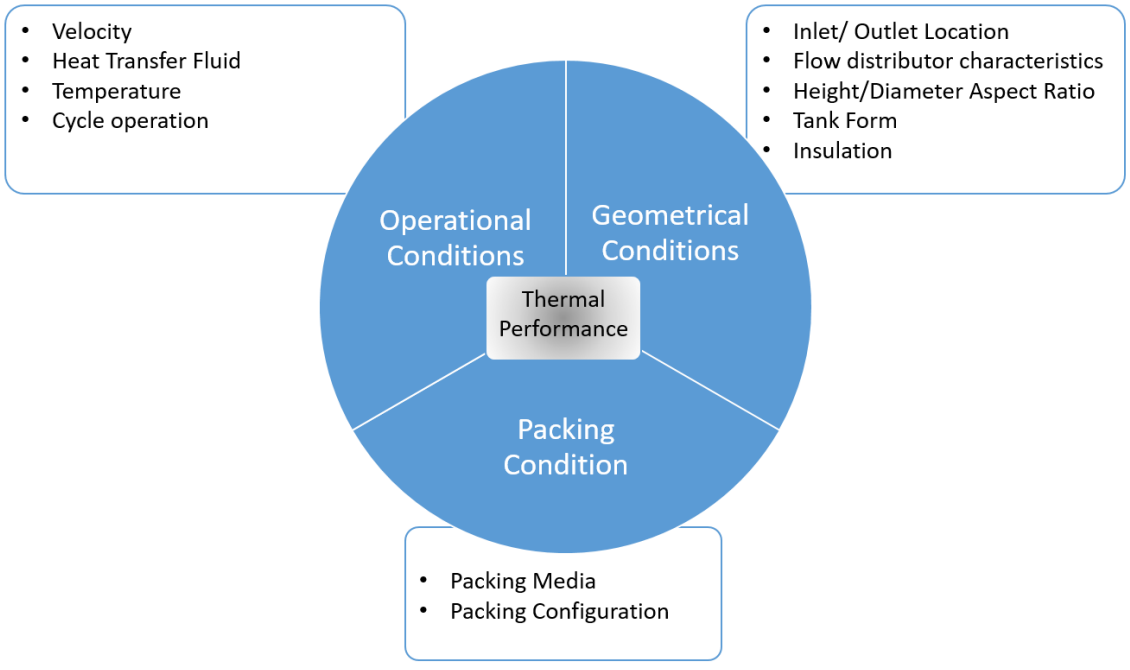

Figure 3.2: TES parameters for optimum thermal performance [4]

(A) **Thermocline TES system performance indicators**
TES performance can be assessed and evaluated even by using the graphical methods (non/dimensional) or by using numerical calculations. Figure 3.3

presents the common performance indicators used to assess the thermocline TES tank, followed by brief summarizing for each performance indicator.

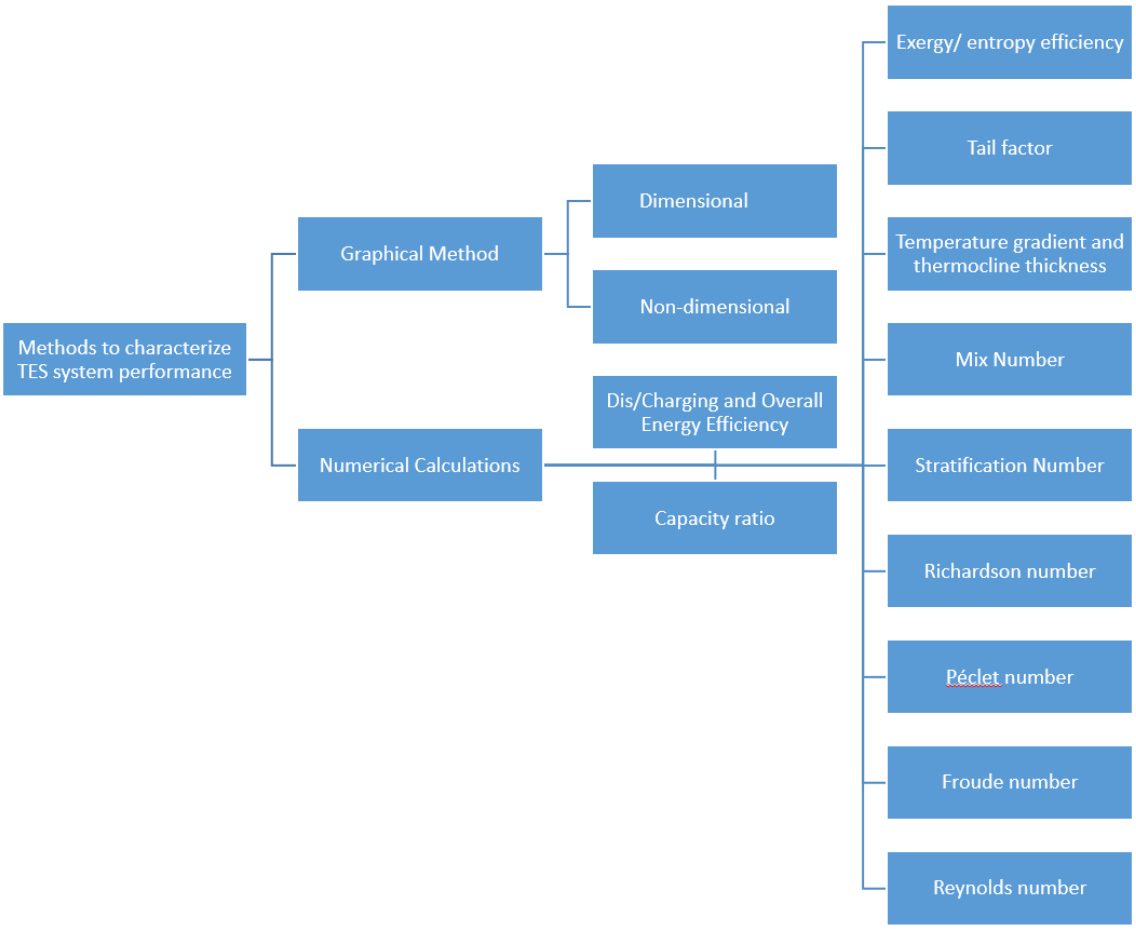

Figure 3.3: Common performance indicators used to assess the thermocline TES tank [5]

(B) **Charging and Discharging Efficiency and Overall Energy Efficiency** The quantity of stored thermal energy can be expressed using indicators that follow the first law of energy conservation, where charging efficiency (Eff.ch) is the ratio of net stored energy to the integral of full incoming energy, whereas the discharging efficiency (Eff.dis) is the ratio of net extracted energy to the integral of initially stored energy. The ratio of the net difference between input and output to the total input energy can be found, knowing the inlet and outlet temperature of the heat transfer medium, which is functionally dependent on time. The effectiveness of the cycle of operation can be expressed by the overall efficiency [5].

By selecting the right cut-off temperature at the end of charging and discharging, it will ensure achieving large storage capacity while avoiding overheating/ sub-cooling of the heat transfer medium.

i. **Capacity ratio**
Same as the overall energy efficiency, the capacity ratio depends on the first law of the energy conservation and it presents the ratio between the difference of the energy in and out to the maximum theoretical energy that can be stored inside the storage [5].

ii. **Exergy/ entropy efficiency**
The indicator of exergy and entropy efficiency follows both the first and the second law of energy conservation and it is used to determine how much usable work is transported and extracted during the process when the energy is released. In another word, it formulates the ratio of the actual exergy to the amount of exergy from a 100% stratified tank, as presented by Shah and Furbo [19].

iii. **Tail factor**
It represents the amount left from full charge and stores the energy in the tank, and it varies between 0 and 1. This factor is independent of the operation conditions, the heat transfer medium thermal properties, and the storage geometry[18].

iv. **Temperature gradient and Thermocline thickness**
One of the most frequent methods of evaluating thermocline/ stratification behavior is to plot the change of the temperature gradient against time or height. However, monitoring the temperature gradients is not suitable to compare the thermal performance between different TES [20]. And it is more appropriate to estimate the thermocline surface or volume due to temperature gradient using 2D or 3D CFD simulation.

On the other side, the thermocline thickness is a suitable to use as an indicator in situations when the formation of the thermocline is regular and the evolution of thermocline is stable, this can be seen in packed-bed TES, in the contracts the use of this indicator is unsuitable for single-medium thermocline[18].

v. **Mix Number**
It focuses on the deteriorated energy that occurs in real-time during the mixing process. The value is between 0 and 1, which the smaller the value means the better stratification and weaker mixing inside the tank[21].

vi. **Stratification Number**
The stratification number is used to assess the stratification decay gradients against the height of the tank; it describes the ratio between the mean temperature decay for each radial position at each time interval and the temperature decay at the beginning of the charging process[22].

vii. **Richardson number**
It is the ratio of buoyancy force to mixing force, which is affected by the length

of the storage tank and the velocity of the fluid under a certain temperature difference and flow rate. A larger Richardson number means a higher stratification level and this can be achieved by ensuring lower inlet velocity of the fluid[23] [24].

viii. **Péclet number**
It is the ratio of the convective to the diffusive transport rates, which is affected by the tank diameter, flow velocity, and the thermal diffusion factor. This indicator value can relate directly to the thermocline thickness[4].

ix. **Froude number**
This indicator is to reflect the ratio of the inertial to buoyancy forces, for the diffuser or inlet design in the tank. The recommended value for the Froude number is to be smaller than 2[4].

x. **Tail factor**
This indicator represents the ratio of inertial to viscous forces. This factor is issued to determine if the flow is laminar (with a low Reynolds number) or turbulent (with a high Reynolds number)[25].

(C) **Thermocline monitoring and measure**
In stratified storage tanks, a vertical row of temperature sensors to be bundled and hung from roof plugs, or use sensors attached to individual shells with extended thermowells, can be used. These measures are used to determine current storage inventory and thermocline thickness by monitoring the levels of warm and cold water inside the tank [26].

(D) **Thermocline relation with temperature difference inside the TES**
Increasing the temperature difference between cold water supply and return water increases the storage capacity of a certain amount of water. Because storage costs are based on tank capacity, the cost per kWh decreases as the temperature differential increases. Furthermore, the higher the temperature differential, the higher the improvement of the thermocline construction and maintenance, reducing transfer pump flow and energy consumption [7].

(E) **Thermocline relation with TES efficiency**
Any loss of usable energy produced by mixing or heat conduction across the thermocline is not factored into the storage efficiency of chilled water tanks, and therefore the storage efficiency is not the best measurement of the availability of cooling in the tank compared with the storage tank figure of merit (FOM). As the FOM accounts for the real loss of usable stored cooling capacity due to thermal conduction and blending within the tank due to thermocline thickness and the temperature differential loss [27].

(F) **Thermocline relation with dis/charge from TES**
Because of conduction heat gains and water blending inside the tank, stored

water typically gains 0.5°C in storage during a 24-hour period. Water should be discharged from the tank at a consistent temperature in the ideal situation. But in reality, as the thermocline begins to be dragged into the lower diffuser, the discharge temperature progressively rises during the discharge duration, increasing more rapidly at the conclusion of the discharge period.

In reality, this steady climb is undetectable unless the charging temperature varies greatly, resulting in layers within the tank. The quality of stratification within the tank, which is a direct result of diffuser design and heat transfer within the tank and through the tank walls, determines the degree of temperature rise during discharge [7].

3.2 Energy Dispatch Modelling of District Cooling System

The modelling of energy dispatch schedule for a energy system was widely investigated by linear optimization. Moreover, non-linear optimization were also used in energy system design. Linear programming refers to the problem which both objective function and constraints are linear functions. Otherwise, it is non-linear programming [28]. Linear optimization such as mixed integer linear optimization is suitable for optimization energy with various interaction with energy carriers in the energy system. Nottrott et al [29] implemented a modelling of energy storage dispatch schedules for a photovoltaic and battery storage energy system by linear programming. Marco et al [30] compared 24 mixed-integer linear programming models with different levels of details of input of various energy systems. It illustrated that simple linear programming model can estimate the total capacity of investments fairly accurately. But for individual units, it is challenging to obtain an accurate result as it depends on details of input and operational constraints. Weber et al [31] developed a mixed integer linear optimization model to optimization the investment of district energy system in a ecotown in the United Kingdom.

On the other hand, non-linear programming is used when the non-linear relations are decisive for obtaining a reasonable results, including the efficiency factors of combined heat and power plants, pressure and heat losses constraints in district energy network. Jie et al [32] established a non-linear optimization model for the district heating network to optimize the operation by accounting the pump work and heat loss of the heating network, including pipes and heat exchangers. Ommen et al [33] pointed out that the linearization of heat and electricity relation in both extraction and back-pressure combined heat and power plant will impose significant error to the results. However, Accounting part load efficiencies of individual technology in the model results in extra long computational duration which may not be appropriate for preliminary planning phase [30]. The comparison of linear and non-linear programming methods showed that mixed integer programming optimization is the most appropriate method in terms of accuracy and computing time for energy system dispatch modelling[33].

4
Methodology

4.1 Introduction

The study of future district cooling system in Gothenburg is divided into two parts, namely the modelling of computational fluid dynamics simulation of the thermal energy storage tank and the investment modelling of district cooling system. The first part presents the methodology of CFD modelling of operating scenarios in the cooling thermal storage tank, and the second part includes the methodology of energy dispatch modelling of district cooling system in Gothenburg.

4.2 Modelling of Cooling Thermal Energy Storage Tank

The computational fluid dynamics modelling in this section intends to gain an insight into the operation of stratified thermal energy storage tank with low loading temperature, to understand the three-dimensional transient dynamics of the development and stability of thermocline layer and the interface dynamics in the TES. In order to achieve this, various futuristic operation scenarios of three-dimensional unsteady simulations are performed. Three-dimensional charging and discharging scenarios in the thermal energy storage tank is modelled by computational fluid dynamics software workbench Ansys Fluent. A tank is first constructed with the design dimensions and geometry. A mesh of the simulation domain is thus defined to discretize the element so that the solution can be calculated. Boundary conditions, assumptions and initial condition are be thus given to define the working condition. Transient conditions are then set for different operational scenarios with respect to time. The model is then run and and the results are analysed and discussed. Figure 4.1 illustrates the schematic of computational fluid dynamics modelling.

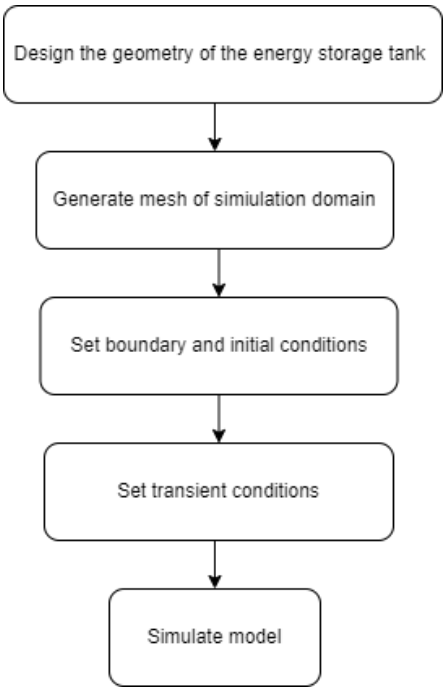

Figure 4.1: Schematic of CFD Modelling

4.2.1 Tank configuration

The tank is constructed based on the realistic data with simplified configuration to reduce complexity and computational time. The tank is cylindrical in shape with two concentric radial type diffusers at the top and the bottom of the tank respectively, as shown in figure 4.2 and 4.3. Practically, the two diffusers are connected to pipes to the outside. Each diffuser can be used for both charging and discharging depending on the operation scenarios. They are working concurrently during operation. When one of them is charging water to the tank, the other is discharging water from the tank, vice versa. The aim of concurrent operation is to keep the tank filled up water at all time in a closed loop. This is to keep the pressure inside the system stable, so that the pressure drop across the system is not affected by the operation of the tank [34].

The volume of the tank of the model is designed to be 22000 m^3, which corresponds to the volume needed for discharging of chilled water for 7 hours with a power rating of 40MW, which is approximated according to the practical operation of charging the tank fully during the night time. The height of the tank was determined by Göteborg Energi at 65 meters due to practical constraints, with the diameter of 20.76m, which correspond to the height-diameter aspect ratio of 3.13. This aspect ratio is good for reducing mixing and stratification [35].

The diffusers are radial type which ensure that chilled water enters the tank with a linear flow of low velocity. This is to minimize disturbance on the stratification and thermocline development. They are located at the top and bottom of the tank

concentrically with the tank. The ratio between the cross-section area of the radial diffuser and the storage tank is at its optimum from 0.0327 to 0.131 [36]. In this model a value of 0.1 is taken. The cross-section area of the discs are 33.8 m^2 while the cross-section area of the tank is 338 m^2.

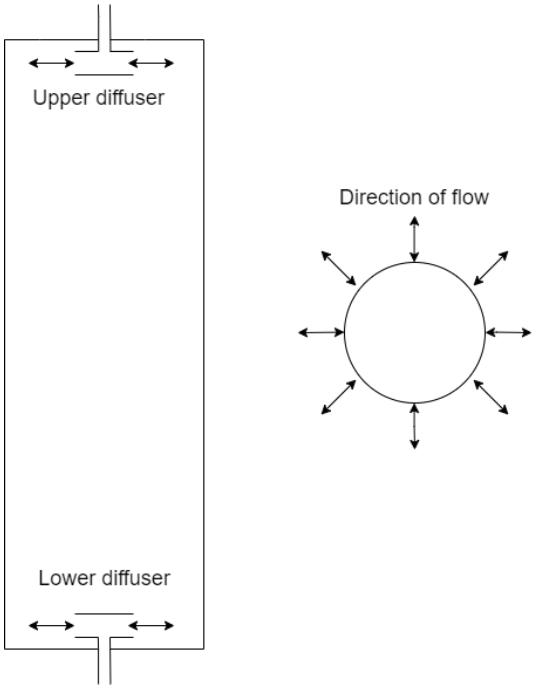

Figure 4.2: Schematic of Stratified thermal storage tank with radial parallel plate diffusers

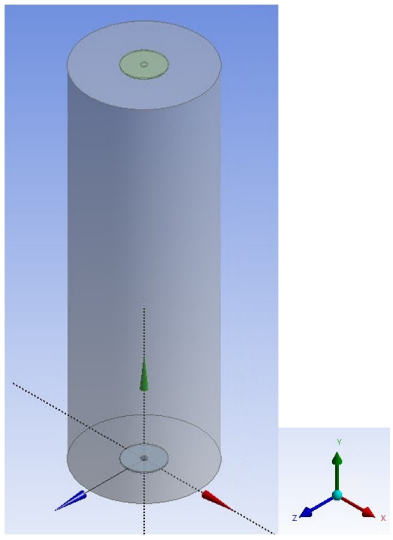

Figure 4.3: Tank Configuration

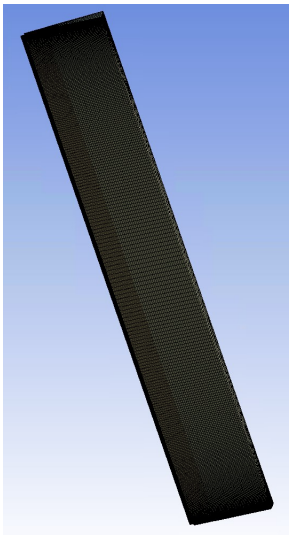

Figure 4.4: Meshing of Tank

Table 4.1: Dimensions of the tank

Parameter	Value
Volume of the tank(m^3)	22000
Height of the tank(m)	65
Diameter of the tank(m)	20.76
Diameter of the inlet and outlet pipe(m)	0.75
Diameter of the disc of the diffuser(m)	6.56
Vertical distance between 2 discs of the diffuser(m)	0.165

4.2.2 Assumptions

ANSYS FLUENT R1 2021 is utilized to solve transient, three-dimensional energy equations. It implements simple algorithm to solve Navier-Stokes equations for flow with various densities because of temperature difference. Mesh is created at vertical cross-section area of the tank to model the change in temperature of water within the tank during charging and discharging. Gravitational acceleration of 9.81 m/s^{-2} is included in model. Pressure-based approach is chosen for the simulation as it is appropriate for low speed and incompressible flow.

A second-order upwind scheme is used for spatial discretization of convective fluxes. For the transient formulation, a first-order implicit scheme is used for pressure-based simulation. The time step used for the simulation is set to be 10 seconds with a maximum iteration of 30 times per each time step. The settings are summarized as follows:

- State: Transient
- Approach: Pressure-based
- Type of flow: Laminar and incompressible flow
- Insulation: Fully insulated from ambient condition
- Momentum: Second order upwind
- Energy: Second order upwind
- Pressure: Second order

4.2.3 Initial and Boundary Conditions

For simplification, the storage tank's envelop is assumed to be fully insulated. That means an adiabatic thermal condition is applied for the tank envelop and the heat flux is set to be zero. All the inlet planes are assigned with no-slip condition. The initial tank is filled with water with one single temperature and temperature profile in the tank is unified.

4.2.4 Input Data

The design return temperature of water from the district cooling network is 13°C. The inlet charging temperature of chilled water can be 1°C or 4°C.

Table 4.2: Operating parameters of the tank

Parameter	Value
Design Pressure(kPa)	101
Design maximum charging flow rate(m^3/h)	3823
Design maximum discharging flow rate(m^3/h)	3823
Charging cycle(h)	7
Discharging cycle(h)	7
Hot water temperature(K)	286
Cold water temperature(K)	274 & 277

4.2.5 Governing Equations

Navier-Stokes Equations

The equation of conservation of mass, or continuity equation:

$$\frac{\partial \rho}{\partial t} + \nabla \cdot (\rho \overrightarrow{v}) = 0 \tag{4.1}$$

The Momentum Conservation Equation:

$$\frac{\partial (\rho \overrightarrow{v})}{\partial t} + \overrightarrow{\nabla} \cdot [\overline{\overline{\rho v \otimes v}}] = -\overrightarrow{\nabla} p + \overrightarrow{\nabla} \cdot \overline{\overline{\tau}} + \rho \overrightarrow{f} \tag{4.2}$$

The Energy Equation:

$$\frac{\partial (\rho e)}{\partial t} + \overrightarrow{\nabla} \cdot ((\rho e + p) \overrightarrow{v}) = \overrightarrow{\nabla} \cdot (\overline{\overline{\tau}} \cdot \overrightarrow{v}) + \rho \overrightarrow{f} \overrightarrow{v} + \overrightarrow{\nabla} \cdot (\overrightarrow{q}) \tag{4.3}$$

where $\overline{\overline{\tau}}$ being deviatoric stress tensor.

$$\overline{\overline{\tau}} = \mu[\nabla \overrightarrow{v} + (\nabla \overrightarrow{v}^T) - \frac{2}{3} \nabla \cdot \overrightarrow{v} I] \tag{4.4}$$

where $\otimes$ denotes the tensor product, creating a tensor from the constituent vectors. A double bar denotes a tensor.

4.2.6 Scenarios

A storage process for TES includes charging, storing and discharging. The tank is always full of water during all scenarios. During charging process, chilled water is

charged to the tank by one diffuser while warm water is discharged from the tank by the same mass flow rate by another diffuser. During discharging process, chilled water is discharged from the tank by bottom diffuser, and at the same time, return warmer water is charged to the tank from the top diffuser.

For freshwater, the relation between temperature and the density is not always negatively related. As shown in figure 4.5 below, the density of water increases with decreasing temperature from 13 °C until 4 °C and the density peaks at 4 °C. And the density decreases again from 4 °C down to 0 °C. Theoretically, in order to attain desired stratification of water layers, for chilled water of temperature lower than 4 °C, it should be stacked on top of water of 4 °C and chilled water of temperature close to 0 °C should be at the top. However, practically, it is unclear about how stratification will happen under low-temperature charging and discharging.

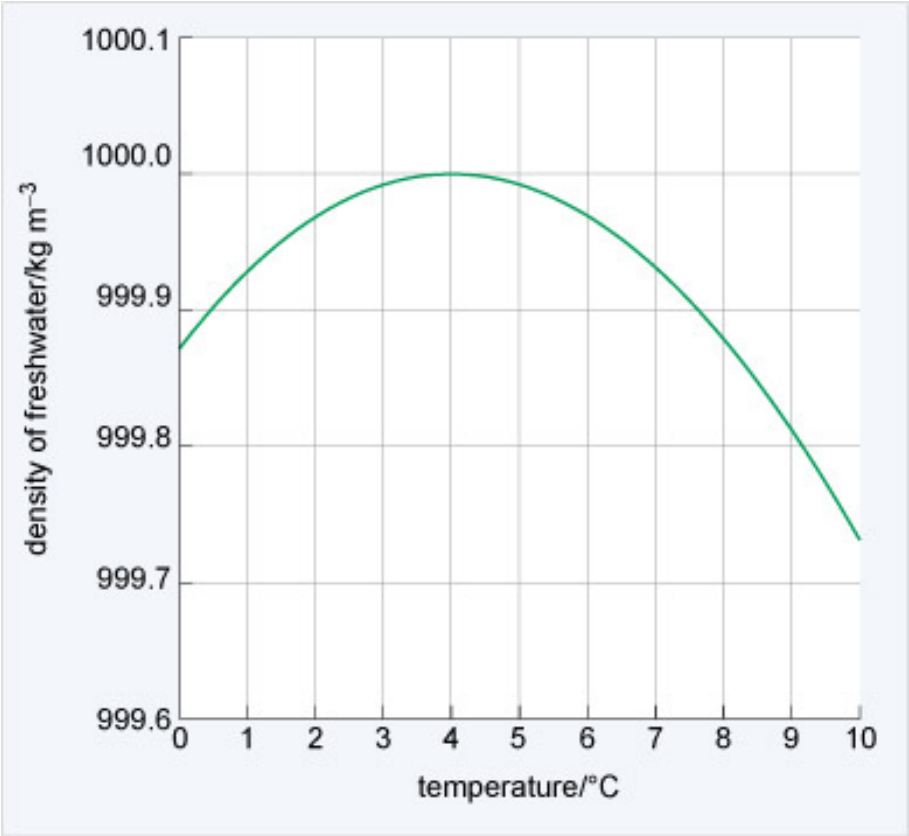

Figure 4.5: Freshwater density against temperature. *Adapted from [37]*

Therefore, in order to study low loading temperature scenarios down to 1 °C, different charging strategies are implemented with different charging and discharging sequences. Two operating scenarios, which are based on future operating scenarios, are modelled in this part, as shown in the following figures 4.6 and 4.7.

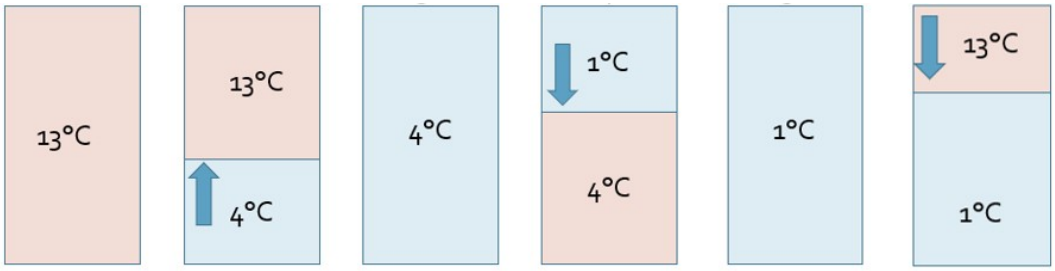

Figure 4.6: Modelling Scenario A.

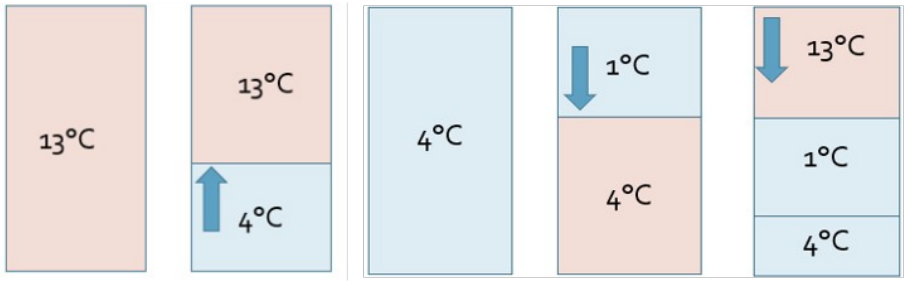

Figure 4.7: Modelling Scenario B.

Table 4.3: Operating details of scenario A

Sequence	Action	Duration(hours)	Flow rate(L/s)
1(Initial Condition)	Filled with water of 13 °C	/	/
2	Charging from the bottom with water of 4 °C	5.75	1062
3	Charginig from the top with water of 1 °C	11.9	512
4	Charging from the top with water of 13 °C	2	796

Table 4.4: Operating details of scenario B

Sequence	Action	Duration(hours)	Flow rate(L/s)
1(Initial Condition)	Filled with water of 13 °C	/	/
2	Charging from the bottom with water of 4 °C	5.75	1062
3	Charging from the top with water of 1 °C	4	512
4	Charginig from the top with water of 13 °C	1	1062

Figure 4.6 illustrates the modelling scenario A. Initially, the tank is filled with water of 13 °C, which is the temperature of the return water of the district cooling

network. Chilled water of 4°C is then charged from the bottom of the tank, while water of 13 °C is discharged from the top of the tank at the same time, which corresponds to the charging operation. Chilled water with 4 °C is the standard chilled water outlet temperature of existing system. This corresponds to the temperature of water after passing through the chilling system. The tank is charged with water of 4 °C continuously for 5.7 hours with a flow rate of 1062 L/s until the tank is fully filled with chilled water of 4 °C. This flow rate refers to a power rating of 40MW.

Then, chilled water of 1 °C is charged to tank from the top of the tank while 4 °C water is discharged from the tank. In order to try to keep the stratification stable, water of 1 °C should be displaced at the top of the tank. Theoretically, as the density of water at 1 °C is lower than at 4 °C. Chilled water of 1 °C refers to the targeted charging and storage temperature of the new TES and it also refers to temperature of chilled water outlet of the new chiller. In reality, the new chiller, which is responsible for cooling down water to 1 °C, has a temperature difference of 7-8 °C between the inlet and outlet, which is also called delta temperature(Δ T) of the chiller. Therefore, the discharged water of 4 °C from the tank has to mix with return water of 13 °C to bring up the temperature to 8-9 °C before going to the new chiller for further cooling down to 1 °C. This operation corresponds to the situation when more cooling demand is expected during peak hours in the future. The tank is charged with 1 °C water continuously for 11.9 hours with a flow rate of 512 L/s. The duration chosen is the theoretical time that 1 °C chilled water can fully displaced 4 °C water in the tank. Finally, return water of 13 °C is charged to the tank for 2 hours from the top with a flow rate of 796 L/s while chilled water is discharged from from the bottom. This corresponds to discharging operation of 40MW.

For modelling scenario B (Figure 4.7), a more intense stratification of water with 1 °C, 4 °C and 13 °C is simulated. The initial stage of operation is same as scenario A, which the tank is filled with return water of 13 °C and water of 4 °C is charged to the tank from the bottom diffuser until it is filled with chilled water of 4 °C. Subsequently, chilled water of 1 °C is charged to the tank by displacing water of 4 °C for 4 hours with a flow rate of 512 L/s, which corresponds to the charging operation. Return water of 13 °C is thus charged to tank by displacing chilled water of 4 °C with a flow rate of 1062 L/s, which corresponds to the discharging operation.

Table 4.3 and 4.4 demonstrate the operating details of 2 scenarios. The flow rate is based on the intended energy input and output from the tank with a maximum energy rating of 40MW.

The transient simulation model will return the characteristics of thermocline dynamics, mixing phenomenon, change of temperature profile and discharging temperature of chilled water. The model will give an insight into the feasibility of lowering down the loading temperature down to 1 °C.

4.3 Energy Dispatch Investment Modelling

This part illustrates the methodology of the energy dispatch investment model in the year 2040 scenario. The model aims at determining the optimal capacity of the new chillers cooling production plant in Spårvagnsdepan and the thermal storage tank by minimizing the total annualized cost. It is done by linear optimization technique by setting up linear constraints and finding the global minimum of the objective function. In the following subsections, assumptions, operational and investment costs of the system, and the formulation of objective function and constraints will be explained.

4.3.1 Assumptions

It is assumed that waste heat from the industry is always available when needed. Moreover, the cost of getting waste heat from the industries is assumed to be zero.

It is assumed that the thermal energy storage tank can be charged by all the chiller units in the network and there is no difference in cost by charging in different locations.

The thermal storage tank is formulated like a battery, with a capacity, rate of charging and discharging , and cycle efficiency.

The coefficient of performance of the chiller units is assumed to be constant. For the absorption chiller, it is assumed to be 20, by only accounting for electricity use alongside free heat. The COP of the compressor is assumed to be 5, including the efficiency of cooling towers and pumps.

4.3.2 Generation and storage

This subsection explains the details of generation and storage units in the year 2040, including capacities, costs, and operational constraints.

(A) **Capacity of units**
The capacity of units is based on the expected installation in the year 2040, as shown in the following Table 4.5. As the new chiller in Spårvagnsdepan is next to the thermal storage tank, it is expected that the chillers will be used mainly for charging the tank when the electricity prices in their lowest and also fulfilling the cooling demand requirements in the system. Therefore, the optimal capacity of the new chiller in Spårvagnsdepan and the thermal storage tank is to be determined.

Table 4.5: Capacity of cooling units

Location	Total Capacity (MW)
Skeppsbron	20
Gullbergsvass	11.2
Gasklockan	30
Odin	4.7
Ceres	5.6
Medicinareberget	10
Almedal	11
Spårvagnsdepan	to be determined
Lindholmen	15.6
Nya Mässan	5
Sahlgrenska	3
Thermal Storage Tank	to be determined

(B) **Investment Cost**

The investment cost for much technical equipment does not have a linear relationship with its capacity [38]. Energy generators and storage units that are larger usually have lower specific costs than smaller ones [39].

As part of the study is aiming to investigate which chiller plant type, absorption or compression, is more suitable to achieve the optimization goal. The investment cost of both types of chiller plants, including the building, chillers, cooling towers, pumps, piping, and controls, has been studied. The investment costs of district cooling projects vary widely depending on the local construction environment and site conditions such as the labor rates, the shipment of equipment, permits, and fees, local authorities and restrictions, etc. The investment cost of a chiller plant in North America is typically in the range between (9510 - 8085 SEK per KW) including the design fees, contingencies and taxes [3].

A previous study was done in Sweden to evaluate the economic aspects of using an absorption cooling system have compared between installing compression and absorption cooling system, where the study presented that the compression cooling system installation was around 20% cheaper than the installation of an absorption cooling system [40]. Based on the above mentioned and for simplicity due to not acquiring actual data from the Swedish market to be used in the comparison, the investment cost for the installation of compression and absorption cooling systems was assumed 9510 SEK and 7610 SEK per KW respectively.

The investment costs of the energy storage system comprise the cost of the tank and the two diffusers, the cost of building up the foundation, the cost of pumps, piping, and valves etc... [7]. The following figure 4.8 shows the non-linear relation between specific investment cost and storage capacity of the

chilled water cooling energy storage tank[7]. For all high, average, and low-cost estimations, the specific investment cost for the tank is much higher when the storage capacity is below 10MWh and it starts to flatten out gradually with the increase of storage capacity. In the simulation, data from average estimation will be utilized as an investment input, the value considered is 210 SEK per KWh.

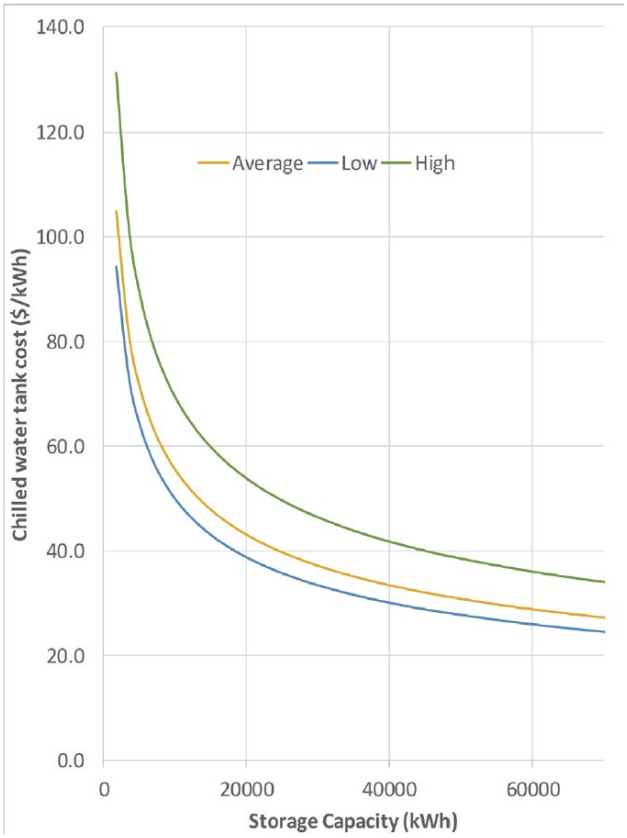

Figure 4.8: Relation between Specific cost against storage capacity of tank. *Adapted from [7]*

The investment cost of the thermal energy storage tank in this study is not linearly related to its capacity. By taking into consideration that for larger TES, the investment cost will become flattened as shown in the graph above, but also noting that a lower discharge temperature from the TES means an even cheaper total investment cost is required for the TES. Therefore, a value between 21.71 to 31.48 SEK/KWh was selected between 2°C and 7°C discharge temperature respectively, taking into consideration the expected storage capacity.

Annualized investment cost can be calculated by multiplying the investment cost and the annuity factor, as shown in the equation 4.5. It is assumed that the number of years is 25, which corresponds to the expected service lifetime of the generation unit and the tank, with an assumed discount rate of 3%.

$$af = \frac{r}{1 - (1 + r)^{(-n)}} \tag{4.5}$$

where r represents the discounted rate, and n represents the number of years the amount will be annualized. Based on the equation above, the annuity factor is 0.05.

(C) **Operational Cost**
One of the main factors to determine the operating cost of the system is the electricity price, which will be highlighted in the upcoming section. Each cooling system, absorption, and compression chillers, have different COP values and this will reflect on how much consumption of electricity is required for each system to operate, and eventually, this will reflect on the overall operational cost of the cooling system. This means the system with the higher COP has the advantage over the other system when it comes to the cost of operation.

Another factor that has been taken into account in this study is the maintenance cost requirements for each chiller system, absorption, and compression. The district cooling guide from ASHARE has given a guideline for an estimated annual maintenance cost for different chiller types. For this study, it was assumed that the compression chillers are electric centrifugal (single compressor industrial-field erected) type with a maintenance cost of 2.7 SEK per KW per year, and a hot water absorption chillers (single effect) type were assumed for the absorption chiller cooling system with the maintenance cost of 4.6 SEK per KW per year [3].

The cost of other operational factors has been not been taken into consideration for this study as they have similar values disregarding whether the cooling plant and TES are operated using absorption or compression chillers. Therefore, they will have no impact on the results of different optimization model scenarios. This factor includes the labor cost and the pumping cost of the cooling plants (noting that the existing plant was considered as one unit and the cooling distribution network is not part of the study). In addition, the operating cost of the TES is neglected for the same reason mentioned above.

4.3.3 Cooling Loads

The future predicted of the cooling load profile is based on the cooling load profile data of Göteborg Energi for year 2020. Figure 4.9 shows the predicted cooling load profile in the year 2040 based on the prediction that the cooling load will be 3.85 times higher in 2040 compared to 2020 (Figure 4.10. Therefore, the cooling load profile in the year 2040 is established based on the one in the year 2020. In addition, the cooling demand is multiplied by a factor of 3.85 to generate the predicted cooling load hourly profile in the year 2040.

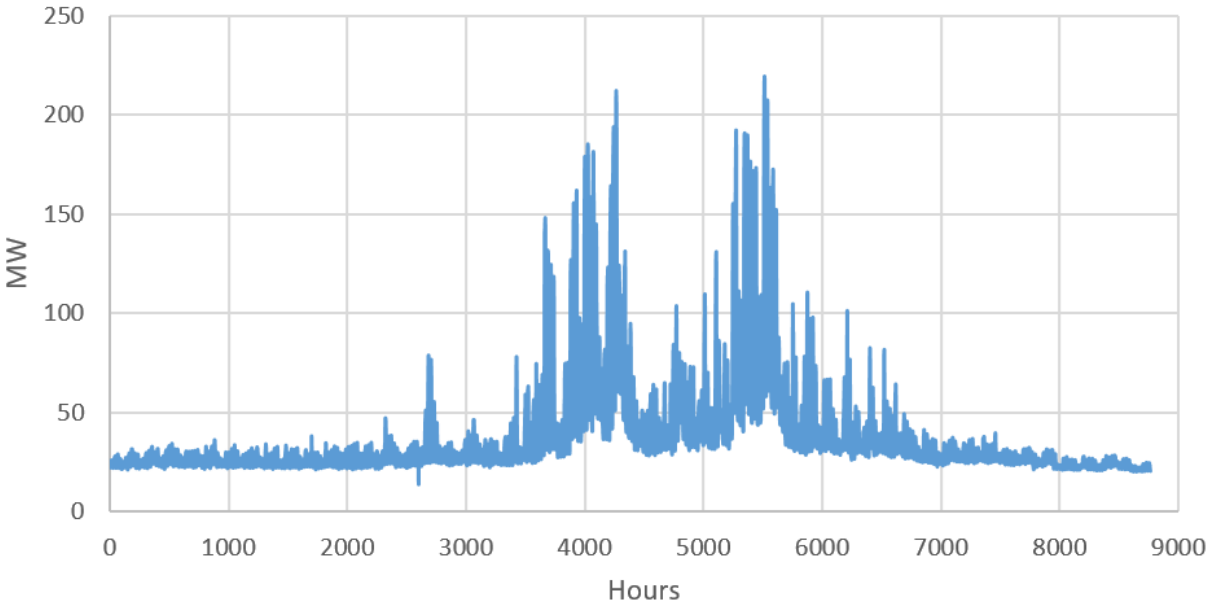

Figure 4.9: Predicted Cooling Load Profile in 2040.

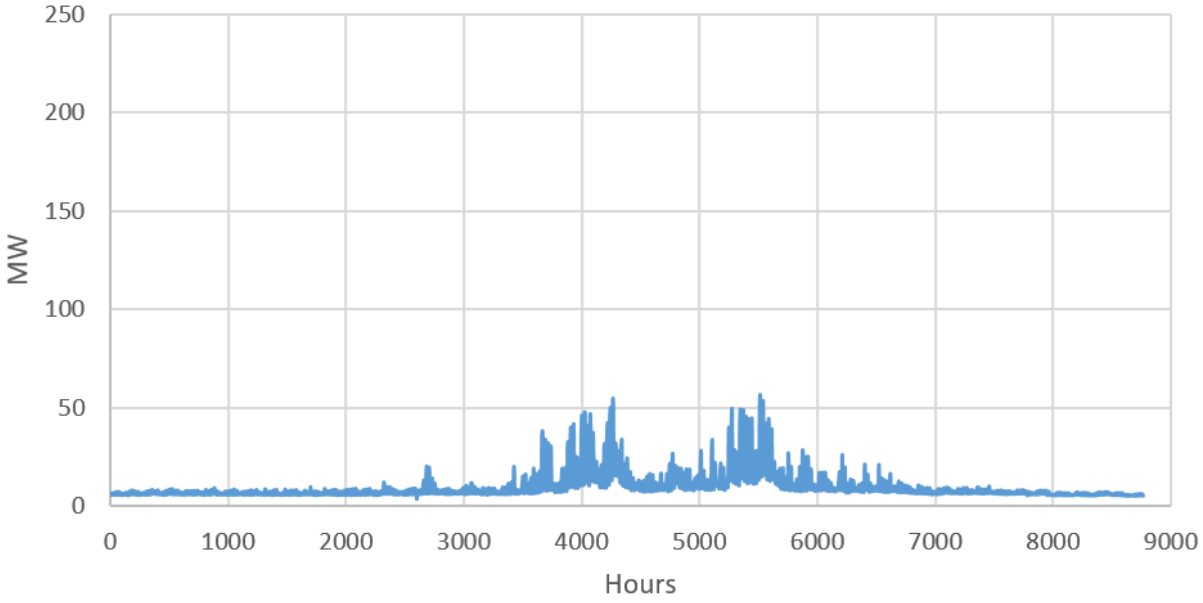

Figure 4.10: Cooling Load Profile in 2020.

In Gothenburg year 2040, the cooling production system by Göteborg Energi will be designed to fulfill the maximum cooling demand with a capacity of 163.7 MW (100% of cooling load) at a maximum outside design temperature of 25°C, where this value will be presented later as DUT 100%.

In terms of daily demand profile, four cases are considered. Four daily load profiles are extracted from the hourly demand profile in 2040 and their generation characteristics will be studied. Their daily peak demands correspond to the utilization of 50%, 75%, 100% and exceeding 100% of the total capacity of the generation system.

In the future operation, there will be a cap imposing on the cooling generation. Once the maximum generation is reached, the system will not provide more cooling energy even if the outdoor ambient temperature is higher and more energy is needed. Figure 4.11 shows the four daily load cases that will be considered. The rated power that can be generated is 163MW. Therefore 50%, 75% and 100% of generation corresponds to 81.5 MW, 122 MW and 163 MW. Those four load cases refer to the load on June 22nd, June 23rd, August 19th and August 17 th respectively.

Figure 4.11: Daily Load Profile.

The cooling loads that needed to be fulfilled by chillers and the operation from the tank is the net cooling demand. The net cooling demand refers to the difference between the total cooling demand and the free cooling demand, which is fulfilled by free cooling from river water.

4.3.4 Loading temperature

The intended loading temperature of district cooling system is below 7 °C. Loading temperatures from 1 to 7 °C will be investigated in the model. It will be simplified by modelling as the maximum power output of the tank. Under constant flow, for a low loading temperature down to 1 °C, the power output is higher due to higher temperature difference for the same amount of volume flow.

Referring to this, it is desirable to go as low as possible achieving 1 °C, but the investigation will demonstrate if this is possible and will also demonstrate how much is possible for the loading temperature to go low before mixing happening within a certain time constrain.

4.3.5 Energy costs

The electricity price implemented in the model is based on the prediction of the year 2040. The future average electricity price prediction will be modeled based on a suggestion from Göteborg Energi. The future predicted average electricity price is expected to increase around 6.5 times from 2020 to 2040 (221 SEK/MWh to 1427 SEK/MWh respectively), as per Göteborg Energi's average electricity price suggestion and the historical average electricity price in 2020 as per Nordpool. The hourly electricity profile for year 2020 from Nordpool is taken and multiplied by the correction factor to predict the future hourly electricity price pattern in the year 2040.

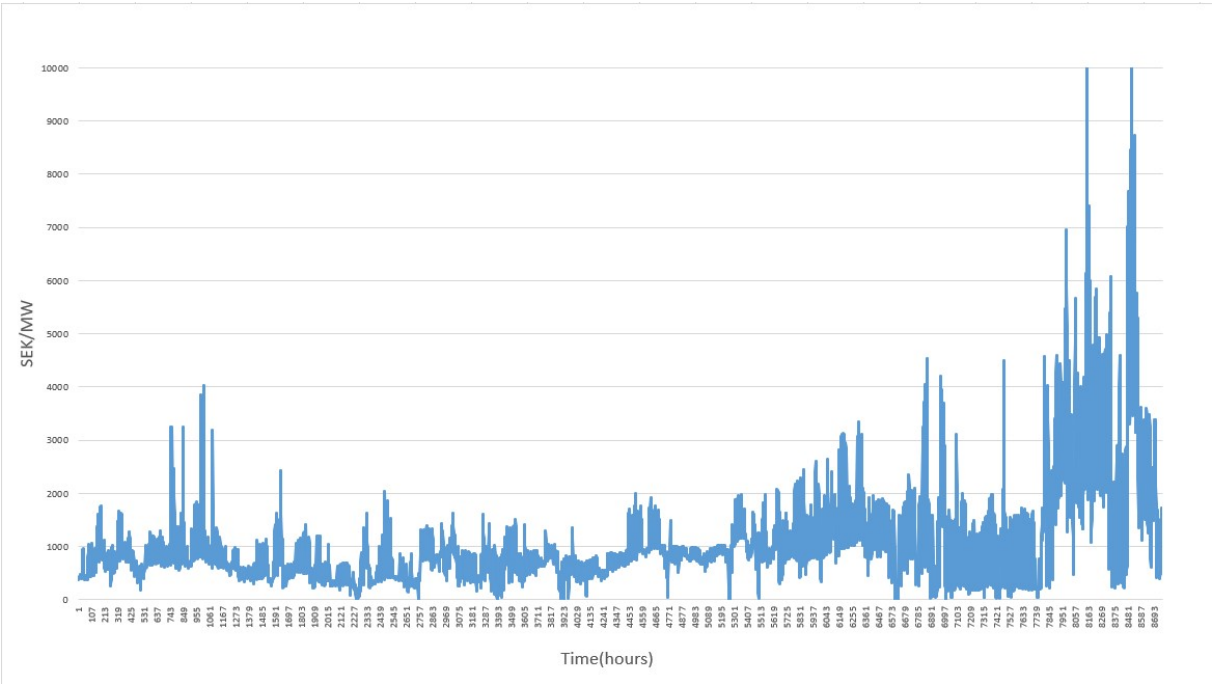

Figure 4.12: Electricity Price Profile in 2040.

4.3.6 Thermal Efficiency and Coefficient of Performance

The thermal efficiency of the cooling thermal energy storage tank is considered as the ratio of energy output from the tank to the energy input to the tank during one charging and discharging cycle. For a well-designed tank, the daily energy loss is about 1% [31]. However, due to the presence of a thermocline layer, a layer with a large temperature gradient will reduce the amount of cooling energy available. The efficiency of thermal storage thus will be affected. Equation 4.6, 4.7 and 4.8 explains efficiency of storage tank.

$$\eta_{ch} = \frac{E_{In} - E_{Out}}{E_{In}} \times 100\% \tag{4.6}$$

$$\eta_{dis} = \frac{E_{Out} - E_{In}}{E_{St}} \times 100\% \tag{4.7}$$

$$\eta_{st} = \eta_{ch} \times \eta_{dis} \tag{4.8}$$

The value will be taken from the result of computational fluid dynamics modelling. The coefficient of performance of chiller is calculated as follows:

$$COP = \frac{E_{Out}}{W} \tag{4.9}$$

Here η_{ch} and η_{dis} refer to the charging and discharging efficiency respectively. E_{In} and E_{Out} refer to the energy input and energy output respectively. E_{St} refers to the Energy stored. η_{st} refers to the storage efficiency. W refers to the work input.

The COP of centrifugal compressor chiller varies depending on the percentage of cooling load. Figure 4.13 shows the relation between cooling load and coefficient of performance. The range of COP varies between 2.2 and 9.4 depending on the lading and reaches its maximum when the loading is at around 60%.

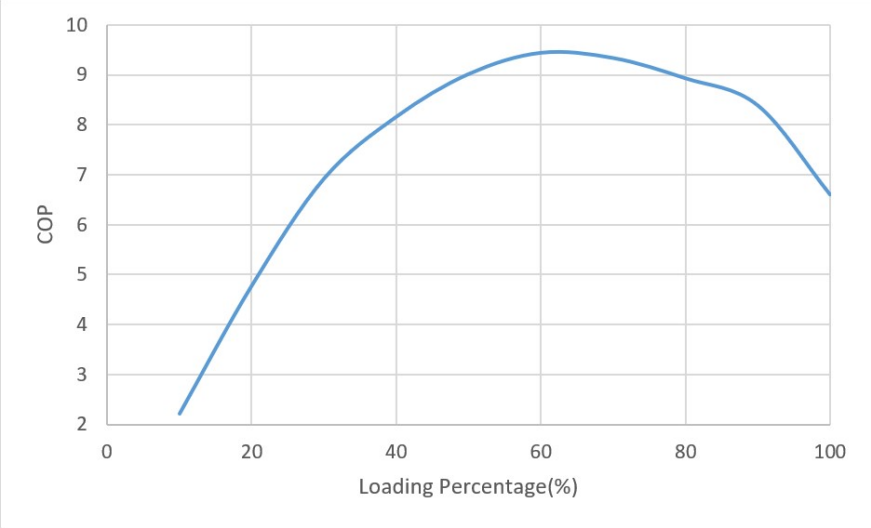

Figure 4.13: Coefficient of performance against cooling load of centrifugal compressor chiller.

In a linear optimization model, the relationship between the load of the chiller and the COP should be a linear relation, but as has been seen in the figure above, the relation is non-linear and can not be presented in the model program. To avoid this issue and as the COP will be used to compute the chillers' operating expenses, the SEER (seasonal energy efficiency ratio) with a constant value will be assigned and used as the final value for COP. Equation 4.10 is used to calculate the ESEER [41]:

$$\begin{aligned} SEER = COP_{100\%} \times WC_{100\%} + COP_{75\%} \times WC_{75\%} + COP_{50\%} \times WC_{50\%} \\ + COP_{25\%} \times WC_{25\%} \end{aligned} \tag{4.10}$$

Where 100%, 75%, 50% 25% are the various load ratio % of the chillers WC present the Weighting Coefficient for that load and it is 3%, 33%, 41%, and 23% respectively

for each load ratio. from the equation and the graph of the COP curve above, the ESEER have a value of 8, however in our model we look at the overall COP for the plant, taking into consideration the cooling tower and the pumps. Therefore, for modelling, a constant value of 5 will be chosen for the COP as an input for production plants using compression chillers, the same was confirmed with Göteborg Energi. And since the chillers will operate for the entire year then the level of inaccuracy of the results due to the use of constant COP can be treated as insignificant.

On the other hand, the absorption chillers have constant COP irrespective to the load on the chiller and the energy input includes waste heat from industries and electricity used by pump work. As the waste heat is assumed to be for free and sufficient, the only work input we considered in the equation is electricity. Therefore, a COP value of 20 is considered for the overall production plant using absorption chillers in the optimization modelling.

4.3.7 Modelling Scenarios

In this study, several cases have been investigated to decide what would be the optimum scenario of cost optimization for the new cooling production plant and TES in the year 2040 within the district cooling network. The main two scenarios are a new cooling absorption chillers production plant with TES and a new cooling compression chillers production plant with TES. Each scenario of those will be divided into sub-scenarios based on the ability to achieve different discharge temperatures, from 1°C to 7°C, and what would be the lowest temperature possible for achieving the study purpose.

Figure 4.14 below demonstrate the different scenarios that will be further investigated in the next chapter.

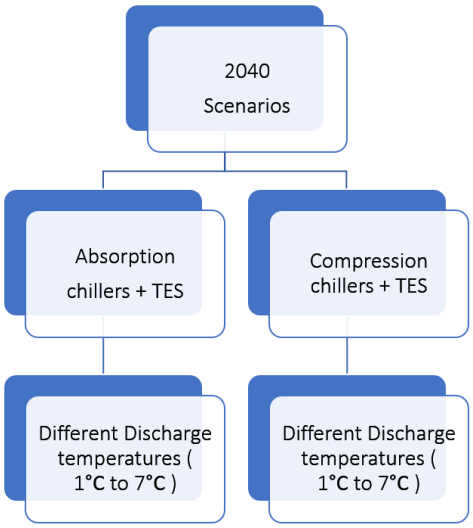

Figure 4.14: New cooling production plant scenarios in year 2040

(A) **Scenario 1: New cooling production compression chillers cooling plant and TES**
The main aim of this scenario is to identify if considering the installation of compression chillers for the new cooling production plant in Spårvagnsdepån would be the optimum solution with the use of TES and what would be the optimum capacity for the plant and the required volume of TES.

Sub-scenarios: different discharge temperature (1°C to 7°C)
For modeling, seven sub-scenarios will be considered for the first scenario, the main difference between the sub-scenarios is considering a constant maximum flow rate for all scenarios while changing the discharge temperature from 1°C to 7°C. Several other parameters have been taken into the model but remained the same for all sub-scenarios. These parameters are the TES efficiency of 0.95, existing compression chillers COP as 5, the new cooling production plant COP as 5 (considering the new plant using compression chillers), the available existing chillers capacity in the district cooling network is 116 MW, the investment cost of the new cooling production plant is 7.608 MSEK per MW, the investment cost of TES is as shown in the table below. In addition, the annuity factor (af) is 0.05, the electricity prices are SEK per hour, and the maintenance cost for the new and old cooling production plants is 2.7 SEK per KW per year.

Table 4.6 below summaries the difference between each sub-scenario in scenario 1.

Table 4.6: Scenario 1: general data input

Scenario 1							
Discharge Temperature (°C)	1	2	3	4	5	6	7
TES capacity (MW)	43.33	40	36.67	33.33	30	26.67	23.33
TES efficiency	0.95						
Existing compression chillers, COP	5						
Existing absorption chillers, COP	20						
New compression chillers, COP	5						
Existing available chillers capacity in the district cooling network (MW)	116						
New cooling production plant investment cost (MSEK/ MW)	7.608						
TES investment cost (MSEK/ MWh)	0.18	0.19	0.21	0.22	0.24	0.26	0.28
Annuity Factor	0.05						
Existing cooling production plant maintenance cost (SEK/ KW)	2.7						
New cooling production plant Maintenance cost (SEK/ KW)	2.7						

(B) **Scenario 2: New cooling production absorption chillers plant and TES**

Similar to scenario one, the objective is to identify if the installation of absorption chillers with TES would achieve the study purpose. In addition, to what would be the optimum capacity of the plant, and the volume required by the TES.

Sub-scenarios: different discharge temperature (1°C to 7°C)

For modeling, seven sub-scenarios will be considered for the second scenario, the sub-scenarios are similar to the first scenario, however, some parameters will have different values such as the new cooling production plant COP (considering the new plant using absorption chillers), the investment cost of the new cooling absorption chillers plant and the maintenance cost for the new cooling plant.

Table 4.7 below summaries the difference between each sub-scenario in scenario 2.

Table 4.7: Scenario 2: general data input

Scenario 1								
Discharge Temperature (°C)	1	2	3	4	5	6	7	
TES capacity (MW)	43.33	40	36.67	33.33	30	26.67	23.33	
TES efficiency	0.95							
Existing compression chillers, COP	5							
Existing absorption chillers, COP	20							
New absorption chillers, COP	20							
Existing available chillers capacity in the district cooling network (MW)	116							
New cooling production plant investment cost (MSEK/ MW)	9,510							
TES investment cost (MSEK/ MWh)	0.18	0.19	0.21	0.22	0.24	0.26	0.28	
Annuity Factor	0.05							
Existing cooling production plant maintenance cost (SEK/ KW)	2.7							
New cooling production plant Maintenance cost (SEK/ KW)	4.6							

4.3.8 Investment Dispatch Model Formulation

The aim of the model is to find out the optimized investment capacity of the new chillers and the thermal energy storage tank. The model outputs the energy dispatch pattern, the operation of chillers and the thermal storage tank, and the optimized investment capacity of new technologies. The model comprises an objective function, an energy balance equation and several constraints. This part will explain the formulation of all the equation input into the Python model.

Objective function: The objective function is to minimize annual cost of the district cooling system. The equation comprises annual operational costs and annualised investment cost. The optimization function is shown in equation 4.11.

$$Min(\sum_{t=1}^{8760}[Q_{com}(t)/COP_{com} \times e_{price}(t)] + [Q_{new}(t)/COP_{new} \times e_{price}(t)]$$

$$+ [\text{inv}_{Q_{new}} \times P_{Q_new} \times af] + [inv_{TES_{new}} \times C_{TES_{new}} \times af]) \tag{4.11}$$

Where Q_{com} and Q_{new} represents the cooling load generated by all the existing compressors chillers and the new chilling units, in MWh/hr; COP_{com} and COP_{new} represents COP of compressors and new chillers (compression or absorption) respectively; e_{price} represents the electricity price SEK/MWh; $inv_{Q_{new}}$ and $inv_{TES_{new}}$ represent the investment costs of new chilling unit and thermal storage tank respectively, in SEK/MW hr and SEK/MWh hr respectively. P_{Q_new} and $C_{TES_{new}}$ represent the invested capacity of the new chiller and the cooling thermal energy storage tank, in MW and MWh, respectively.

The objective function has an hourly resolution, all the operations are based on an hourly basis. The annual cost thus is the summation of all the hours throughout the year.

Energy Balance: The energy balance constraint is implemented to ensure the cooling supply and demand is always met, as expressed in equation 4.12.

$$Q_{com}(t) + Q_{new}(t) + Q_{discharge}(t) = Q_{demand}(t) + Q_{charge}(t), \quad \forall t \in \mathcal{T} \tag{4.12}$$

where Q_{charge} and $Q_{discharge}$ represent the cooling load charged and discharged from the tank, in MWh, respectively. The left hand side of the equation represents total cooling energy supply to the system, including energy generation from the existing compressors(Q_{com}), new chillers(Q_{new}) and energy discharge from the tank($Q_{discharge}$). The right hand side of the equation represents the total cooling energy demand, including cooling demand from the consumers(Q_{demand}) and cooling energy charging to the tank(Q_{charge}).

Constraints: Constraints for the generation units and the cooling thermal energy storage tank are presented below.

(**A**) The charging and discharging condition of the thermal energy storage tank is limited to the state of charge (SOC). This represents the energy storage level of the tank at each time step, as shown in equations 4.13 and 4.14 .

$$SOC_{TES}(t) = SOC_{TES}(t-1) + Q_{charge}(t) - Q_{discharge}(t), \quad \forall t \in \mathcal{T} \tag{4.13}$$

$$SOC_{tes,min} \leq SOC_{tes}(t) \leq C_{tes_{new}}, \quad \forall t \in \mathcal{T} \tag{4.14}$$

Where the state of charge (SOC_{tes}) represents its energy level of the tank, Q_{charge} and $Q_{discharge}$ represent the amount of cooling energy being charged and discharged at specific time step t. The time step (t-1) represents the previous time step.

Equation 4.14 limits the range of storage of the tank. $SOC_{tes,min}$ represents the minimum state of charge in the tank. $C_{tes_{new}}$ represents the invested capacity of the tank, which represents the maximum storage level of the tank.

(**B**) The amount of energy can be charged and discharged is limited by the maximum power that can be drawn and supplied from and to the thermal energy storage tank, as shown in equations 4.15 and 4.16.

$$0 \leq Q_{charge}(t) \leq Qtes, \quad \forall t \in \mathcal{T} \tag{4.15}$$

$$0 \leq Q_{discharge}(t) \leq Qtes, \quad \forall t \in \mathcal{T} \tag{4.16}$$

Where $Qtes$ refers to the maximum charging and discharging power of the tank.

(**C**) The cooling energy generation from the chillers is limited by the power rating of them, as shown in the equations 4.17 and 4.18.

$$0 \leq Q_{com}(t) \leq Pcom, \quad \forall t \in \mathcal{T} \tag{4.17}$$

$$0 \leq Q_{new}(t) \leq P_{new}, \quad \forall t \in \mathcal{T} \tag{4.18}$$

Where P_{com} and P_{new} represent the power rating of the existing compressors chillers and the new chillers (compression or absorption) respectively.

4.4 Sensitivity Analysis Scenarios

The results output from the modeling scenarios depends on several set of inputs (parameters and assumptions which was made), and due to the uncertainty of the assumptions used, the outcome of the results might have significant impact if the assumptions input changed. Therefore, the impact of the assumptions on the outcomes will be examined in this chapter, analyzing the importance and dependency of input parameter to the results and a sensitivity analysis will be carried out accordingly.

4.4.1 Electricity price

The impact of future electricity prices on the optimization output will be tested. The future electricity prices in the year 2040 were reflected originally based on the electricity prices of the year 2020, to be also consistent with the historical data chosen for the cooling demand. However, there were several occasions such as the Covid-19 pandemic which make a possibility that this reflection might not be accurate. Therefore, several other years 2021, 2019, 2018, and 2017 were investigated to examine the prediction of the electricity prices in 2040 and see how this will impact the overall results. The historical data of the electricity hourly prices were retrieved and collected from Nordpool website [6], and the predicted average electricity price of 2040 was given from Göteborg Energi. From collecting the data it was noticed that the jump in the electricity prices from the chosen year to the year 2040 varies from 1.62, 4.9, 2.68, 2.38, and 3.62 from the year 2021 to 2017 respectively. which indicates our concern that there is no certain pattern to be followed in predicting the future electricity prices and confirms our choice to choose of doing a sensitivity analysis for the electricity prices.

Table 4.8 below presents the average electricity prices as per Nordpool data, which was used in the sensitivity analysis in combination with the predicted electricity price for the year 2040, 1427 SEK as given by Göteborg Energi. The average electricity prices were used to see how much the hourly electricity prices should expand to achieve an average electricity price of 1427 in the year 2040.

Table 4.8: Yearly average electricity prices as per Nordpool. [6]

Year	2021	2020	2019	2018	2017
Electricty price (SEK)	671.60	221.03	405.49	457.78	300.90

Figure 4.15 presents the historical electricity profile data for different years, 2021, 2020, 2019, 2018, and 2017 as per Nordpool data.

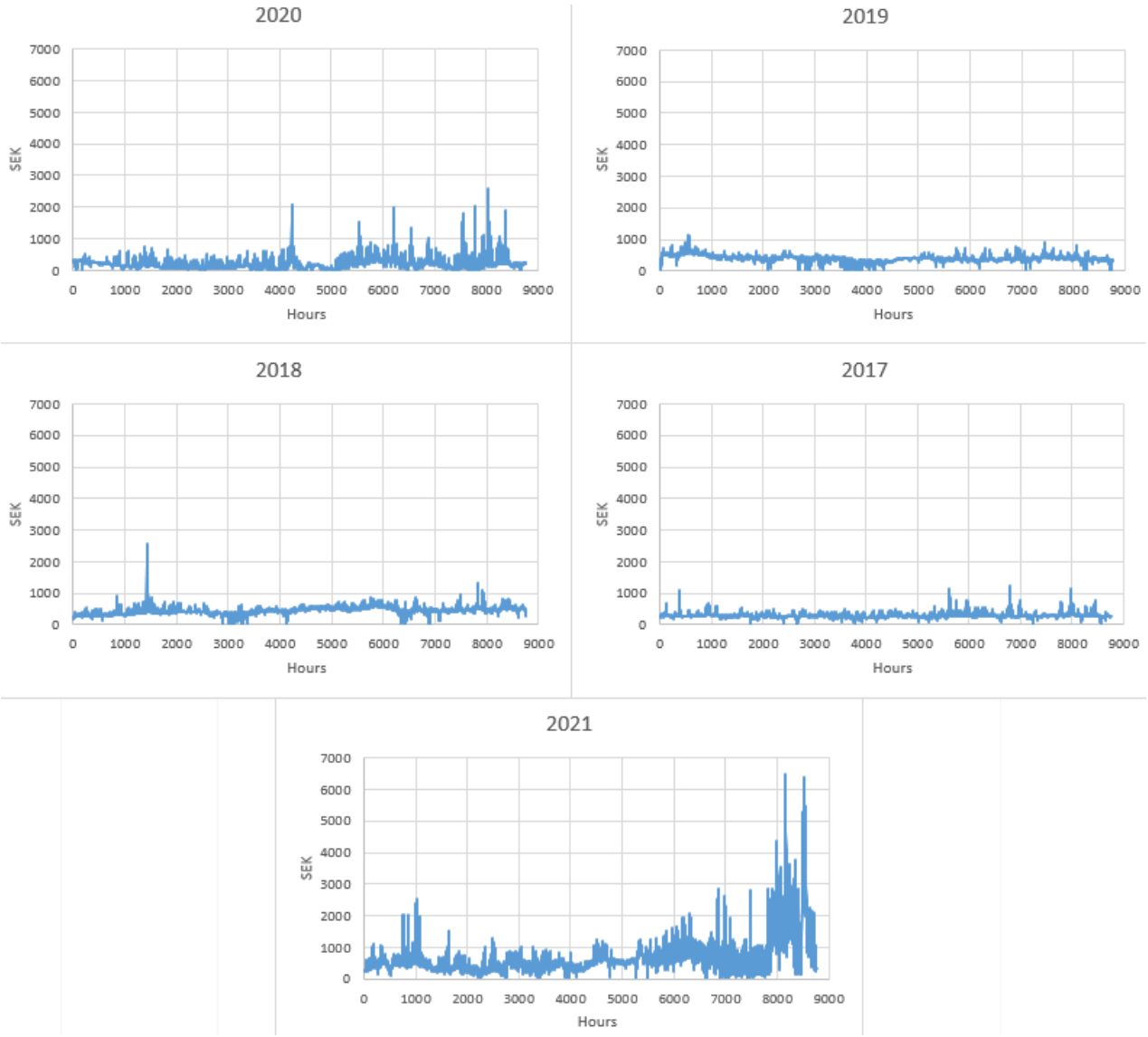

Figure 4.15: Historical electricity prices data *[6]*

4.4.2 Cooling Demand Profile

Similar to the electricity price, historical data for the load profile was used to predict the load profile pattern in the future, the year 2040. The future hourly cooling load demand in the year 2040 was reflected originally based on the hourly cooling load demand of the year 2020, as it is the latest available cooling demand data year. As mentioned in the sensitivity analysis - electricity price section, several uncertainties can be related to the cooling demand in the year 2020. Therefore, investigating additional previous years, and their cooling demand reflection is necessary to examine how the cooling demand would impact the decision of selecting the optimum model.

Figure 4.16 present the historical cooling demand data for different years, 2020, 2019, 2018 and 2017 as given by Göteborg Energi.

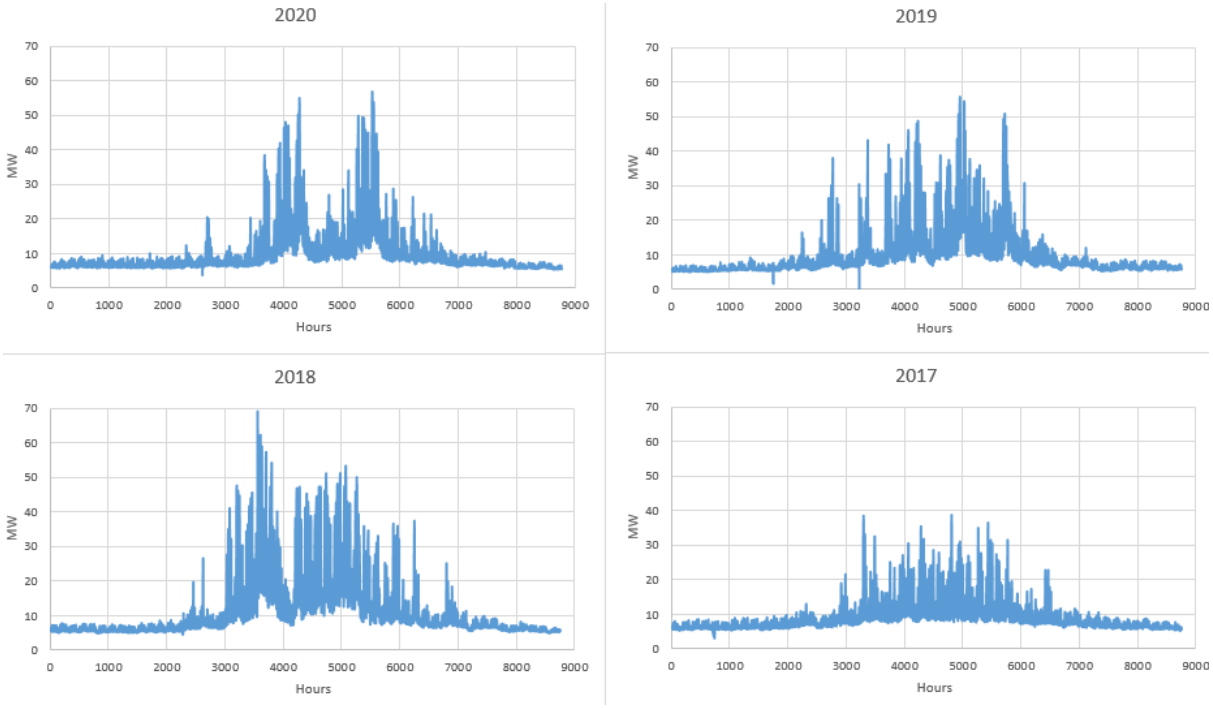

Figure 4.16: Historical cooling demand data

5

Results

5.1 Computational Fluid Dynamics Modelling

This section embodies the outcomes from computational fluid dynamics modelling of cooling thermal energy storage tank. It includes the results from the two modelling scenarios and further observation and analysis from them.

5.1.1 Summary

In two modelling scenarios, charging and discharging operation of 1 °C, 4 °C and 13 °C with several sequences are modelled. Numerous aspects are analysed, including stratification between different temperature zones, development of thermocline layers, propagation of water after diffusing to the tank and storage efficiency. Overall, the result showed that extensive mixing occurs between 1 °C and 4 °C and no clear temperature zone can be established within the cold zone. On the other hand, thermocline layer was established between the return 13 °C and chilled water of 1-4 °C. A clear separation between warm and cold zone enables efficient energy storing by stratification within the tank.

5.1.2 Scenario 1

During the charging of 4 °C from the bottom of the tank, 13 °C warm water will be discharged from the top diffuser concurrently. In the process, a thin layer of thermocline layer is developed from the beginning of charging process. Chilled water at 4 °C and warm water of 13 °C are thus be separated. When more chilled water is charged from the bottom, the thermocline layer became thicker. When charging process of 4 °C finishes, the chilled water replaced 13 °C completely without mixing. The stratification is effective in this process without significant energy loss except for the thermocline layer.

After the tank is filled with 4 °C water, 1 °C water chilled is charged to the tank from the top while 4 °C water is discharged from the bottom. In the process, there is no stratification between 1 °C and 4 °C water and no thermocline is formed between them. Instead, mixing phenomenon happens instantly when 1 °C water is charged to the tank. 1 °C water mixes with 4 °C at the upper part of the tank first, making the upper part colder. The colder water then diffuses to the bottom of the tank

unified the chilled water temperature inside the tank. The resultant chilled water temperature of the tank is around 2 °C. After that, chilled water is discharged from the tank at the bottom while water temperature of 13 °C is returned from the top. During the process, thermocline layer is generated to separate the warm and cold layer.

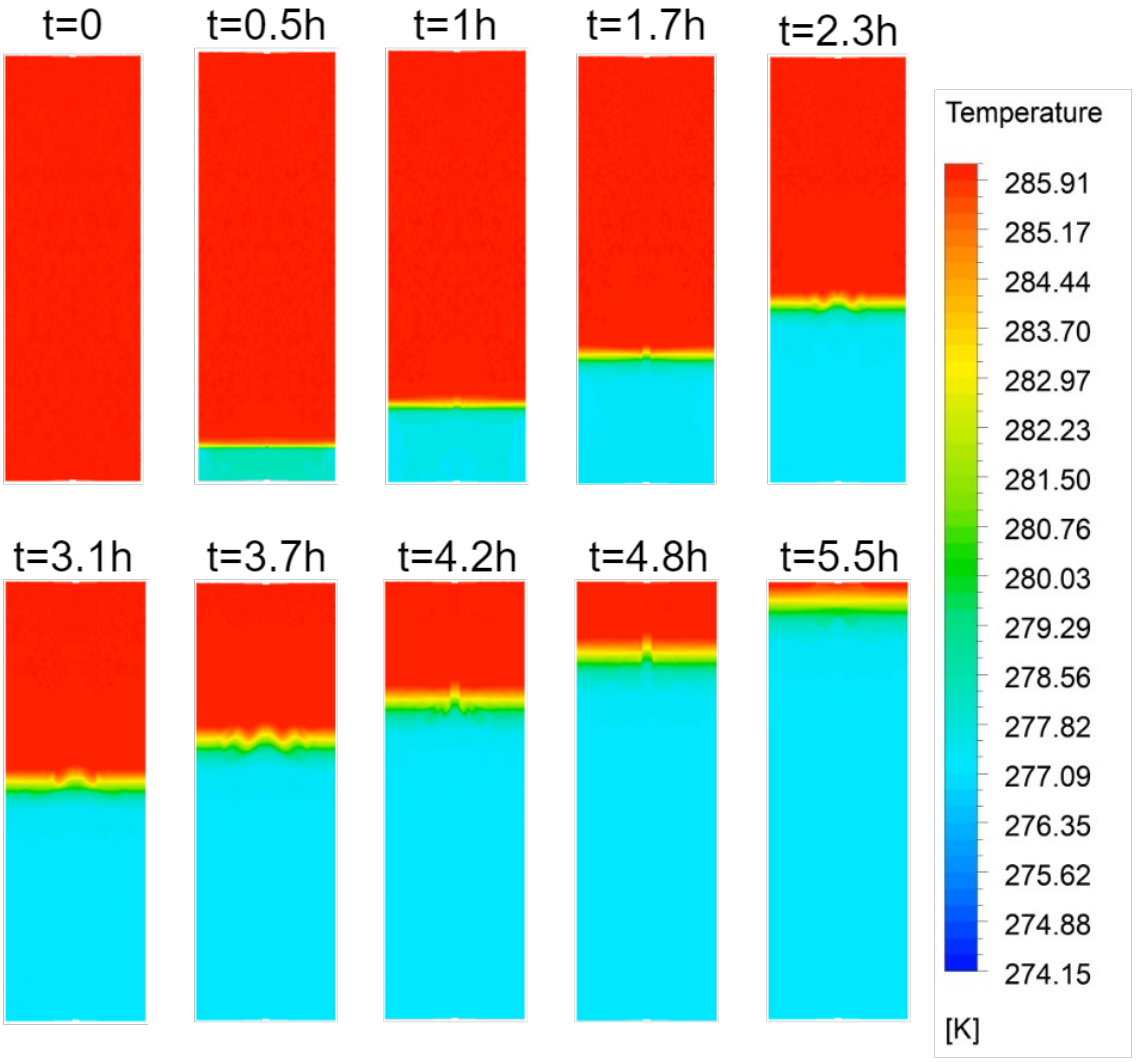

Figure 5.1: Cross-section graphical illustration during charging of 4 °C chilled water at different time steps.

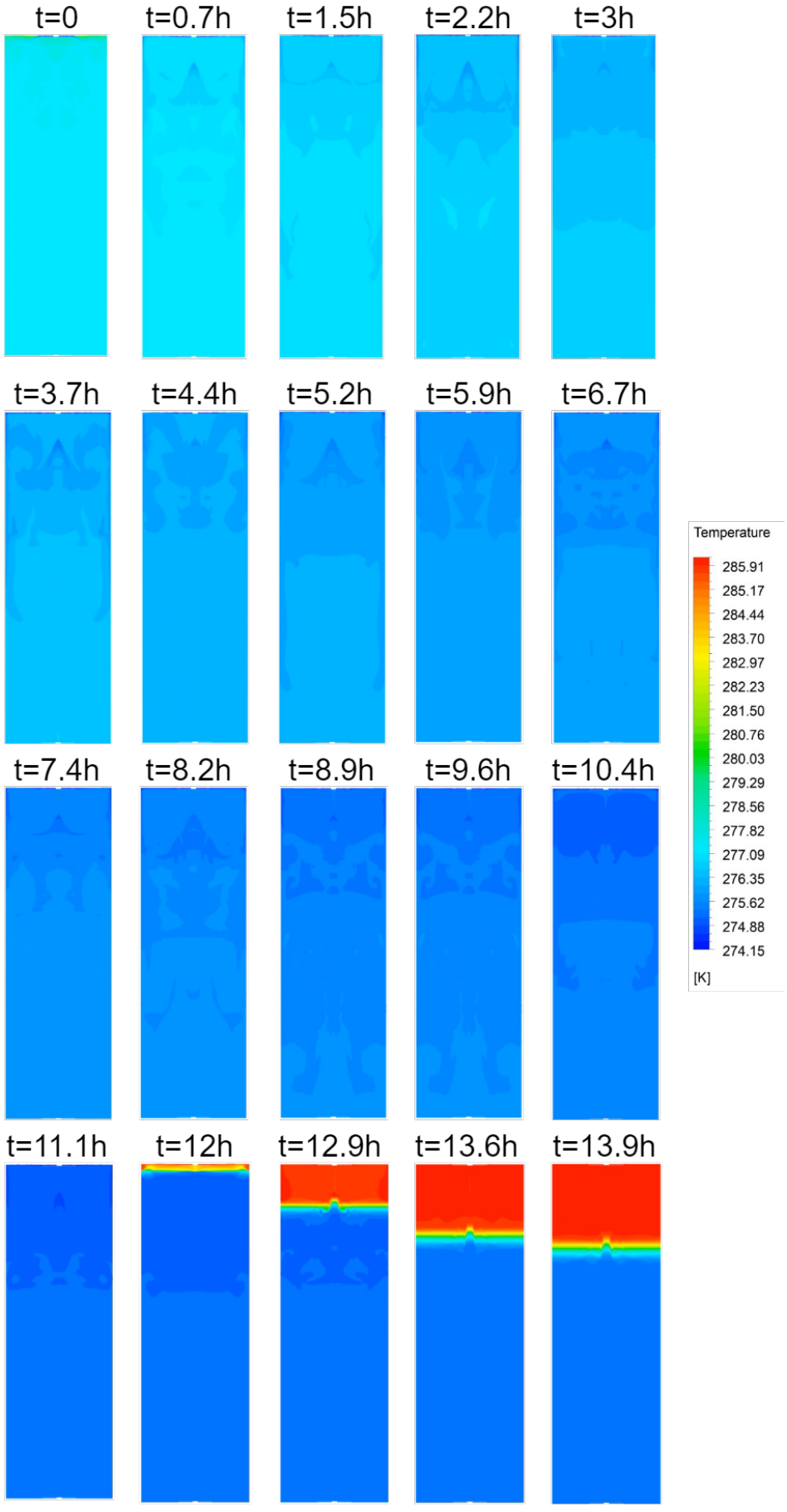

Figure 5.2: Cross-section graphical illustration during charging of 1 °C chilled water and charging of 13 °C return water at different time steps.

5.1.3 Scenario 2

The initial charging of water of 4 °C is the same as scenario A. It corresponds to normal charging operation of water with 4 °C. Subsequently, during charging of tank of 1 °C water to the tank filled with water of 4 °C, it shows similar characteristic with scenario 1. Continuous mixing occurs between them without building up thermocline layer or stratification. The resultant temperature of the tank depends on the volume of chilled water charged to tank. If more water with 1 °C is charged into the tank, the resultant temperature will also be lower due to conservation of energy. A temporary cooler zone was established at the upper part of the tank after chilled water with 1 °C was charged to the tank. The chill water then start to diffuse and mix with the rest of the water inside the tank to form a single gradient temperature zone. However, it should also be noticed that the mixing between 1 °C and 4 °C takes time to achieve a unified temperature within the tank. When 13 °C water is charged from top of the tank, a thermocline layer is formed to separate the warm and cold layer. Only 2 temperature zones are formed instead of 3, with the cold layer of around 3.5 °C and the warm layer of around 13 °C.

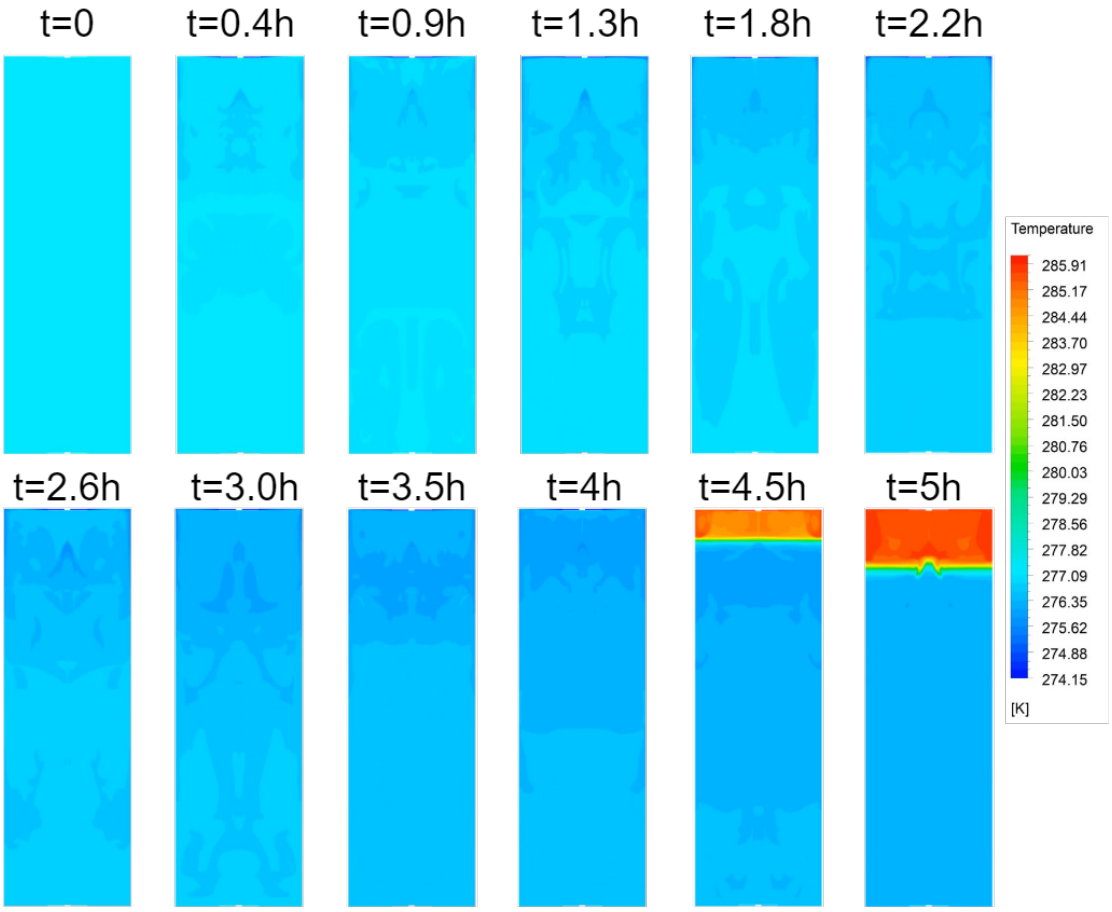

Figure 5.3: Cross-section graphical illustration of Scenario B at different time steps.

5.1.4 Temperature Gradient

A good thermal stratified energy storage tank should have a high value of temperature gradient in the thermocline zone. A high temperature gradient in the zone indicates a weak mixing, also good stratification, between the hot and cold side of water inside the tank [42]. Figure 5.4, 5.5 and 5.6 shows the temperature distribution across the tank's height during different time horizon in charging and discharging cycles of scenario A. Figure 5.4 refers to the charging operation of water of 4 °C from the bottom of the tank. It is observed from the figure that the temperature gradient decreased gradually in the thermocline zone with time from the hour of 1.25 to 4.58, resulting in thicker thermocline layer. The flattened temperature gradient can be explained by the axial thermal conduction of fluid due to temperature difference. Additionally, in the cold water zone, the average temperature dropped with time. Within the vertical distance from 0-10 meters , the average temperature of the chilled water dropped from 4.21 °C to 4.04 °C, a temperature difference of 0.17 °C. It can be explained by the influence of diffuser during charging process. In the initial stage of charging process, there was less chilled water presented in the tank and the thermocline had not developed steadily. Therefore, the mixing of water between the warm and cold zone were more prominent, and the resultant temperature in the cold zone was higher. However, during time, more stable thermocline layer was established and more chilled water is charged to the tank. The distance between the thermocline layer and the inlet diffuser thus increased. Therefore, the influence of the inlet bottom diffuser declined during time and the average temperature of the chilled water in the tank dropped. On the other hand, the temperature on the warm side stayed undisturbed at 13 °C throughout the charging process.

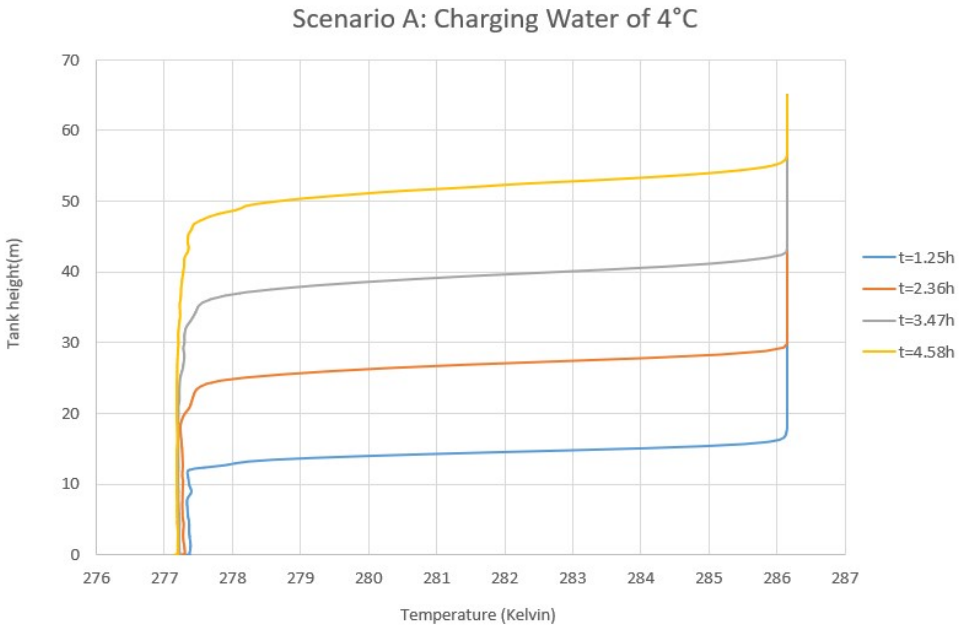

Figure 5.4: Temperature Profile during charging of water of 4 °C of Scenario A.

Figure 5.5 refers to the charging process of water of 1°C from the top of the tank. As shown in the figure, the temperature profile is irregular throughout the charging process. There is no thermocline layer developed throughout the process. Instead, extensive mixing along the vertical axis of the tank. Due to the intensive mixing, when more water of 1 °C was charged to the tank, the average temperature of water dropped gradually with time from 3.57 °C at hour 2.36 to 2.05 °C at hour 12.0.

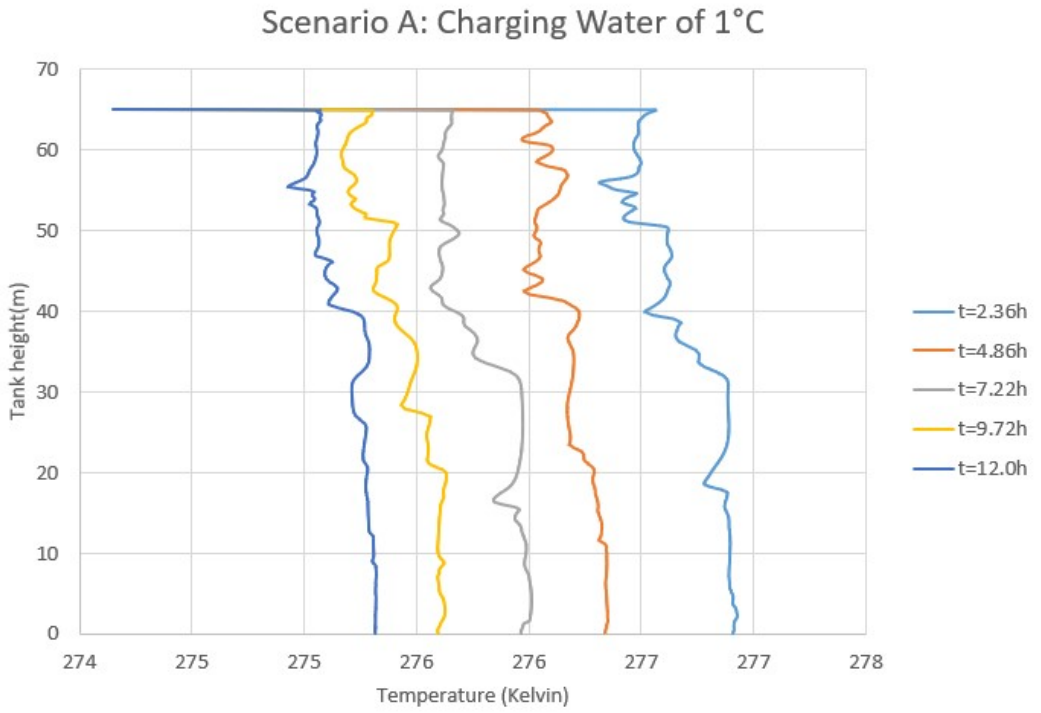

Figure 5.5: Temperature Profile during charging of water of 1 °C of Scenario A.

Figure 5.6 refers to the discharging operation of chilled water and a return water temperature of 13 °C is charged into the tank from the top diffuser. Similar to the charging process of water of 4 °C, the temperature gradient declined with time due to the increased axial heat conduction during the process, creating a thicker thermocline layer. As the water of 13 °is charged from the top of the tank, the diffuser inlet influenced the water temperature of the warm zone in the initial stage, resembling the charging process. After the thermocline was established and moved further away from the diffuser inlet, the temperature of the warm zone increased to the water return temperature of 13 °C.

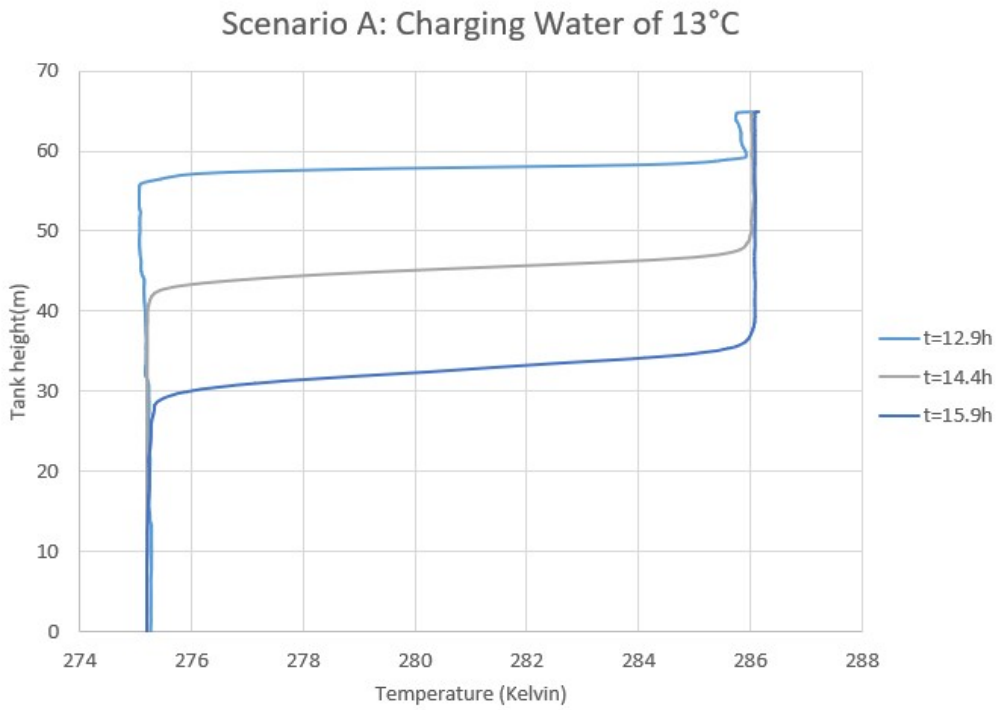

Figure 5.6: Temperature Profile during charging of water of 13 °C of Scenario A.

Figure 5.7 and 5.8 below shows the temperature distribution across the tank's height during different time horizon in charging and discharging cycles of scenario B. Figure 5.7 refers to the charging operation of water of 1°C from the top of the tank. Similar to scenario A, extensive mixing is seen between water of 1 °C and 4 °C in the charging process with no development of thermocline layer. The colder water at the top of the tank diffused and mixing with the warmer water at the bottom. Heat transfer is mainly by means of convection until attain a uniform temperature throughout the tank.

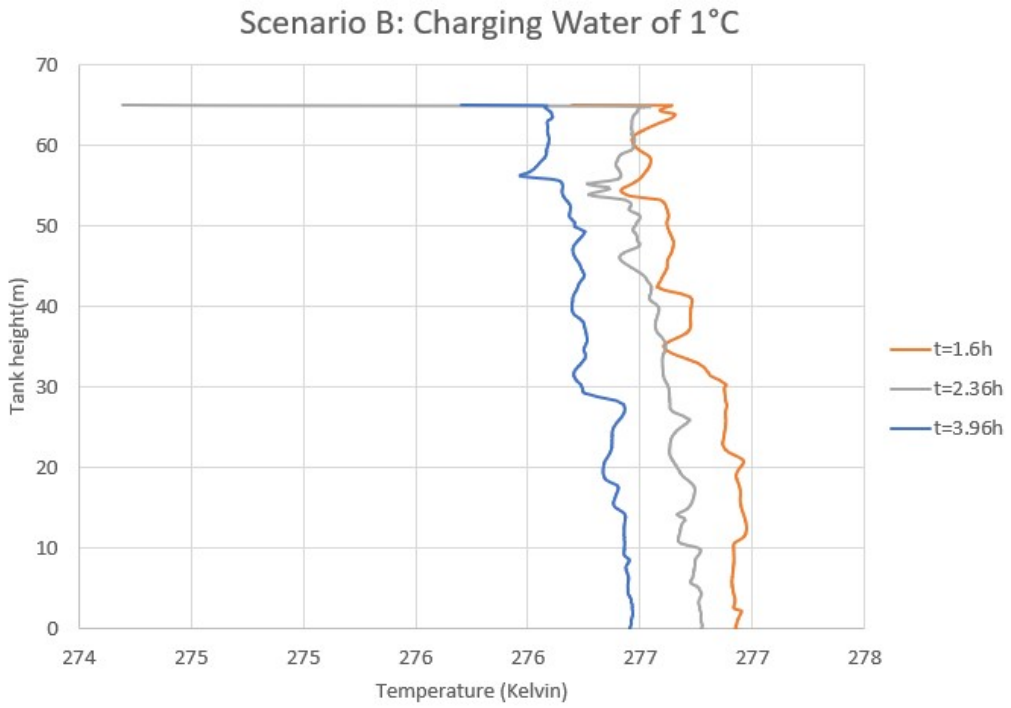

Figure 5.7: Temperature Profile during charging of water of 1 °C of Scenario B.

Figure 5.8 the discharging operation of chilled water and a return water temperature of 13 °C is charged into the tank from the top diffuser. As shown in the figure, the cold zone has a unified temperature of around 3 °C after the mixing during charging process. A steady thermocline was formed between warm and cold zone. Temperature gradient declined and thermocline thickness increased with time, similar to the scenario A.

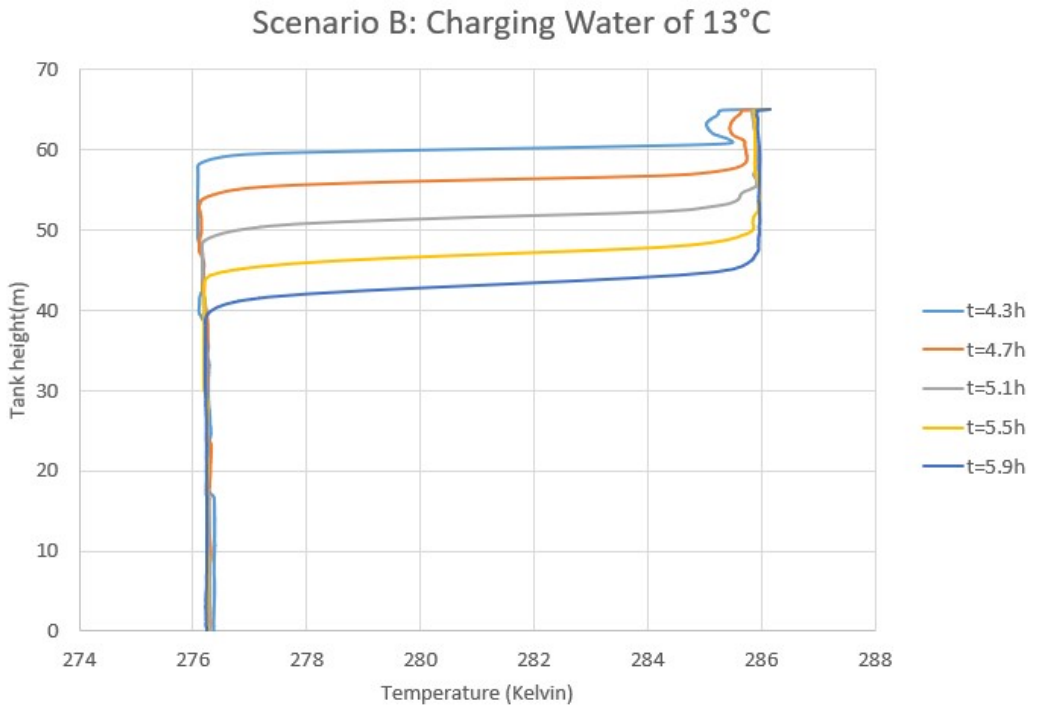

Figure 5.8: Temperature Profile during charging of water of 13 °C of Scenario B.

5.1.5 Thermocline Thickness

Thermocline thickness is a performance indicator to understand the stratification efficiency and storage efficiency of the energy storage tank. It can be assessed by dimensionless temperature(Θ) [43], the relation is shown as follows:

$$\Theta(x) = \frac{T(x) - Tc}{Th - Tc} \tag{5.1}$$

which $\Theta(x)$ is the dimensionless temperature at a certain location in the TES; $T(x)$ is the temperature a certain location in the TES; Th is in the inlet charging temperature of water; Tc is the initial temperature of water inside the TES. $Th - Tc$ in the denominator represents the temperature difference between supply and return water in the TES; $(T(x) - Tc)$ represents the temperature difference between a certain point in the TES and the cold side of chilled water in the tank.

The thermocline thickness can be defined by the distance in the TES tank based on

the range of dimensionless temperature(Θ) selected. In this study, $0.15 \leq \Theta \leq 0.85$ is defined as the temperature range of thermocline. The following equation 5.2 is used to calculate thermocline thickness (Δh):

$$\Delta h = Xh - Xc \tag{5.2}$$

which Xh is the distance from the bottom of the tank when $\Theta = 0.85$; Xc is the distance from the bottom of the tank when $\Theta = 0.15$. For example, for a supply and return temperature of 4 °C and 13 °C, the thermocline zone will be the vertical distance between Xc at 5.35 °C and Xh at 11.65 °C.

At the first stage of operation in scenario A, during charging of water of 4°C, it is observed that the thermocline thickness grew during the charging process and attained its maximum when the thermocline layer was close to the top outlet diffuser. It is in line with the study by Waluyo et al. that the flowing stream near the diffuser affects the mixing within the thermocline layer and degraded the stratification [44]. Additionally, heat conduction between the hot and cold side of water increased due to temperature difference. This thus increased the thermocline thickness over time. As shown in figure 5.9, the thermocline thickness increased steady over time from around 2 meters after 1 hour to more than 4 meters after 4.5 hours of charging.

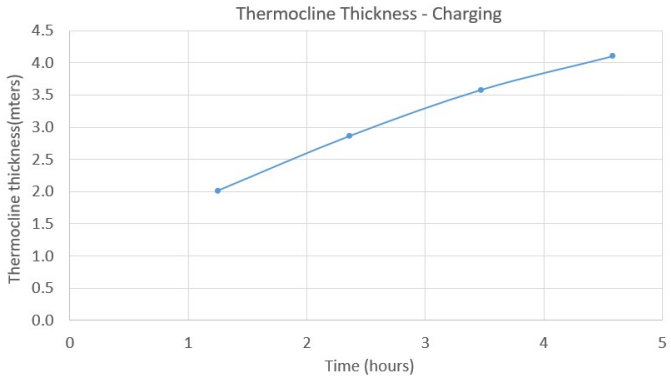

Figure 5.9: Thermocline thickness by time during charging of water of 4 °C of Scenario A.

During the charging of water of 1 °C, there are only mixing with water of 4 °C. No stratification or thermocline layer was developed.

During discharging of cold water, the return 13 °C warm water developed a thermocline with the cold side in a similar way. As shown in figure 5.10, the thermocline grew steadily from 1 meter at 12th hour to 3 meters at 15th hour.

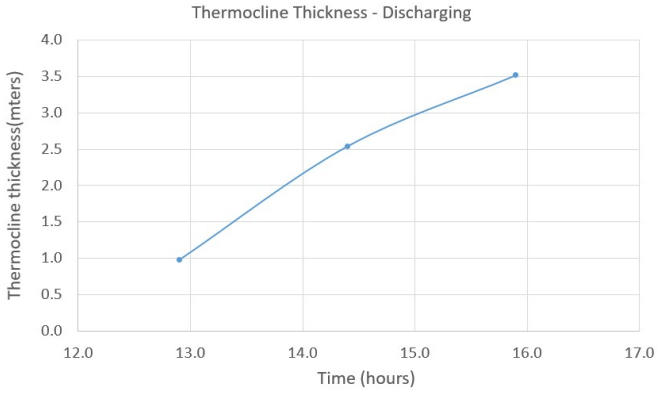

Figure 5.10: Thermocline thickness by time during charging of water of 13 °C of Scenario A.

Similarly, for scenario B, there is no thermocline development during the charging process of water of 1 °C due to the extensive mixing with 4 °C. For the discharging process, during the charging of return water at 13 °C, thermocline developed between the warm and cold zone and thermocline thickness grew over time as seen in figure 5.11.

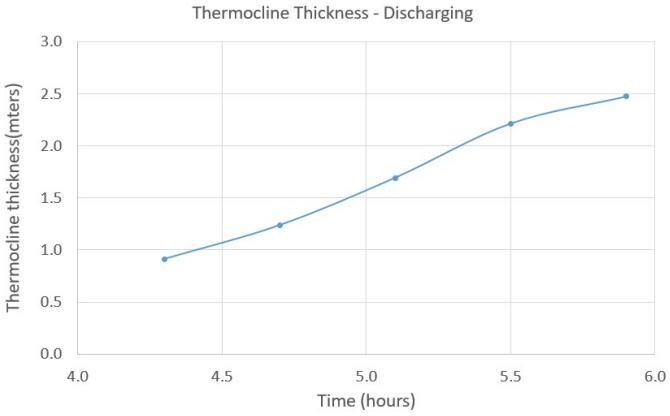

Figure 5.11: Thermocline thickness by time during charging of water of 13 °C of Scenario B.

Efficiency is usually related to the ratio between energy output and energy input, and the energy loss determines its efficiency. Thermal storage efficiency refers to the ratio between the net energy output and net energy input during one cycle of charging and discharging. However, for a decent energy storage tank, the energy loss is around 1 % per day, so it is quite negligible [7]. Thermal efficiency thus is not a good indicator to illustrate the efficiency of the tank, as it does not consider the decline in cooling energy available due to the development of thermocline and the mixing phenomenon between the hot and cold side during storage process. If we consider the loss of available energy due to the formation of thermocline, the thickness of the thermocline at the end of charging water of 4 °C and charging water of 13 °C in scenario A correspond to 6.3% and 5.3% of the total height of the

tank. For scenario B, the thickness of the thermocline at the end of charging water of 13 °C corresponds to 3.8% of the total height of the tank.

5.1.6 Discussion

(A) **Storage Temperature** Due to continuous mixing between 1 °C and 4 °C, storage temperature can be lowered down close to 1 °C if chilled water with 1 °C is constantly charging for a prolonged period of time. However, it will displace existing chilled water in the tank and the displaced water will flow out of the tank to the district cooling network, which may not be desired and realistic. It also takes long time to charge the tank until it reaches a temperature close to 1 °C. For a more practical point of view, the storage temperature should not aim at 1 °C. But instead, lowering water temperature down to 2-3 °C is more realistic to increase the storage capacity of the tank. It can be done by charging chilled water at 1 °C for several hours in the night time to decrease the temperature of water inside the tank.

(B) **Risk of freezing** For charging chilled water near freezing point of 0 °C, there are concerns that freezing of water may occur within the system if the control of temperature in the system is not appropriate. It would have significant destruction on the operation of the system, including obstructing the delivery of water in the pipes, damaging pumps or valves, lowering the storage efficiency etc. This is one of the major concern of existing cooling thermal energy storage system. For storage temperature lower than 4 °C, the existing systems tend to use low temperature fluid which has lower freezing point to prevent any freezing in the system. However, if low temperature fluid is used in this system, a heat exchanger is needed to separate the storage side and the network side, due to the difference in operating medium. The heat exchanger will inflict additional investment cost. Moreover, the heat exchanger imposes a loss of 1-2 °C of delta T due to heat exchange between hot and cold side, in turn, adversely affecting the benefits of low-temperature storage.

(C) **Cooling Operation of Low Temperature Chilled Water** During the charging of water at 1 °C, the return water is first cooled down from 13 °C to 4 °C and store in the tank. Then, water water with 4 °C is discharged from the tank and is mixed with the return water in order increase the temperature to around 8 °C so that the new chiller can operate at a delta temperature of 7-8 °C. The mixed water then cooled down by the new chiller down to 1 °C and charge the tank again from the top. When the process continues, due to mixing, the temperature inside the tank will drop. In order to keep the delta T of the chiller constant, the volume of mixing between chilled water from the tank and the return water is always changing. The flow rate from the tank should decrease and the return water flow rate should increase. Therefore, the control of flow in the tank and the mixing stream are important to optimize the performance of the chiller.

(D) **Stratification Performance** From the literature, there are some decisive parameters that affect the performance of a stratified thermal energy storage tank. They include the water flow rate, diffuser's type and design, tank's

height to diameter aspect ratio, and hot and cold side temperature difference etc [45] [44] [46]. Higher water flow rate has more turbulence influence and increases Reynold's number near the diffuser, and thus increase the thermocline thickness. Diffuser's design affects the direction of flow, flow rate and flow properties, and thus induce mixing between hot and cold side during charging and discharging. Aspect ratio of the tank influences the mixing and the development of thermocline. Moreover, the temperature difference between the hot and cold side of storage affects the thermal diffusion and axial heat conduction between them. A higher temperature difference induces a thicker thermocline, which is in line with the study.

Moreover, in this study, specific parameters are chosen for the study based on information obtained. However, the storage performance can vary by changing design parameters, such as the type of diffuser. Radial parallel-disk diffuser with the same length on the upper and lower disk is chosen for the simulation. It corresponds to the most common type of diffuser for thermal energy storage tank. However, other diffuser types such as slotted-type and octagonal pipe type diffuser will have some differences on storage performance and stratification. The dimension of the diffuser is also an important factors, including the gap between upper and lower disk, cross section area of the disk etc.

5.2 Optimization Modelling

This section embodies the outcome from optimization modeling scenarios for different discharge temperatures of the tank (from 2 °C to 7 °C) with even the use of compression chillers or absorption chillers as the new cooling production plant, in addition to the existing cooling production plants within the cooling network. for that purpose, Python software has been used as the programming language to create the optimization models.

5.2.1 Summary

For the investigation of the results, 12 optimization model has been created, each model represents a different scenario Table 5.1 below present the different scenarios. the section includes the results and a comparison of the different scenarios and further observation and analysis of the output from them, which will be further used to identify which scenario had been able to achieve the lowest annualized cost of the overall cooling system. In addition, to find out what would be the required TES volume and the capacity of the new cooling production plant to achieve the lowest annualized cost.

Table 5.1: Optimization Modeling Scenarios

Scenario name	New cooling production plant type	Discharge Temperature (°C)
Scenario 1-a	Compression Chiller	2
Scenario 1-b		3
Scenario 1-c		4
Scenario 1-d		5
Scenario 1-e		6
Scenario 1-f		7
Scenario 2-a	Absorption Chiller	2
Scenario 2-b		3
Scenario 2-c		4
Scenario 2-d		5
Scenario 2-e		6
Scenario 2-f		7

As observed from the CFD results section, it was not possible to discharge the tank at 1 °C. Therefore, sub-scenarios related to TES discharge temperature at 1 °C has been eliminated and not taken into consideration under this section.

The results are fully presented for one of the optimization scenarios, Scenario 2-a: TES Discharge temperature at 2 °C and absorption chillers as a new cooling production plant, the outcome will include demonstration and observations of the yearly, weekly and daily performance. In addition, a combined result for all sub-scenarios will be presented to compare the outcome of the overall results and to notice the data behaviors when changing the inputs.

5.2.2 Scenario 2-a

Scenario 2a presents the most interesting scenario to look at as it is the one that achieved the cost optimization goal in comparison with the rest eleven scenarios. it became more interesting to look into this scenario in further detail, and how the operational behavior of the TES, new production, and existing production activities during the year. To investigate this, in this section, the data were analyzed from yearly, weekly and daily perspectives. Week 33 and Week 25 were selected as they present the weeks when DUT 100% and DUT 75% occur respectively. And the dates of June 22nd, June 23rd, August 19th and August 17 th were selected to be further analyzed as they present the DUT 50%, DUT 75% and DUT 100%.

The outcomes of this scenario were a TES capacity of 320 MWh, a new cooling production plant using absorption chillers with a capacity of 33 MW, and a total annualized cost of 47.84 MSEK.

(A) **Yearly Case Study, the year of 2040**

i. **Yearly Cooling Demand Profile**
The cooling demand shown in Figure 5.12 below represents the predicted cooling demand in the year 2040 which requires mechanical cooling (Chillers and TES) to fulfill the demand, excluding the cooling demand which can be achieved and cooled by free cooling. As it can be seen, the maximum predicted cooling demand to be achieved at DUT 100% is 163.7 MW in the year 2040 as given by Göteborg Energi. Therefore, the same was ensured in the optimization model and any additional cooling demand above the 163.7 MW was excluded and has not been taken into consideration. This is because only a few hours exceed the cooling demand load at DUT 100%, when enlarging the mechanical cooling system (chillers and TES) are not required to produce cooling for any cooling load above DUT of 100%, above 163.7 MW cooling load.

In addition, it can be noticed that the cooling load during the winter hours can be fully achieved through free cooling from the river, and that the cooling demand required from the mechanical cooling production systems gradually increased during spring and autumn to reach its peak during the summer hours around and between June and August. Two cooling demand peaks were observed around the hour 4,000 and the hour 5500, based on the historical cooling demand data for 2020, which is slightly different from the other historical cooling demand data for the years 2019, 2018, and 2017 when the cooling demand was more fluctuating and have several peaks during the summer hours.

Moreover, it is worth mentioning that there was a minor number of hours when the mechanical cooling production is required to be operated during the winter season, when the cooling demand exceeded the cooling products that can be achieved from the river, or when the river temperature exceeded 15°C.

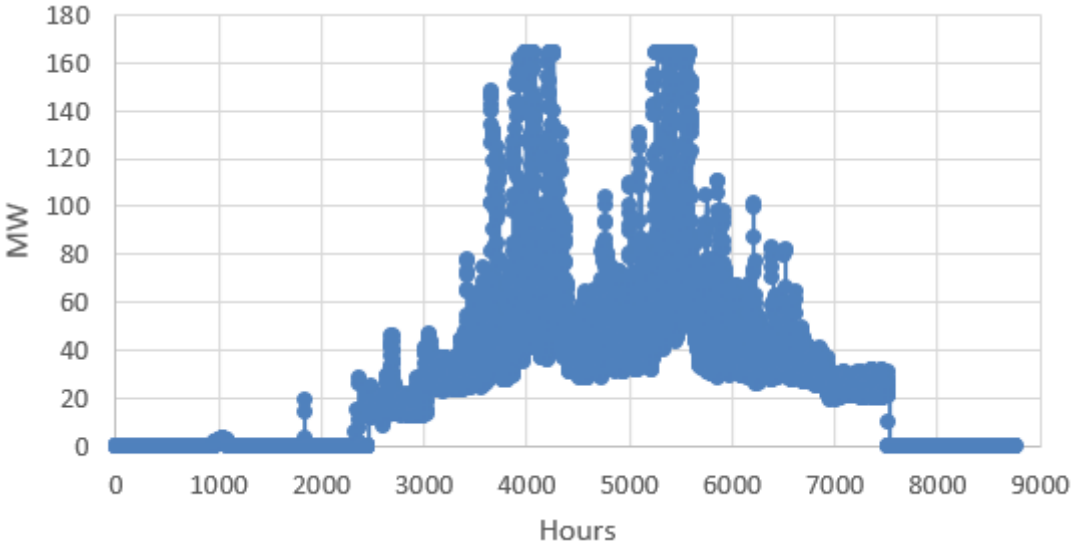

Figure 5.12: Yearly Cooling Demand Profile

ii. **Yearly Electricity Price Profile**
The hourly electricity prices for the year 2040 were based on the historical hourly electricity prices profile for the year 2020, which are as was shown in the methodology section. It had also the lowest average electricity prices compared with the other historical average data, and to predict the hourly electricity profile for the year 2040 and match the average electricity prices. The historical hourly electricity prices data were multiplied with a correction factor based on the difference between the average electricity prices for the year 2020 and the average predicted electricity prices for the year 2040.

Figure 5.13 shows that the electricity prices during the summer hours were similar to the other historical data when it comes to demonstrating that the electricity prices are usually higher during winter hours compared with summer. But it also can be noticed that year 2020 showed more fluctuation in the hourly electricity prices compared with the years 2019, 2018, and 2017. In addition, there were several very high electricity prices jumps during the summer, which has not been seen, in the other historical data. it can be noted that the high electricity prices during the summer have played an important factor in deciding the system capacity and the total annualized cost.

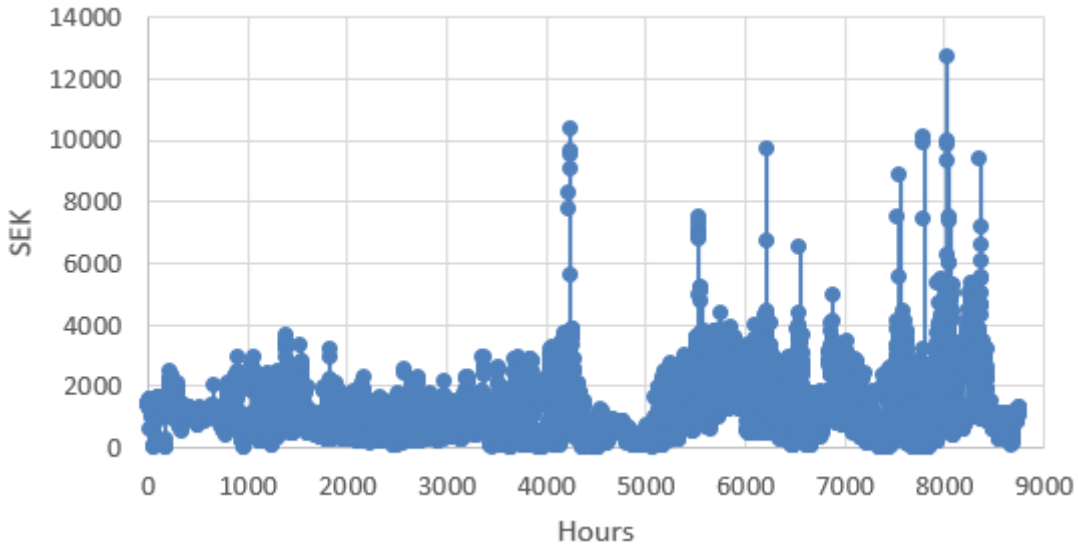

Figure 5.13: Yearly Electricity Price Profile

iii. **Yearly TES State Of Charge Profile**
Figure 5.14 can clearly show that it is always beneficial to use the TES throughout the year when mechanical production is required for operation, and this benefit can be maximized if the electricity prices and the cooling demand can be predicted by every hour, and the more precise data was predicted and collected the more the system can become beneficial. It can be observed that the TES was always prioritized to be fully charged and discharged continuously, as the cooling load requires during the year, especially during spring, autumn, and summer when the mechanical cooling production becomes required (around and between the hours 2500 and 7500, where the TES was generally charged with it full capacity).

The advantage of TES that it can use the cooling production plants to charge the TES when the electricity prices are low during the day. To be later discharged its capacity when the electricity prices are high during the peak cooling demand hours, which will help eventually reduce the operational cost due to the prices of electricity.

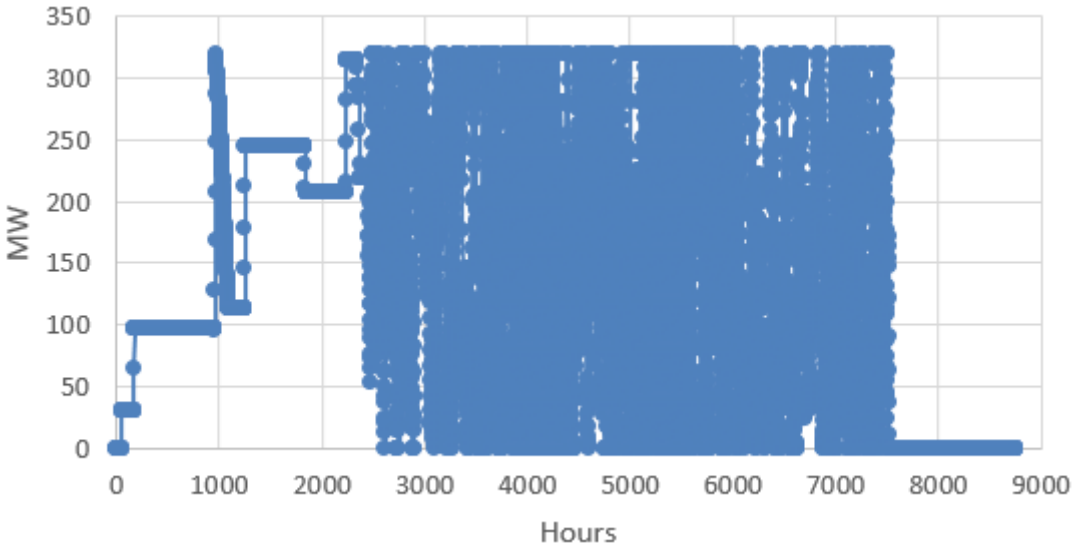

Figure 5.14: Yearly TES State Of Charge Profile

iv. **Yearly TES Charge and Discharge Profile**
Figure 5.15 shows the pattern of charging and discharging all over the year, it can be noticed that the TES was maximized its potential mainly during the summer, especially around and between hours 3500 and 7500, the rest of the year the TES was also used as max but as per the requirements of the cooling demand.

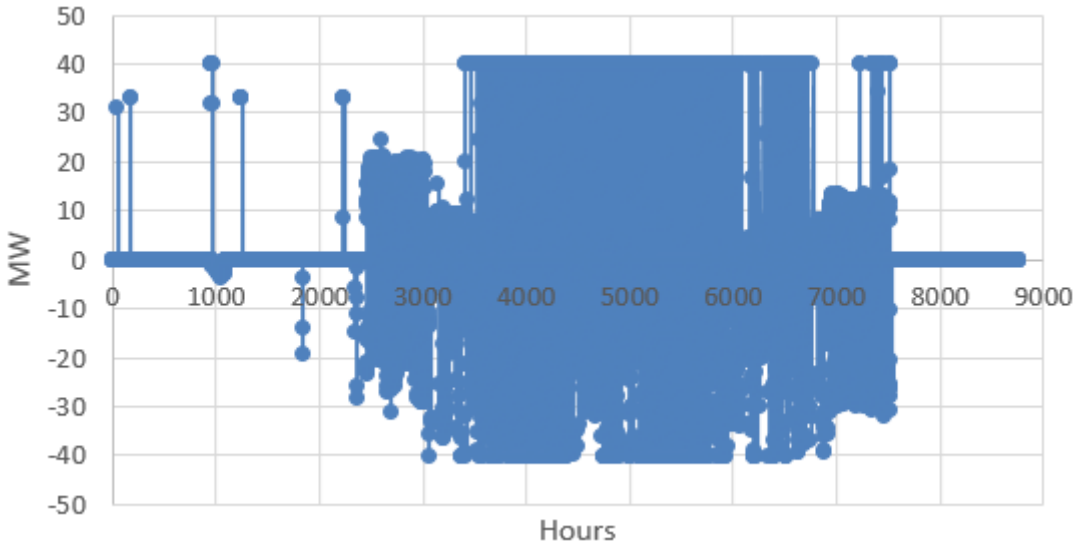

Figure 5.15: Yearly TES Charge and Discharge Profile

v. **Yearly Existing Cooling Production plant Profile**
Figure 5.16 represents the existing cooling production during the year 2040. It can be noticed that the full capacity of 116 MW was fully utilized during the peak cooling demand hours. However, when the cooling demand has not reached its maximum of 163.7 MW, the priority was to utilize the use of TES and the new cooling production plant (in this case as they were absorption chillers), as this will be presented in the next graphs.

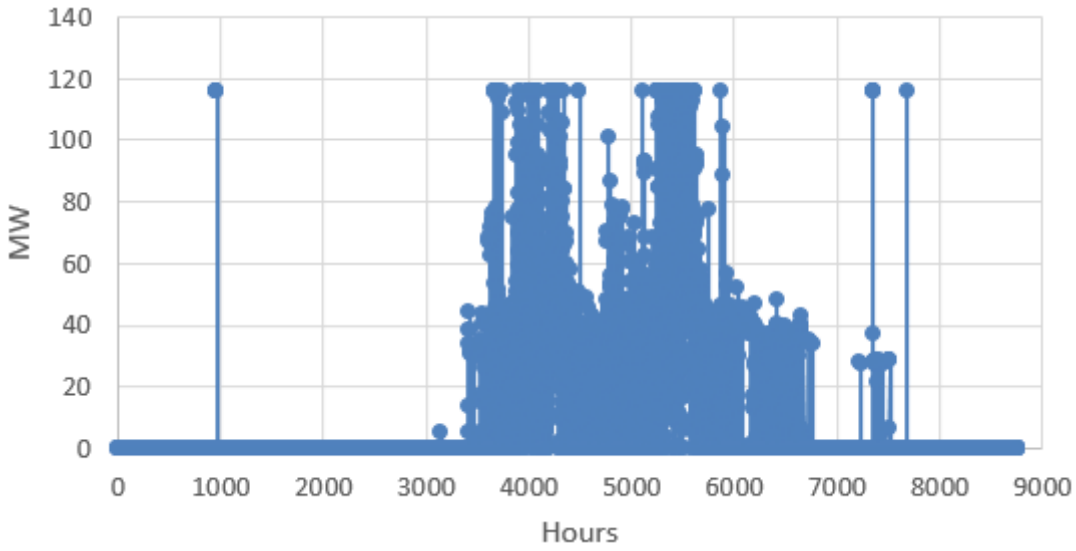

Figure 5.16: Yearly Existing Cooling Production Profile

vi. **Yearly New Cooling Production Plant Profile**
The priority of using the new cooling production plant is to charge the TES and/or fulfill the cooling demand first, before the use of the existing cooling production plants is because the new cooling production plant use absorption chillers with higher COP compared with the existing cooling production plant that uses compression chillers with lower COP. Meaning more consumption of electricity would be required if the existing plant is used first.

Figure 5.17 shows how the new cooling production plant has been utilized to charge the TES and achieve the cooling demand. In addition, it can be noticed that there were certain hours where the plant was not required to operate during the summer season, this is due to that the cooling demand has been covered using the TES mainly or maybe the existing cooling production, whichever would make the system running cost cheaper in overall.

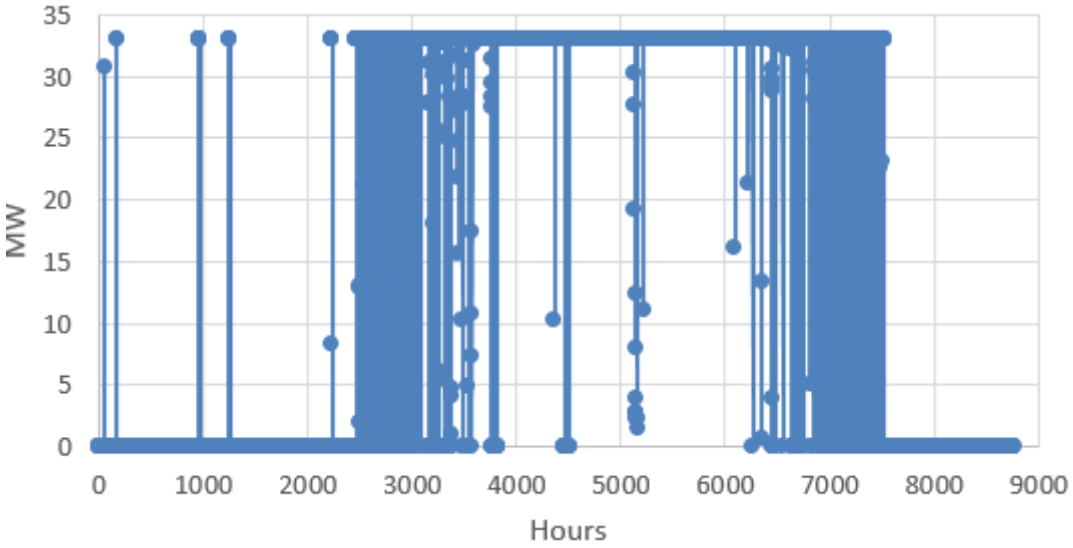

Figure 5.17: Yearly New Cooling Production Profile

vii. **Yearly TES Discharge Profile**
Figure 5.18 shows separately how the TES discharging was utilized to achieve the requirement of the cooling demand.

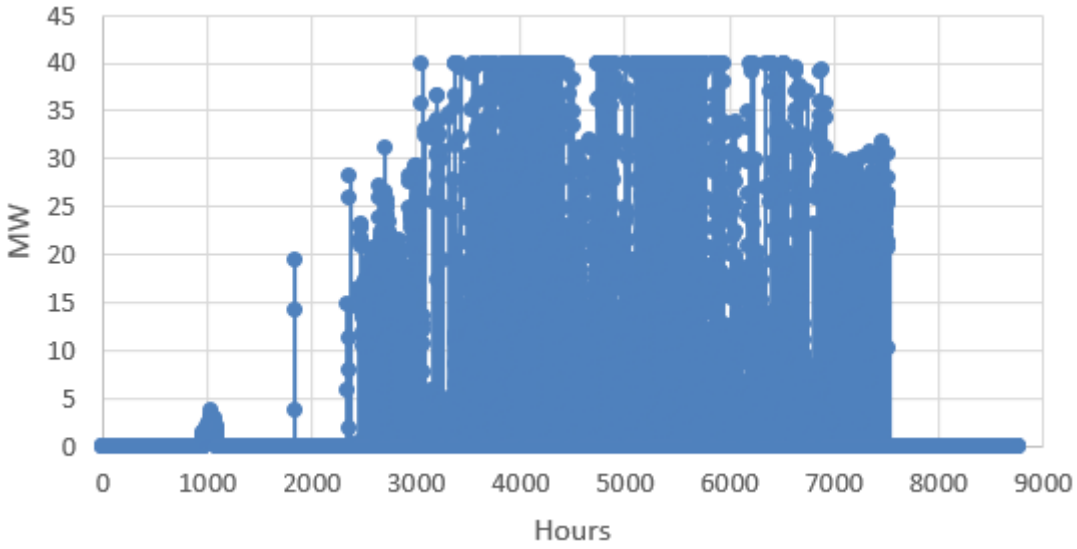

Figure 5.18: Yearly TES Discharge Profile

(B) **Week 33 (15 Aug - 21 Aug, 2040) Case Study**
Week 33, in the year of 2040 represents the week where DUT 100% and above will occur in the year 2040.

i. **Week 33 Cooling Demand Profile**
It can be noticed in Figure 5.19 that the cooling demand has exceeded 163.7 MW over 3 days and reached the DUT 100% on the 19th of August. In addition, the figure shows that the cooling demand pattern is consistent when the peak load for each day happens during the daytime hours and the low load hours happens during the night hours.

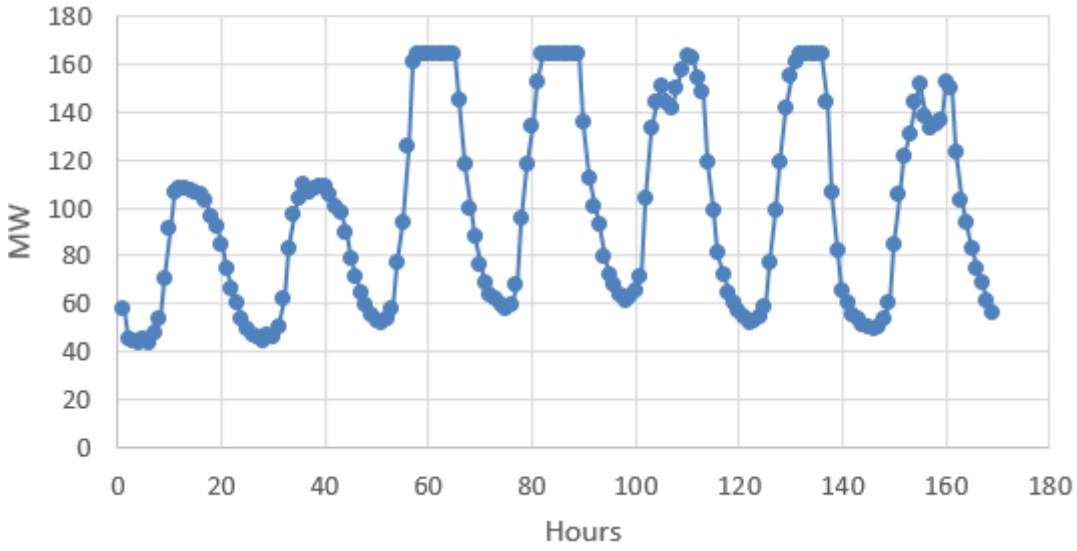

Figure 5.19: Week 33 Cooling Demand Profile

ii. **Week 33 Electricity Price Profile**
Figure 5.20 shows that the electricity prices started to increase gradually to reach their highest in the 18^{th} of August when the cooling demand started also to increase complying with the increase of the outdoor temperature and then later the electricity prices start dropping back as the cooling demand start to decrease.

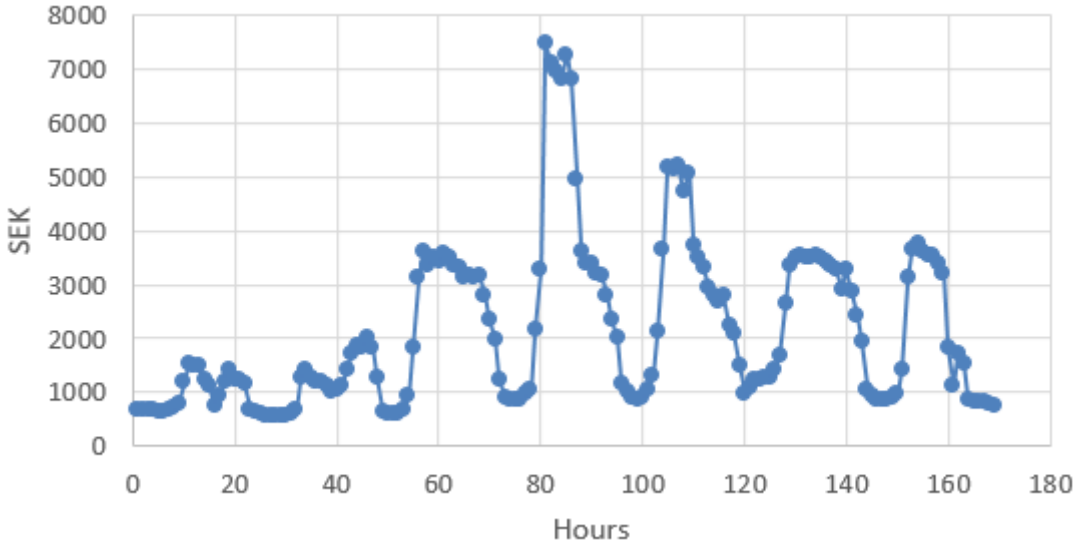

Figure 5.20: Week 33 Electricity Price Profile

iii. **Week 33 TES State Of Charge Profile**
Figure 5.21 shows that the TES starts fully discharging its maximum capacity before recharging again each day when the cooling demand requirement has increased and when the electricity prices started also to increase.

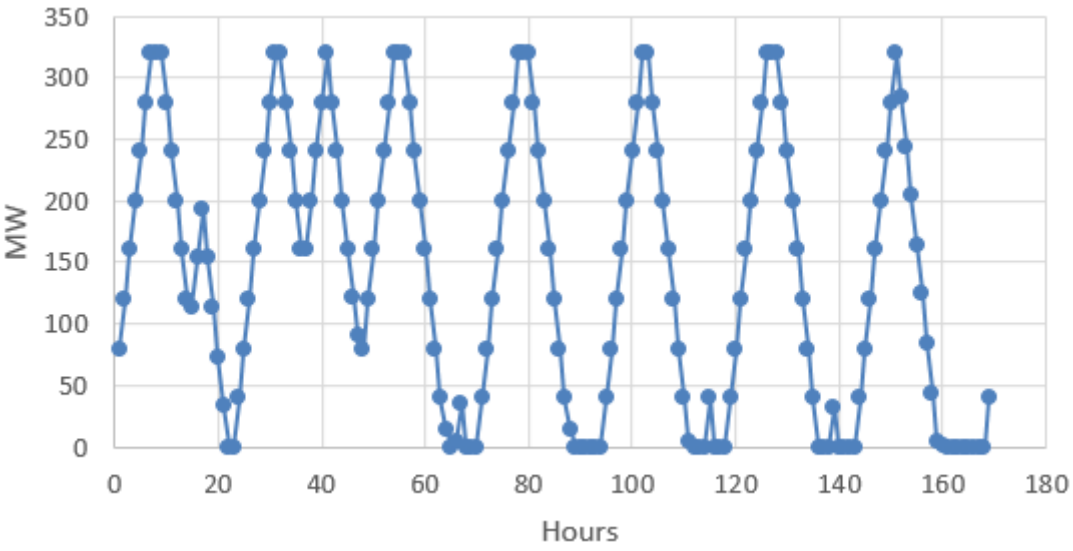

Figure 5.21: Week 33 TES State Of Charge Profile

iv. **Week 33 TES Charge and Discharge Profile**
Figure 5.22 shows the discharge and charging pattern of the TES during the week 33.

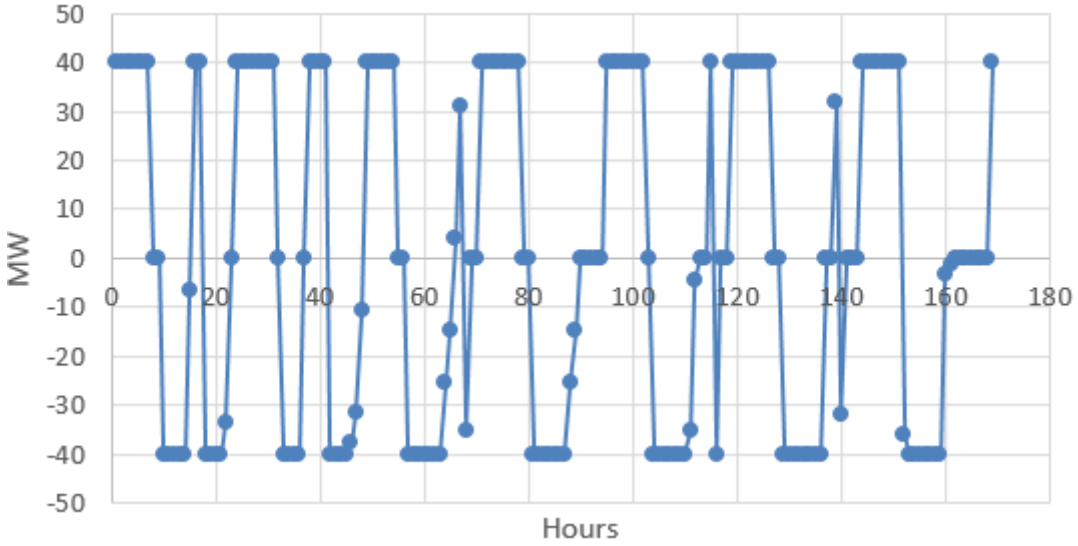

Figure 5.22: Week 33 TES Charge and Discharge Profile

v. **Week 33 Existing Cooling Production plant Profile**
Figure 5.23 shows that the existing cooling production plant was not required to operate to its full capacity during all week hours unless the cooling demand exceeded what is available to be discharged from the TES and the available capacity of the new production plant, then the existing plant production will increase gradually to achieve the required demand.

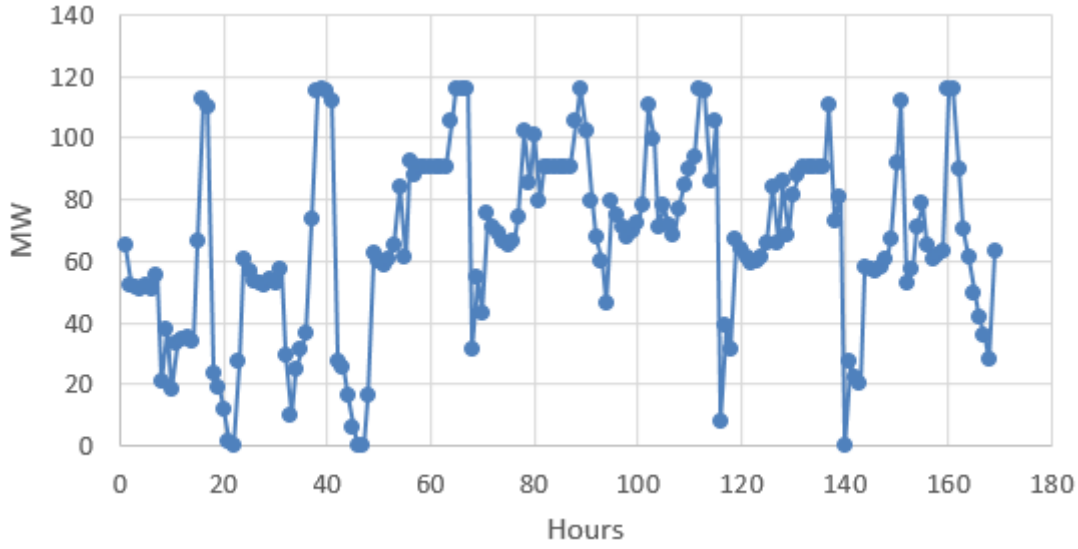

Figure 5.23: Week 33 Existing Cooling Production Profile

vi. **Week 33 New Cooling Production plant Profile**
Figure 5.24 shows that the cooling production of the new production plant will operate during the whole week, as it will have a lower operating cost compared with the existing cooling production plant when it comes to charging the TES or fulfilling the cooling demand.

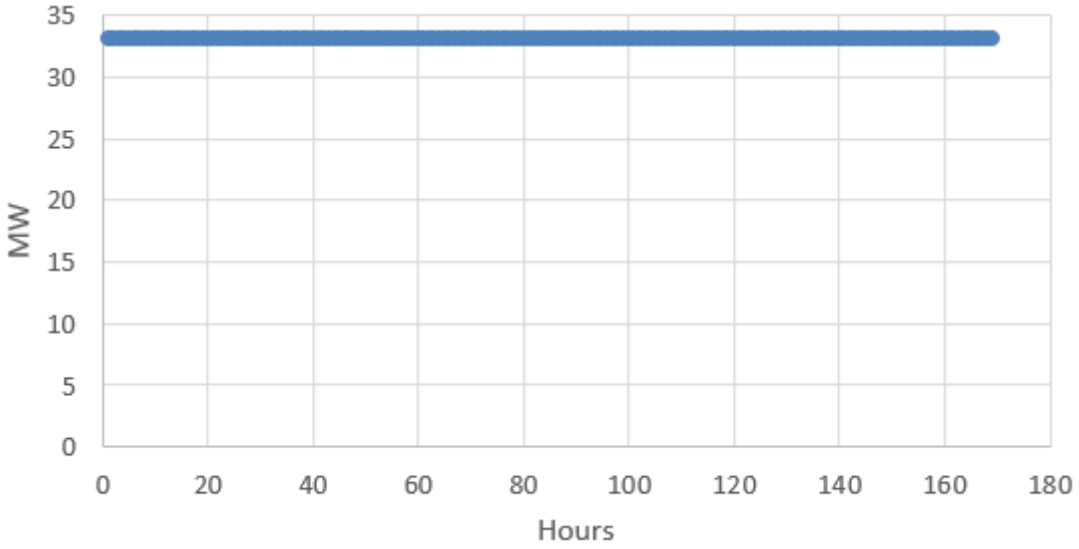

Figure 5.24: Week 33 New Cooling Production Profile

vii. **Week 33 TES Discharge Profile**
Figure 5.25 shows the discharge pattern only from the TES which was utilized to fulfill the peak cooling demand hours.

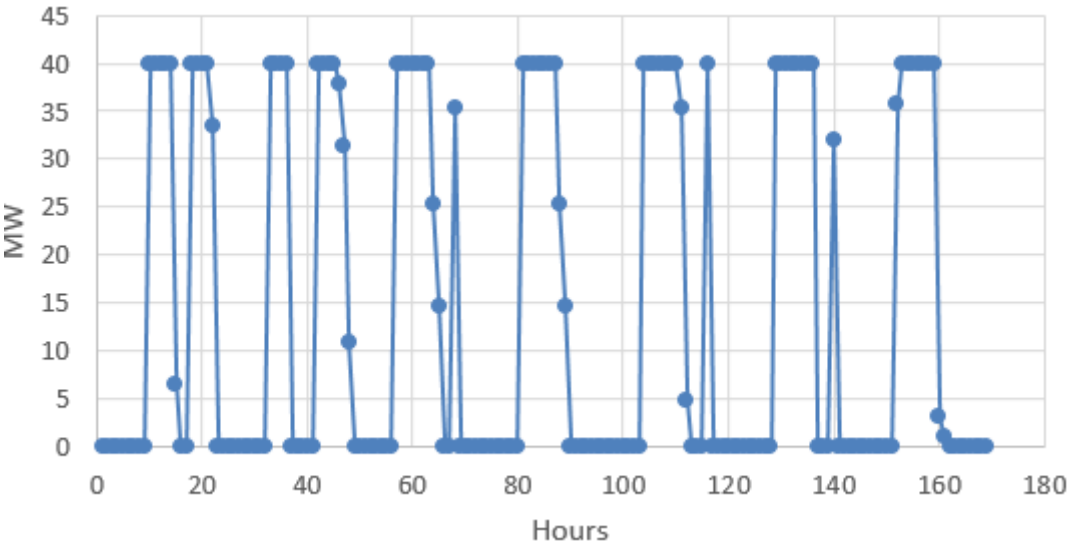

Figure 5.25: Week 33 TES Discharge Profile

viii. **Week 33 Cooling Demand and Production Profile**
Figure 5.26 shows the hours where the new and the existing production plant were operating above the cooling demand requirements during the low cooling demand hours in order to charge the TES, which was utilized later to fulfill the demand at the peak hours.

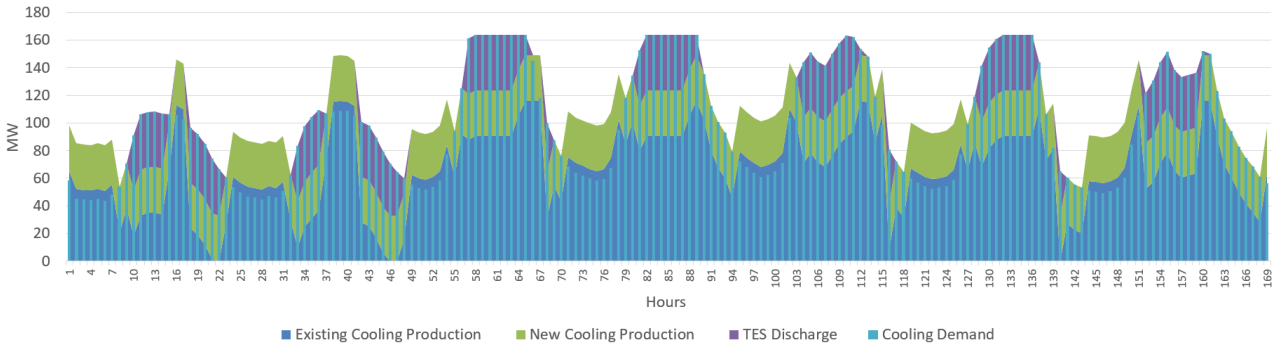

Figure 5.26: Week 33 Cooling Demand and Production Profile

(C) **Week 25 (20 June - 26 June, 2040) Case Study**
Week 25, in year of 2040 represents the week where DUT 75% and DUT 50% will occur in year 2040.

i. **Week 25 Cooling Demand Profile**
Similar to data from week 33, it can be noticed from Figure 5.27 that the cooling demand reached and exceeded 163.7 MW over 3 days and reached the the DUT 75% in the 23th of June. Also the figure shows that the cooling demand pattern is consistent that the peak load for each day happened during the day time hours and the low load hours happened during the night hours.

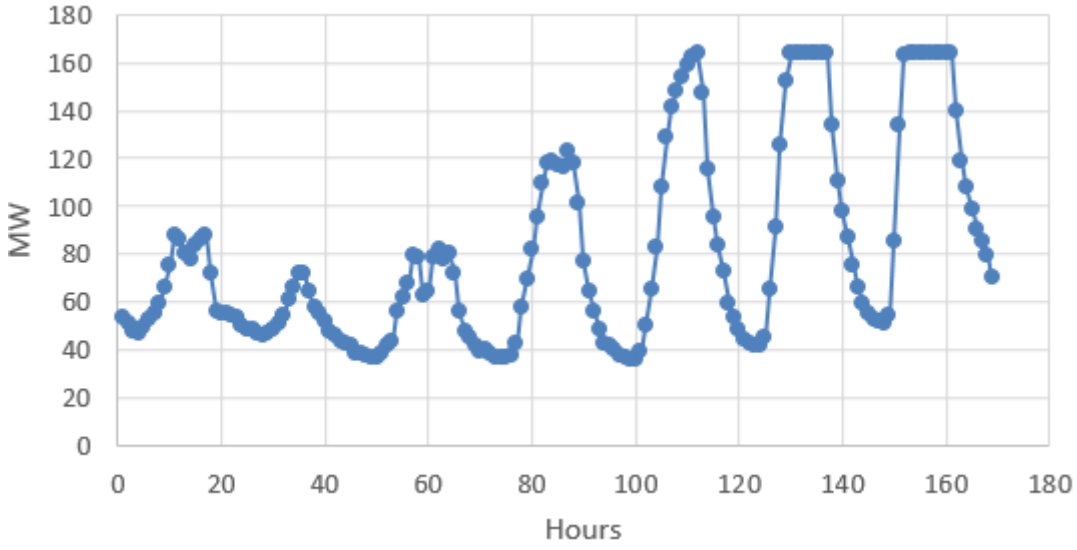

Figure 5.27: Week 25 Cooling Demand Profile

ii. **Week 25 Electricity Price Profile**
Similar to data from week 33, Figure 5.28 shows that the electricity prices started to increase gradually to reach its maximum on 25th of June, when the cooling demand started also to increase complying with the increase of the outdoor temperature, and then later the electricity prices start dropping back as the cooling demand start to decrease.

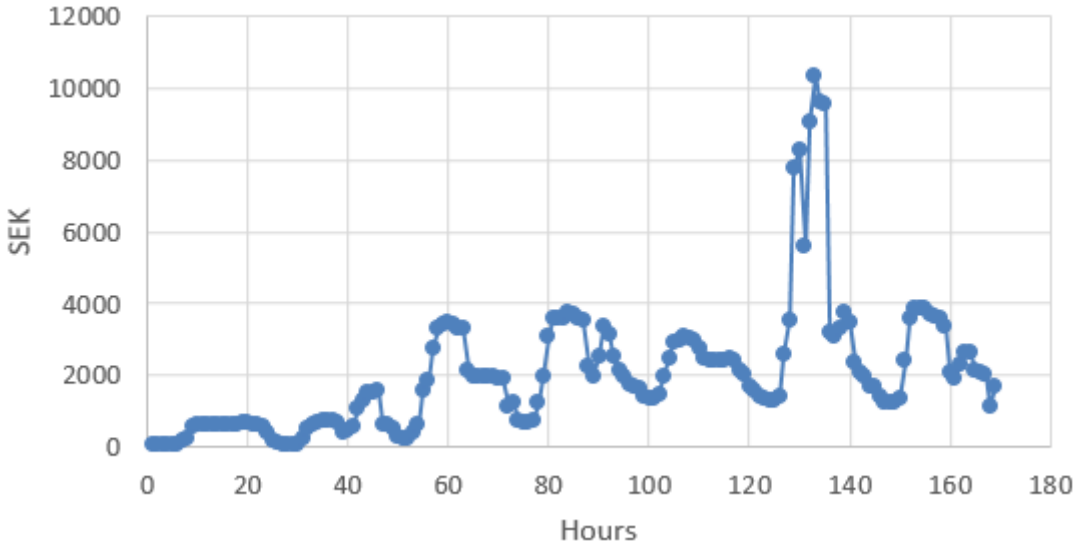

Figure 5.28: Week 25 Electricity Price Profile

iii. **Week 25 TES State Of Charge Profile**
Similar to week 33, Figure 5.29 shows that the TES started fully discharging its maximum capacity before recharging again during each day when the cooling demand requirement has increased and when the electricity prices started also to increase.

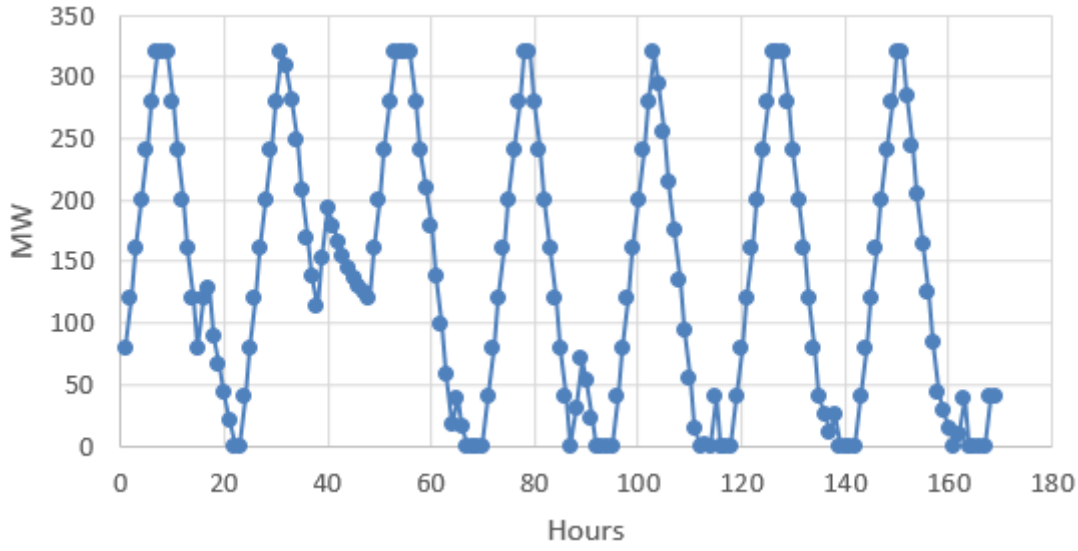

Figure 5.29: Week 25 TES State Of Charge Profile

iv. **Week 25 TES Charge and Discharge Profile**
Figure 5.30 shows the discharge and charging pattern of the TES during the week 25.

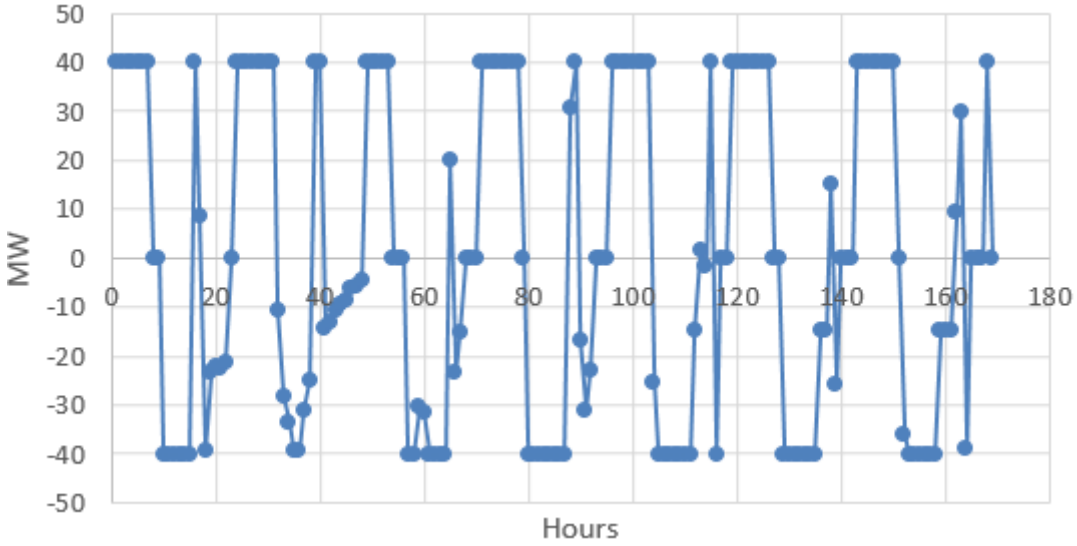

Figure 5.30: Week 25 TES Charge and Discharge Profile

v. **Week 25 Existing Cooling Production plant Profile**
Similar to week 33, Figure 5.31 shows that the existing cooling production plant was not required to operate to it full capacity during all week hours unless the cooling demand exceeded what are available to be discharged from the TES and the available capacity of the new production plant, then the existing plant production will increase gradually to achieve the required demand and where the full capacity was rarely required and only for few hours comparing with week 33.

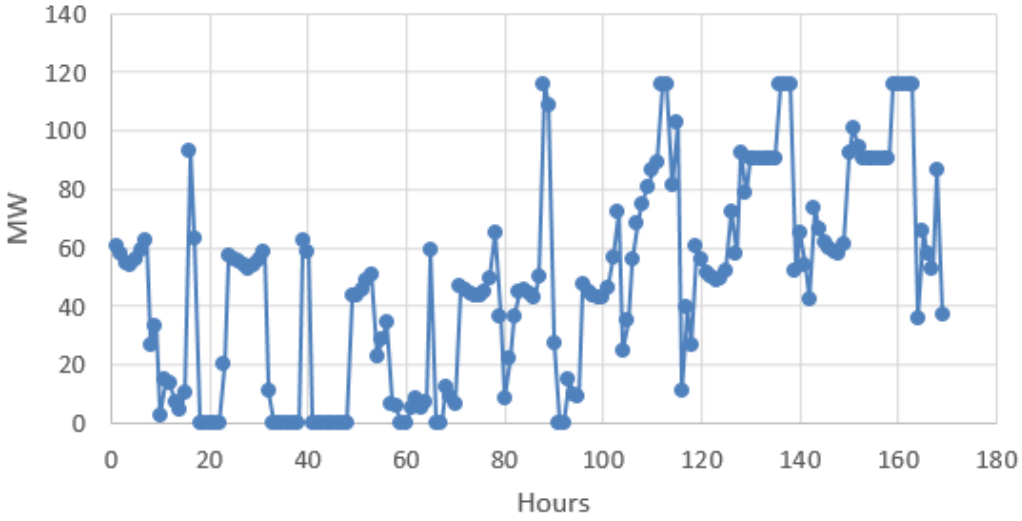

Figure 5.31: Week 25 Existing Cooling Production Profile

vi. **Week 25 New Cooling Production plant Profile**
Similar to week 33, Figure 5.32 shows that the cooling production of the new production plant was required to operate during the whole week to achieve the lowest optimization cost for this scenario, which can be explained as it have a lower operating cost comparing with the existing cooling production plant when it comes to charging the TES or fulfilling the cooling demand.

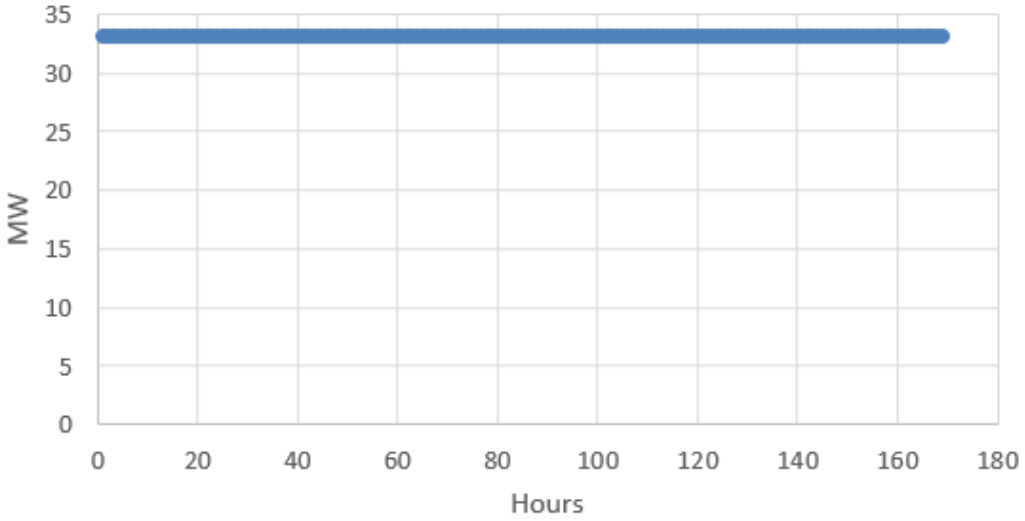

Figure 5.32: Week 25 New Cooling Production Profile

vii. **Week 25 TES Discharge Profile**
Similar to week 33, Figure 5.33 shows the discharge pattern only from the TES and how the TES was utilized to fulfill the peak cooling demand hours.

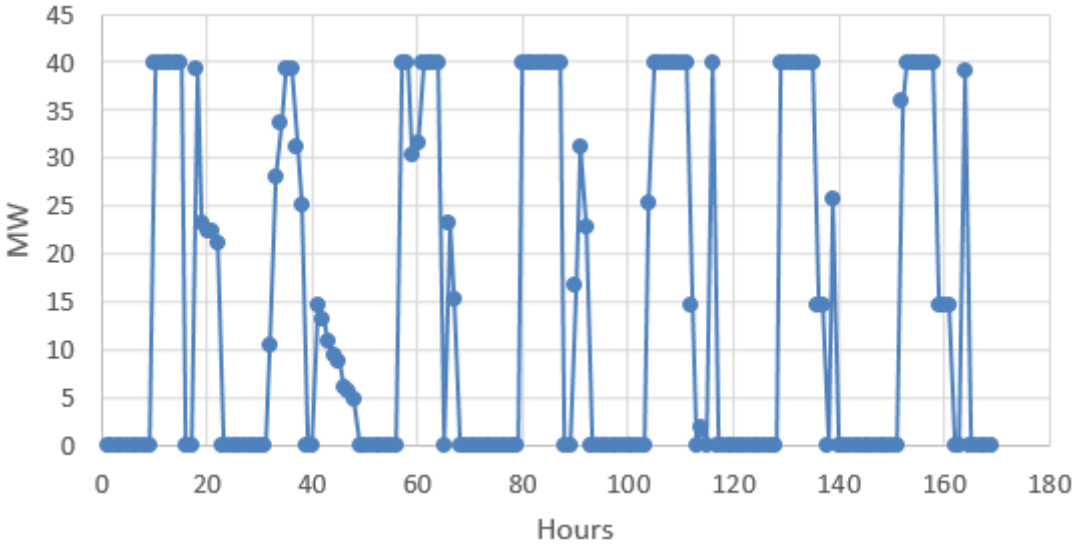

Figure 5.33: Week 25 TES Discharge Profile

viii. **Week 25 Cooling Demand and Production Profile**
Similar to week 33, Figure 5.34 shows the pattern and the hours where the new and the existing production plant where operating above the cooling demand requirements during the low cooling demand hours in order to charge the TES, which was utilized later to fulfill the demand at the peak hours.

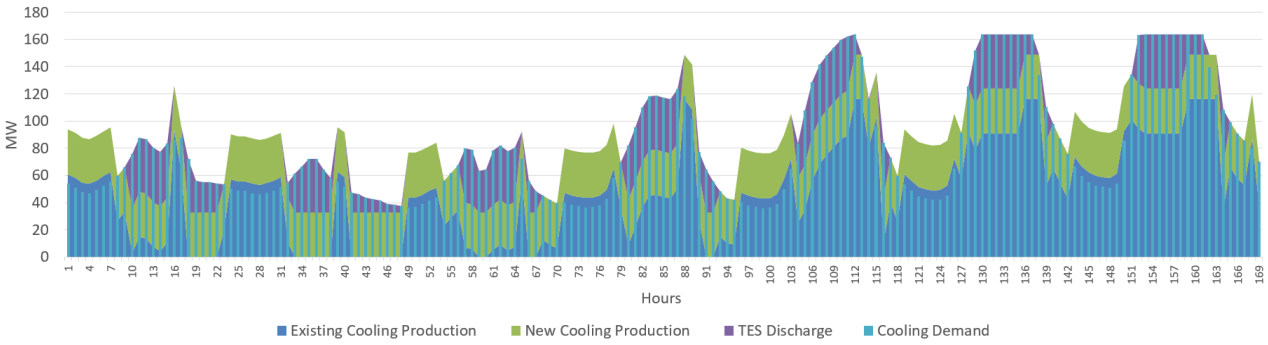

Figure 5.34: Week 25 Cooling Demand and Production Profile

(D) **DUT 100% (19-08-2040) Case Study**

i. **DUT 100% Daily Cooling Demand Profile**
Figure 5.35 represents the cooling demand profile during a day at DUT 100%, it shows that the cooling demand started gradually to increase during the day starting from hour 5:00, reaching the maximum cooling demand, at 163.7MW at hour 14:00, and then gradually decreased after hour 16:00 to reach the lowest cooling demand, at around 60 MW, at around hour 00:00.

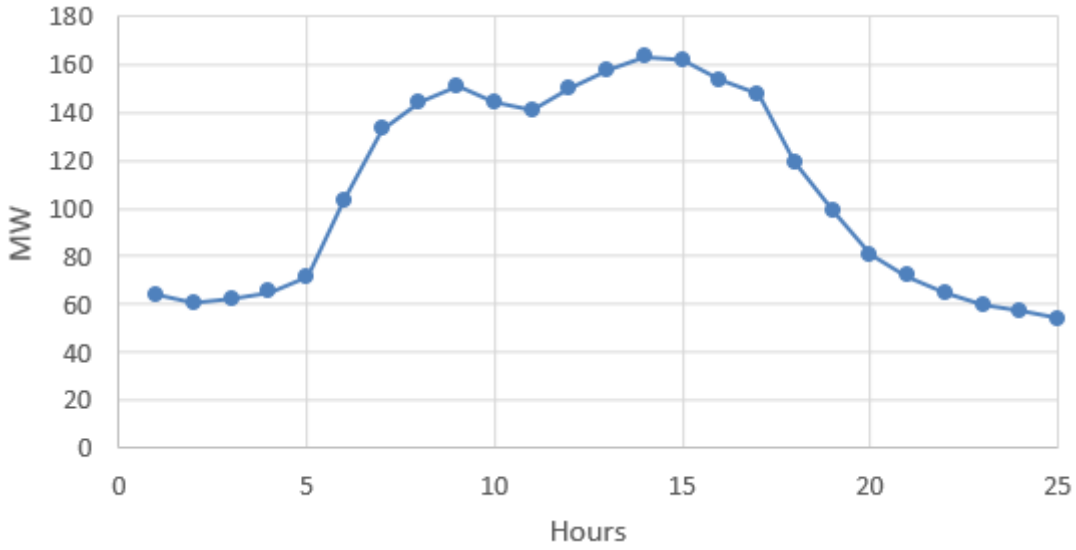

Figure 5.35: DUT 100% Daily Cooling Demand Profile

ii. **DUT 100% Daily Electricity Price Profile**
Figure 5.36 represents the electricity prices profile during a day at DUT 100%, it shows that it is consistent with the increase of the cooling demand, where the electricity prices increase and reach it maximum during the day hours while it gradually drop and reach it lowest prices during the night hours.

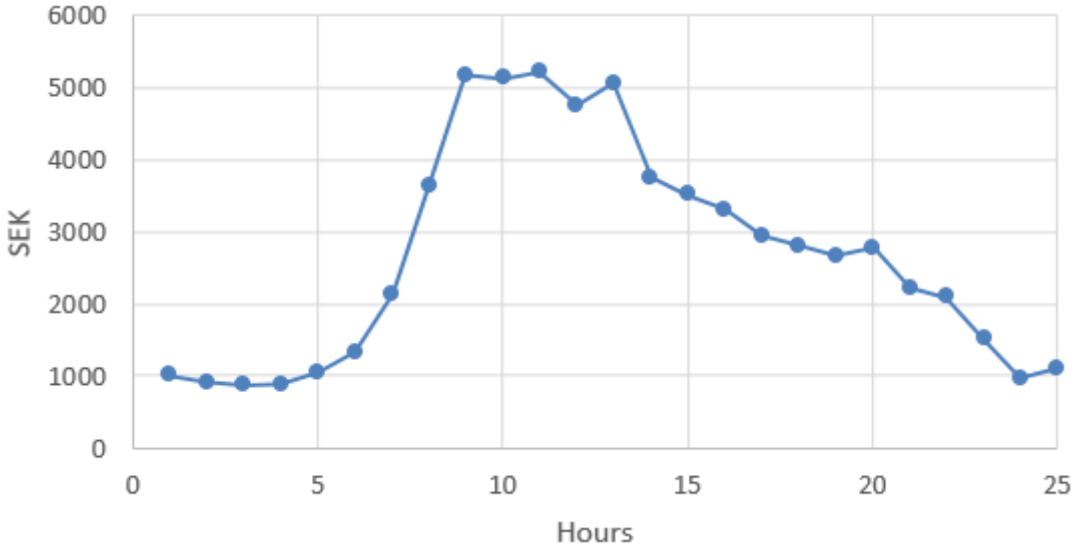

Figure 5.36: DUT 100% Daily Electricity Price Profile

iii. **DUT 100% Daily TES State Of Charge Profile**
Figure 5.37 represents the state of charge for the TES profile during a day at DUT 100%, it shows that the tank starts charging mainly in the off-peak hours between hour 22:00 and hour 5:00 while it discharges during the peak hours between hour 7:00 and 15:00. This is also consistent with the cooling demand profile while the TES is used to discharge during the peak cooling demand hours in order to fulfill the overall cooling demand. This is also consistent with the electricity price profile which shows that the tank starts to charge when the electricity prices are low and then later discharges when the electricity prices are high.

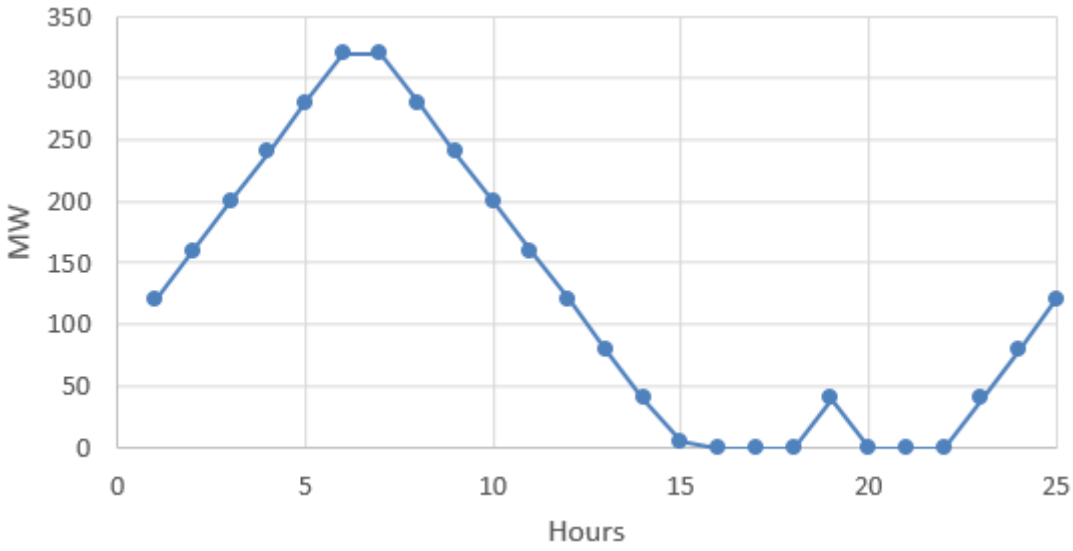

Figure 5.37: DUT 100% Daily TES State Of Charge Profile

iv. **DUT 100% Daily TES Charge and Discharge Profile**
Figure 5.38 represents the charging and discharging profile of the TES during a day at DUT 100%, it shows that the tank starts charging during the night hours (off-peak load hours) with a maximum charging capacity of 40 MW for each hour, to discharge it again during the day hours (peak load hours) with maximum discharge capacity of 40 MW.

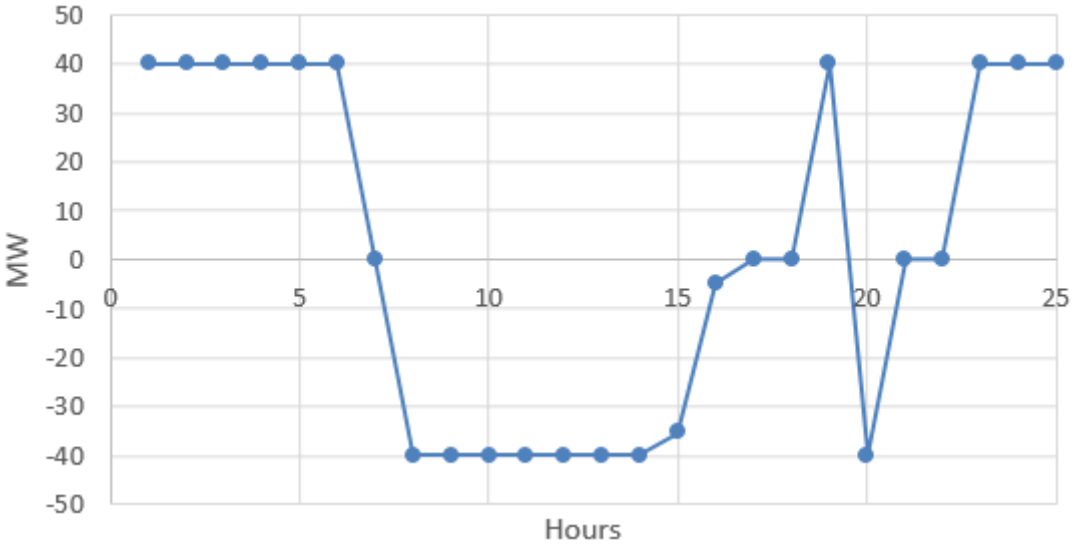

Figure 5.38: DUT 100% Daily TES Charge and Discharge Profile

v. **DUT 100% Daily Existing Cooling Production plant Profile**
Figure 5.39 represents the existing cooling production plant profile during a day at DUT 100%. It shows how the existing plant will operate to achieve the cooling demand. It can be noticed that during the peak hour 14:00 when the cooling demand was 163.7 MW, the existing plant still did not operate to its maximum capacity as the priority was to run the TES and the new production plant. While in hour 16:00 it can be observed that the existing plant start operating to its maximum and that is because there was no more enough capacity left to be discharged from the TES and the demand required for the existing plant to operate using its maximum capacity.

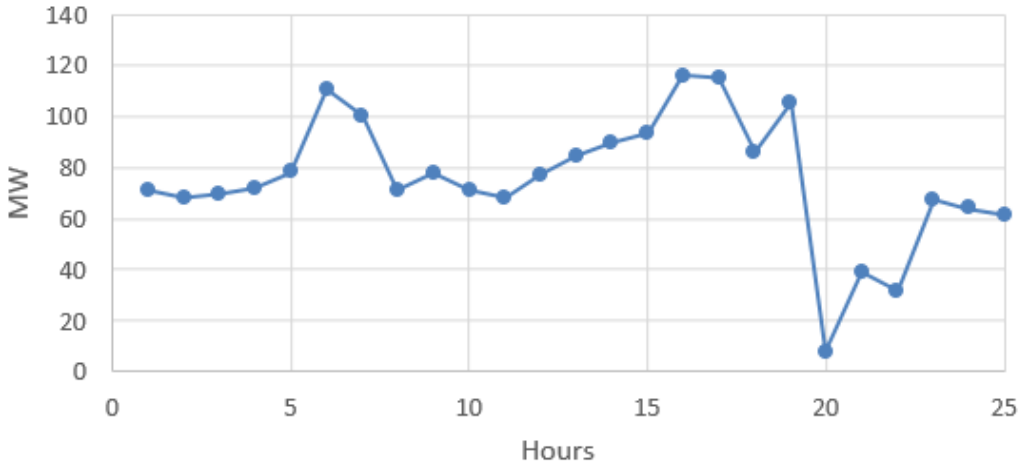

Figure 5.39: DUT 100% Daily Existing Cooling Production Profile

vi. **DUT 100% Daily New Cooling Production Profile**
Figure 5.40 represents the new cooling production plant profile during a day at DUT 100%, it shows that the new production plant was fully utilized during the day as the cost of operation for the new cooling production plant is cheaper than the existing cooling production plant.

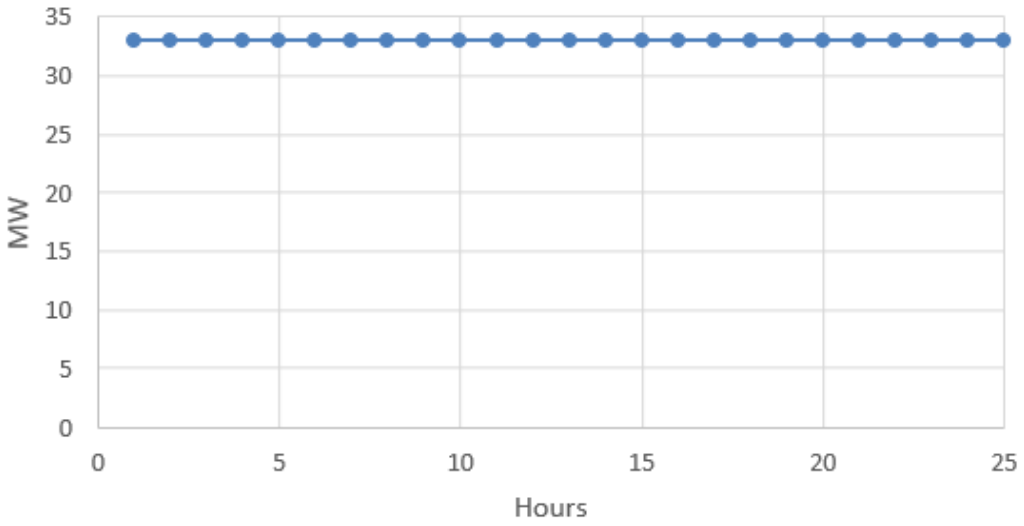

Figure 5.40: DUT 100% Daily New Cooling Production Profile

vii. **DUT 100% Daily TES Discharge Profile**
Figure 5.41 shows only the daily discharge pattern from the TES and how the TES was utilized to fulfill the peak cooling demand hours. Similar to what was mentioned in the state of discharge, the tank start discharging by 40 MW for each hour during day time, between hour 8:00 till 14:00 when the peak load starts gradually to increase to reach its max at hour 14:00.

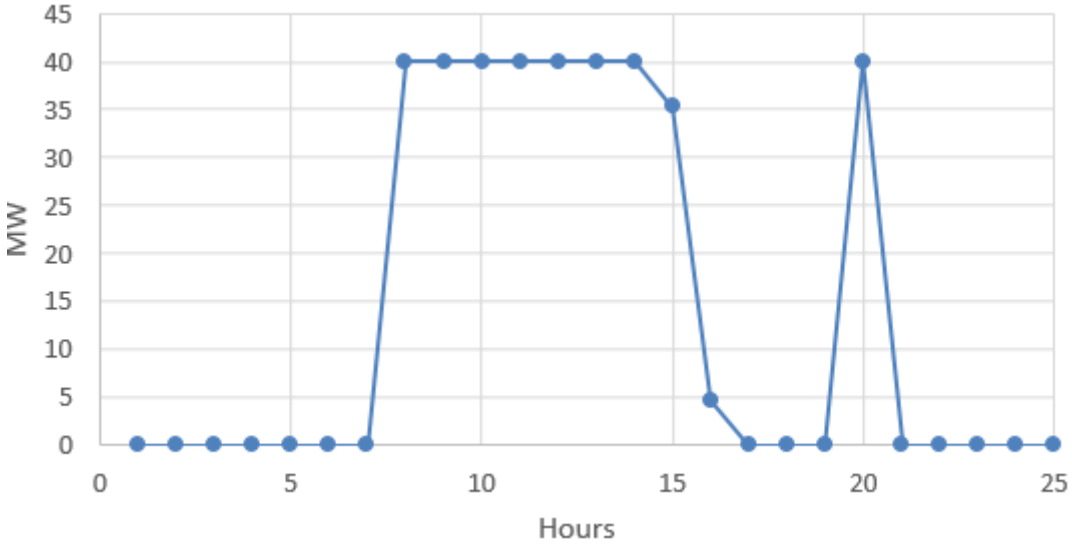

Figure 5.41: DUT 100% Daily TES Discharge Profile

viii. **DUT 100% Daily Cooling Demand and Production Profile**
Figure 5.42 represents the cooling production and demand profile during a day at DUT 100%. It shows the hours which were during the day when the new and the existing production plant were operating above the cooling demand requirements and during the off-peak hours in order to charge the TES, which was utilized later to fulfill the demand at the peak load hours between hour 8:00 till 14:00.

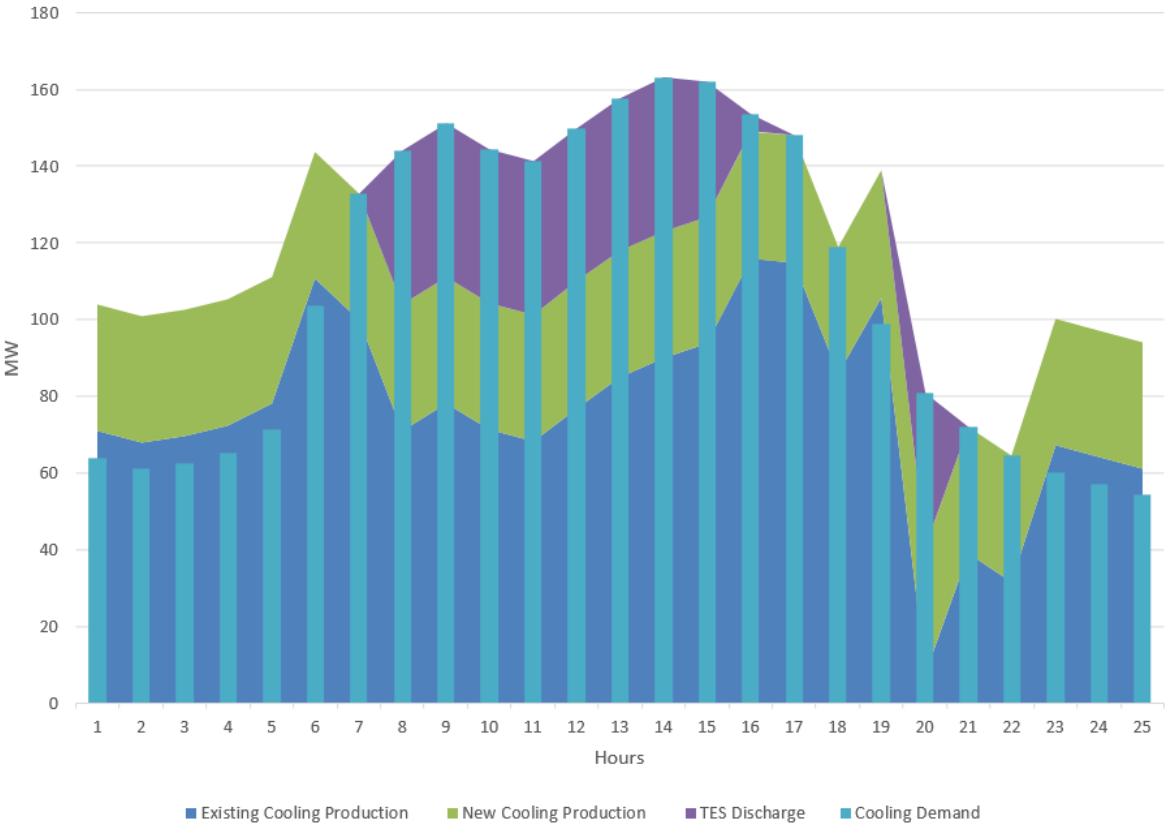

Figure 5.42: DUT 100% Daily Cooling Demand and Production Profile

(E) **DUT 75% (23-06-2040) Case Study**

i. **DUT 75% Daily Cooling Demand Profile**
Figure 5.43 represents the cooling demand profile during a day at DUT 75%, it shows that the cooling demand started gradually to increase during the day starting from hour 5:00, reaching the maximum cooling demand of around 120 MW at hour 15:00 then gradually decreasing after to reach the lowest cooling demand around 40 MW, around hour 00:00. Compared to the profile of DUT 100%, it has a similar pattern but the cooling demand required was less during the day of DUT 75%, around 75% of the maximum load.

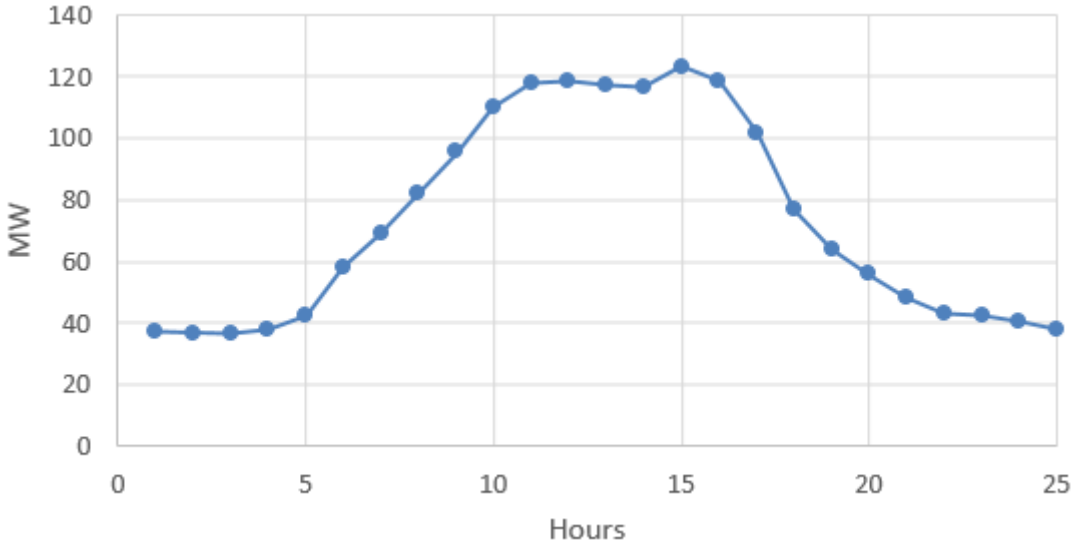

Figure 5.43: DUT 75% Daily Cooling Demand Profile

ii. **DUT 75% Daily Electricity Price Profile**
Figure 5.44 represents the electricity prices profile during a day at DUT 75%. It shows that it is consistent with the increase of the cooling demand, where the electricity prices increase and reach their maximum during the day hours while it gradually drops and reaches its lowest prices during the night hours, except between the hour 17:00 and 18:00 when the electricity prices by a sudden increased again.

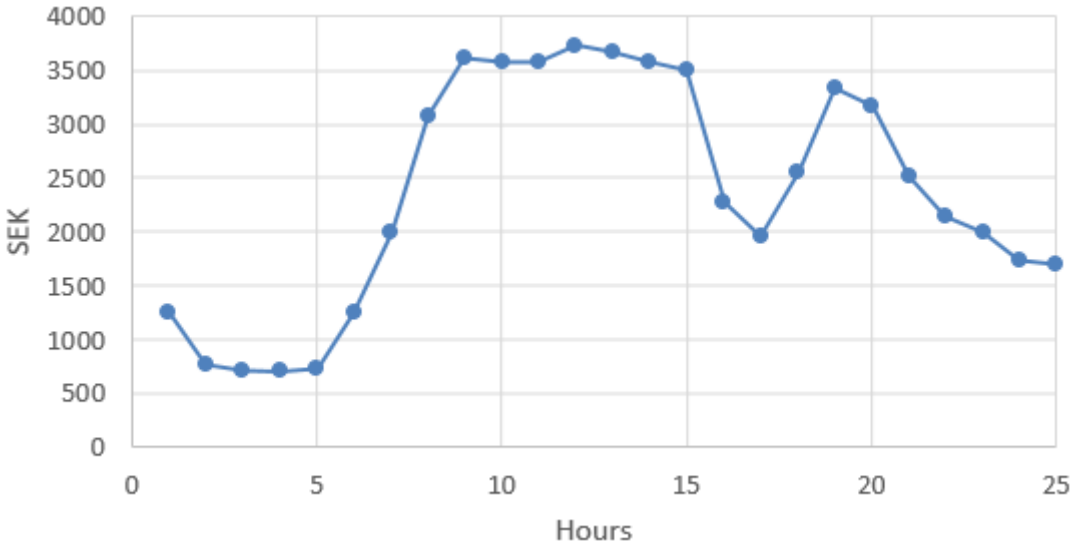

Figure 5.44: DUT 75% Daily Electricity Price Profile

iii. **DUT 75% Daily TES State Of Charge Profile**
Figure 5.45 represents the state of charge for the TES profile during a day at DUT 75%, it shows that the tank starts charging mainly in the off-peak load hours between hour 23:00 and hour 5:00 while it discharges during the peak hours between hour 7:00 and 15:00, to later than slightly charge and discharge between hour 15:00 and 20:00. It is noticed that even though electricity prices went high again but still, it was profitable to charge slightly the tank before the electricity price reach its second peak at hour 17:00. This can be noticed as consistent with the electricity price profile where it shows that the tank starts to charge when the electricity prices are low and then later discharge when the electricity prices are high.

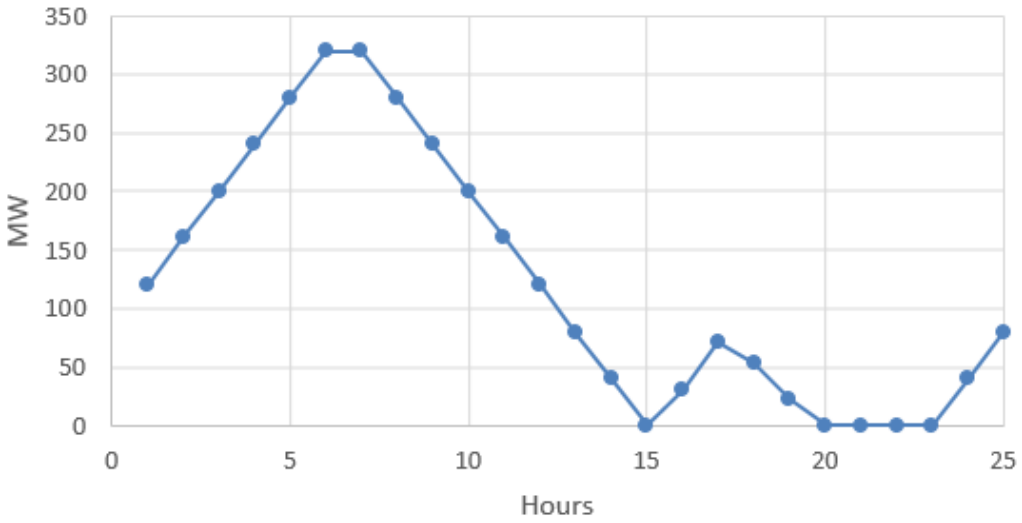

Figure 5.45: DUT 75% Daily TES State Of Charge Profile

iv. **DUT 75% Daily TES Charge and Discharge Profile**
Figure 5.46 represents the charging and discharging profile of the TES during a day at DUT 75%, similar to the profile from DUT 100%. It shows that the tank starts charging during the night hours (off-peak load hours) with a maximum charging capacity of 40 MW for each hour, to discharge again during the day hours (peak load hours) with a maximum discharge capacity of 40 MW. However, a pattern of charging the TES at hour 16:00 was around 30 MW, and an extra 10 MW by hour 17:00 was noticed to reduce the operating running cost for the overall cooling system when the electricity prices went high again at hour 17:00.

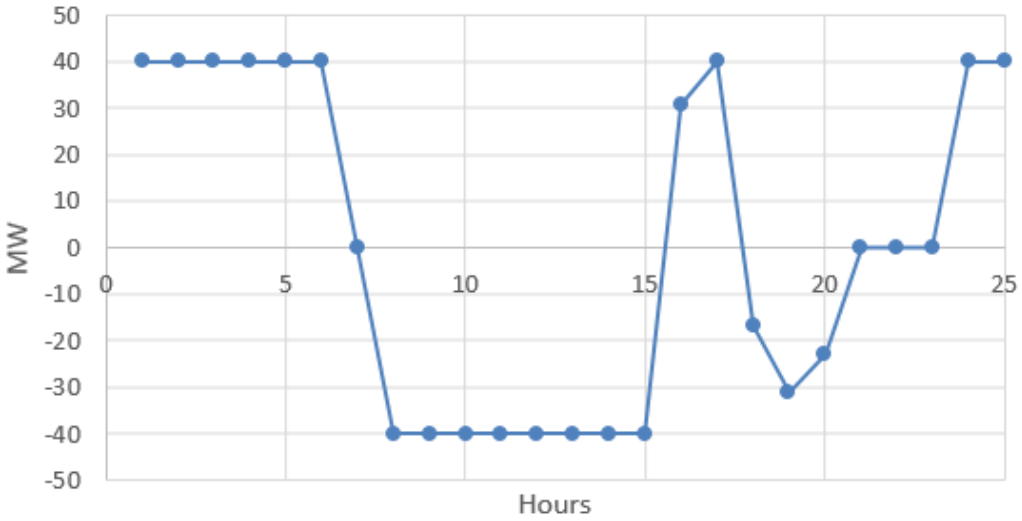

Figure 5.46: DUT 75% Daily TES Charge and Discharge Profile

v. **DUT 75% Daily Existing Cooling Production Profile**
Figure 5.47 represents the existing cooling production plant profile during a day at DUT 75%, similar to the profile of DUT 100%. DUT 75% profile shows how the existing plant will operate to achieve the cooling demand. It can be noticed that during the hour 16:00 when the cooling demand was 120 MW, the existing plant was almost sufficient by itself to produce cooling to cover the cooling demand, while the new production plant capacity remained under operation to fulfill the charging of the TES. And in hour 19:00, the existing plant was switched off as the required cooling load was sufficient to be achieved using the TES and the new cooling production plant, and this had helped to reduce the running cost of using the existing plant which has lower COP.

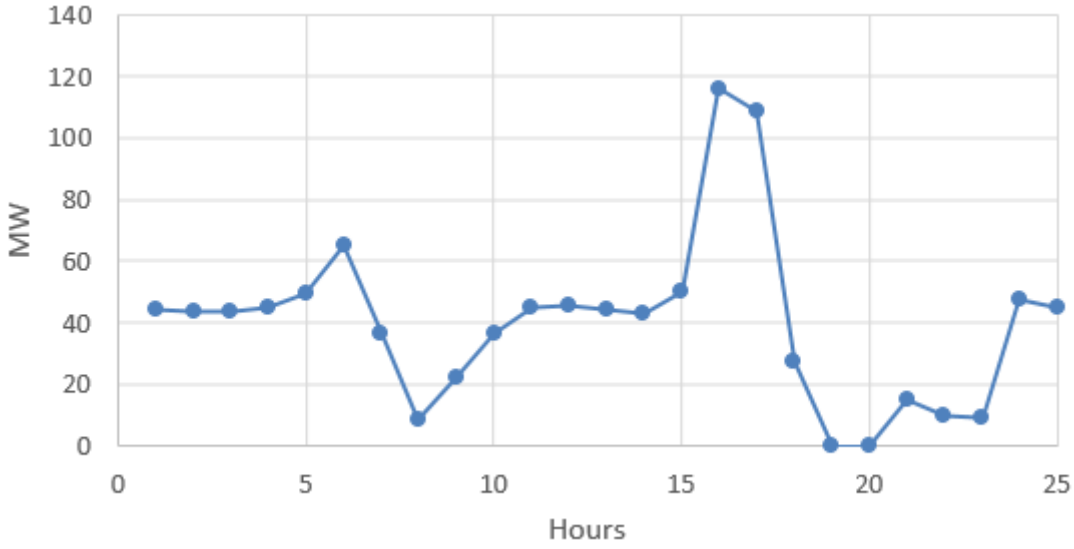

Figure 5.47: DUT 75% Daily Existing Cooling Production Profile

vi. **DUT 75% Daily New Cooling Production Profile**
Figure 5.48 represents the new cooling production plant profile during a day at DUT 75%, similar to the DUT 100% profile. The graph shows that the new production plant was fully utilized during the day, as the cost of operation for the new cooling production plant is cheaper than the existing cooling production plant, which was utilized to charge the TES or to fulfill the cooling demand.

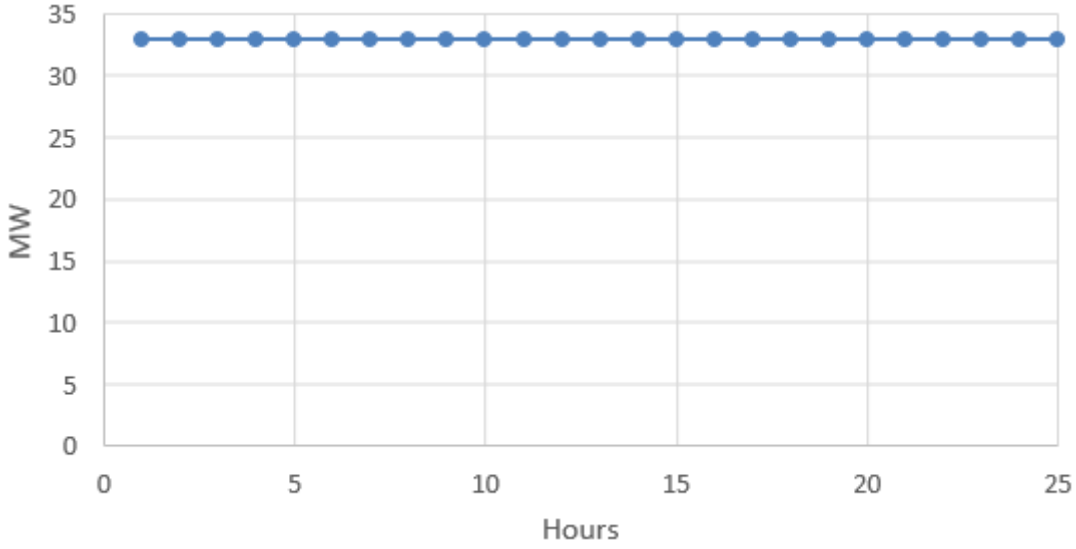

Figure 5.48: DUT 75% Daily New Cooling Production Profile

vii. **DUT 75% Daily TES Discharge Profile**
Figure 5.49 represents the TES discharge profile during a day at DUT 75%, similar to DUT 100%. The graph shows only the daily discharge pattern from the TES and how the TES was utilized to fulfill the peak cooling demand hours, where the tank starts discharging by 40 MW for each hour during daytime, between hours 8:00 until 14:00 when the peak load starts gradually to increase to reach it maximum at hour 14:00. In addition, to be later charged by 30 MW at hour 19:00 to re-discharge later during the day when the electricity prices were high.

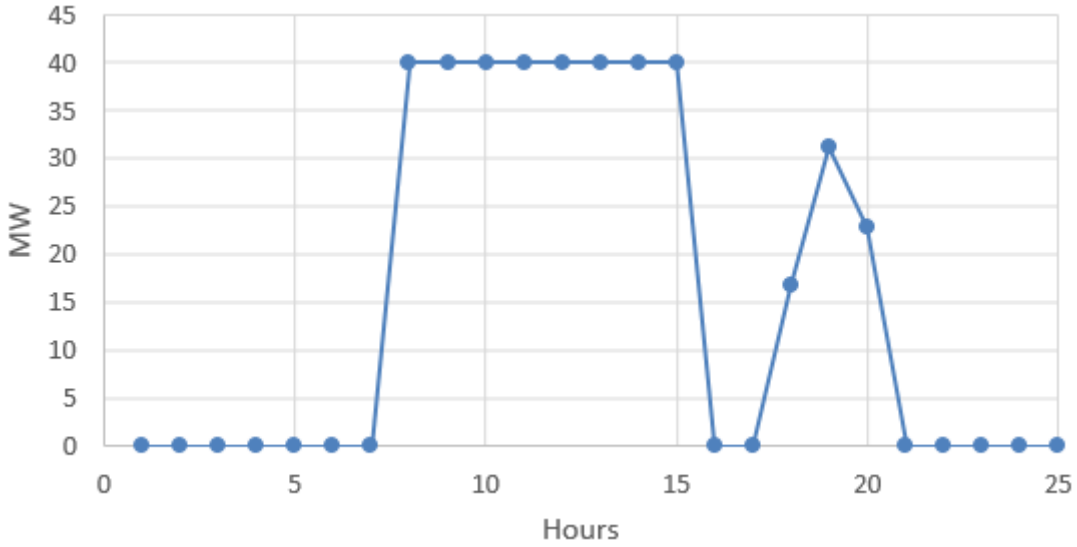

Figure 5.49: DUT 75% Daily TES Discharge Profile

viii. **DUT 75% Daily Cooling Demand and Production Profile**
Figure 5.50 represents the cooling production and demand profile during a day at DUT 75%, similar to the DUT 100% profile. The graph shows the hours during the day where the new and the existing cooling production plant were operating above the cooling demand requirements and during the off-peak hours in order to charge the TES, which was later utilized to fulfill the demand at the peak load hours between hour 8:00 till 15:00.

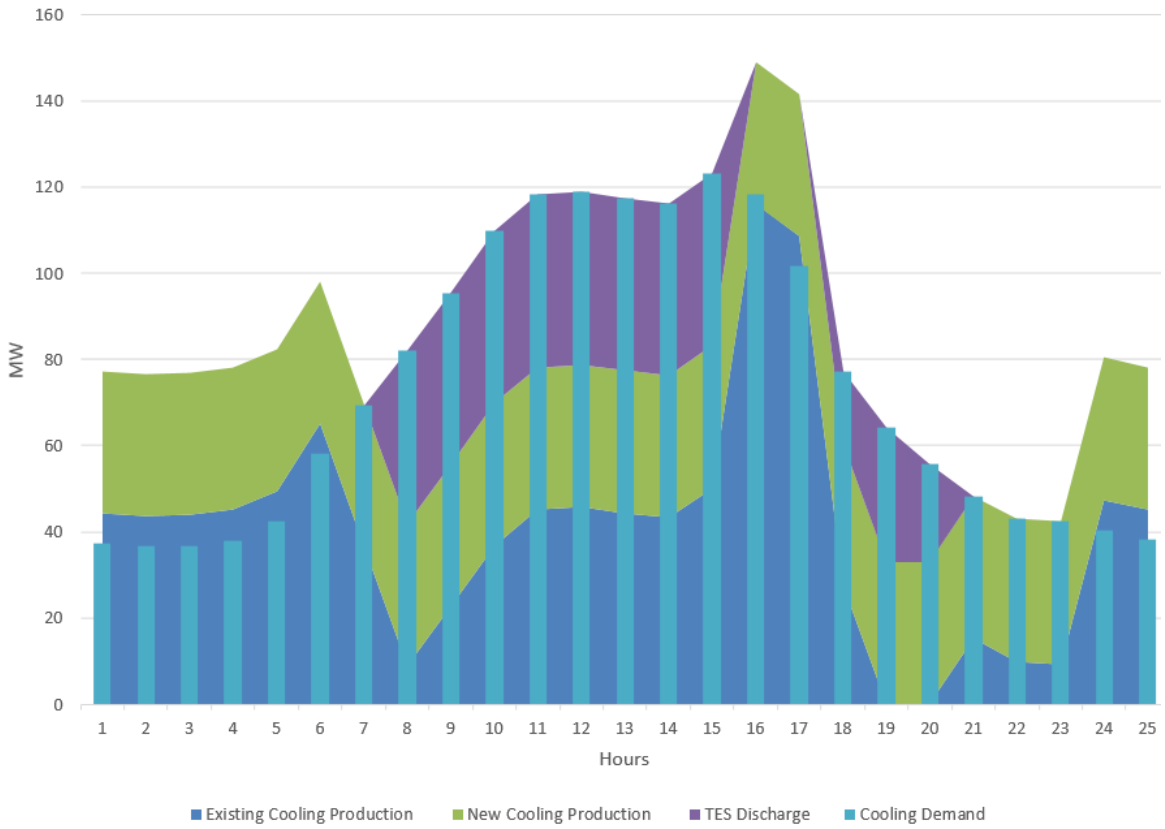

Figure 5.50: DUT 75% Daily Cooling Demand and Production Profile

(F) **DUT 50% (22-06-2040) Case Study**

i. **DUT 50% Daily Cooling Demand Profile**
Figure 5.51 represents the cooling demand profile during a day at DUT 50%. It shows that the cooling demand started gradually to increase during the day, reaching the maximum cooling demand of around 80 MW at hour 9:00 then gradually decreasing slightly to increase and reach the maximum again around hour 14:00 to later drops gradually again and reach the lowest cooling demand around 40 MW, around hour 00:00. Compared to the profile of DUT 100% the pattern is similar and the drop in the cooling demand is more obvious during the daytime hours and the required cooling demand was less during the day of DUT 50%.

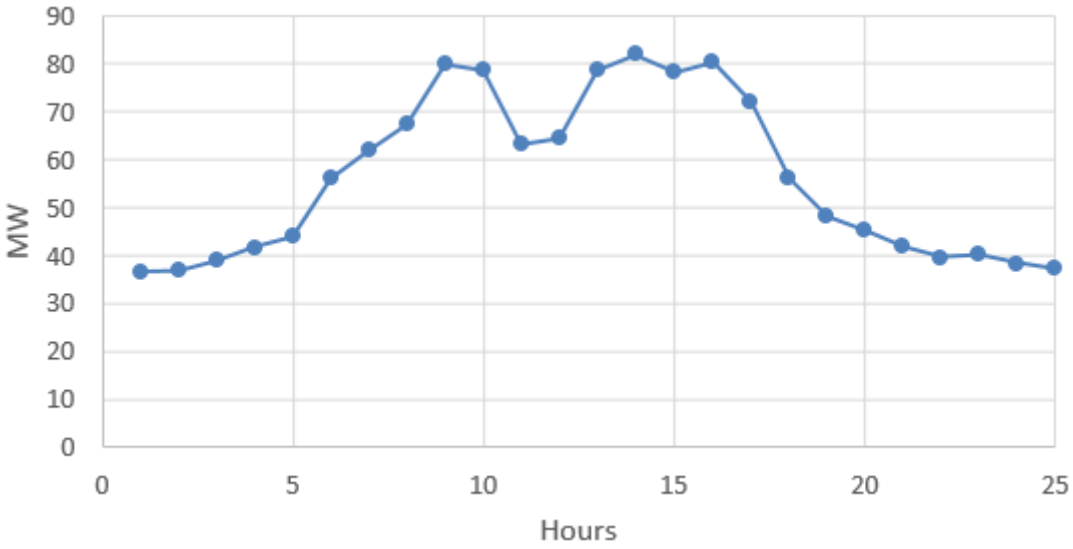

Figure 5.51: DUT 50% Daily Cooling Demand Profile

ii. **DUT 50% Daily Electricity Price Profile**
Figure 5.52 represents the electricity prices profile during a day at DUT 50%. The graph shows that the electricity price increased gradually to reach the highest between hours 10:00 and 14:00 and then drooped again from 15:00 to 00:00 and remained to some extent constant. It is also consistent with the increase of the cooling demand, where the electricity prices increase and reach their maximum during the day hours while they gradually drop during the night hours.

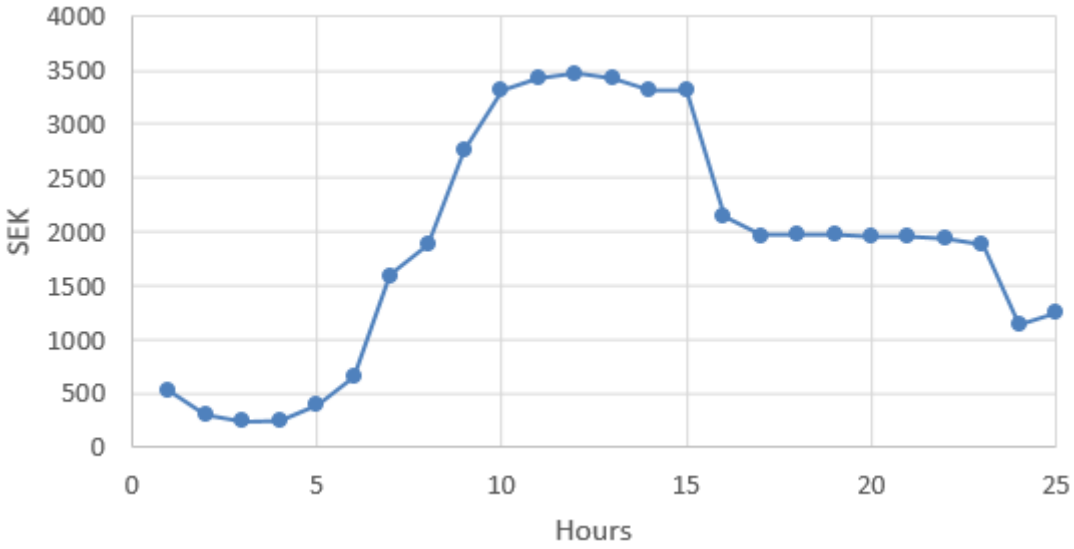

Figure 5.52: DUT 50% Daily Electricity Price Profile

iii. **DUT 50% Daily TES State Of Charge Profile**
Figure 5.53 represents the state of charge for the TES profile during a day at DUT 50%. The graph shows that the tank starts charging in the off-peak load hours between hour 22:00 and hour 4:00 while it discharges during the peak load hours between hour 8:00 and 16:00, to later slightly charge and discharge between hour 16:00 and hour 19:00. This can be noticed as consistent with the cooling demand and electricity price profile where it shows that the tank starts to charge when the electricity prices and when the cooling demand is low and then later discharge when the electricity prices and the cooling demand are high.

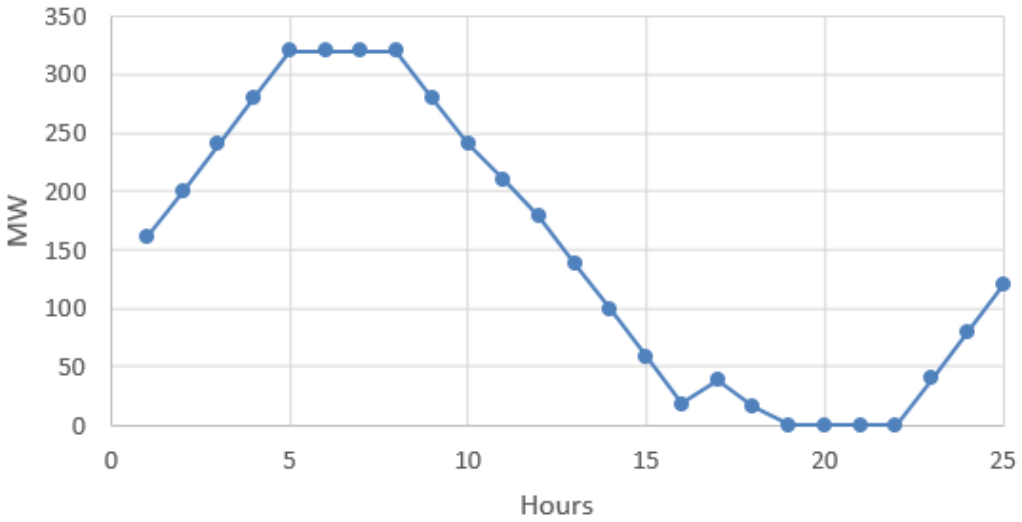

Figure 5.53: DUT 50% Daily TES State Of Charge Profile

iv. **DUT 50% Daily TES Charge and Discharge Profile**
Figure 5.54 represents the charging and discharging profile of the TES during a day at DUT 50%. Similar to the profile from DUT 100%, it shows that the tank starts charging during the night hours (off-peak load hours) with a maximum charging capacity of 40 MW for each hour, to discharge it again during the day hours (peak load hours) with maximum discharge capacity of 40 MW. However, a pattern of charging the TES at hour 17:00 by around 20 MW was noticed to reduce the operating running cost for the overall cooling system when the electricity prices were still considered high compared to the early hours of the day.

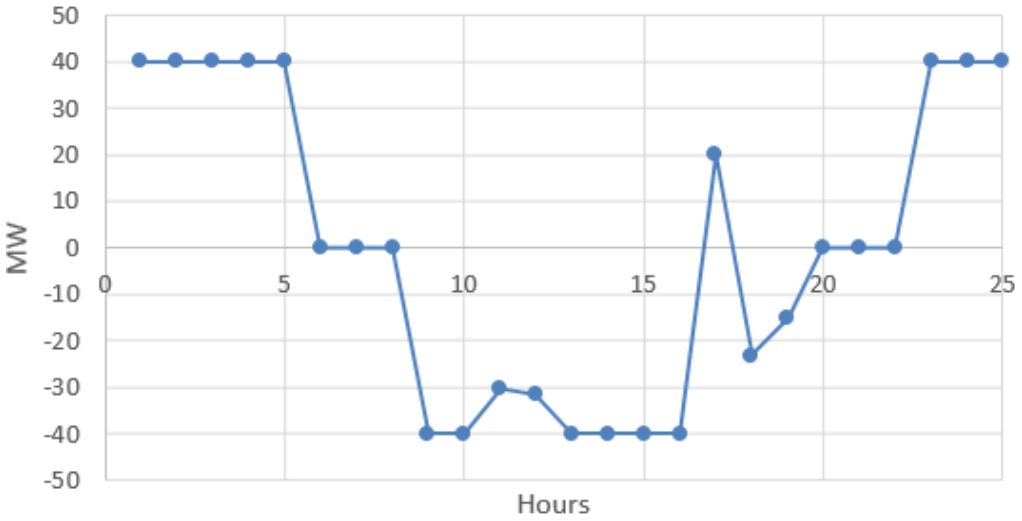

Figure 5.54: DUT 50% Daily TES Charge and Discharge Profile

v. **DUT 50% Daily Existing Cooling Production Profile**
Figure 5.55 represents the existing cooling production plant profile during a day at DUT 50%. Similar to the profile of DUT 100%, the profile shows how the existing plant will operate to achieve the cooling demand. It can be noticed that during the hour 17:00 when the cooling demand was around 70 MW, the existing plant had the highest operation hour during this specific day with 60 MW per hour almost sufficient by itself to produce cooling to cover the cooling demand. While the new production plant capacity remained fully under operation to fulfill the charging of the TES. In addition, in hours 10:00 and 18:00 the existing plant was switched off, as the required cooling load was sufficient to be achieved using the TES and the new production plant, which helped to reduce the running cost of using the existing plant, which has low COP.

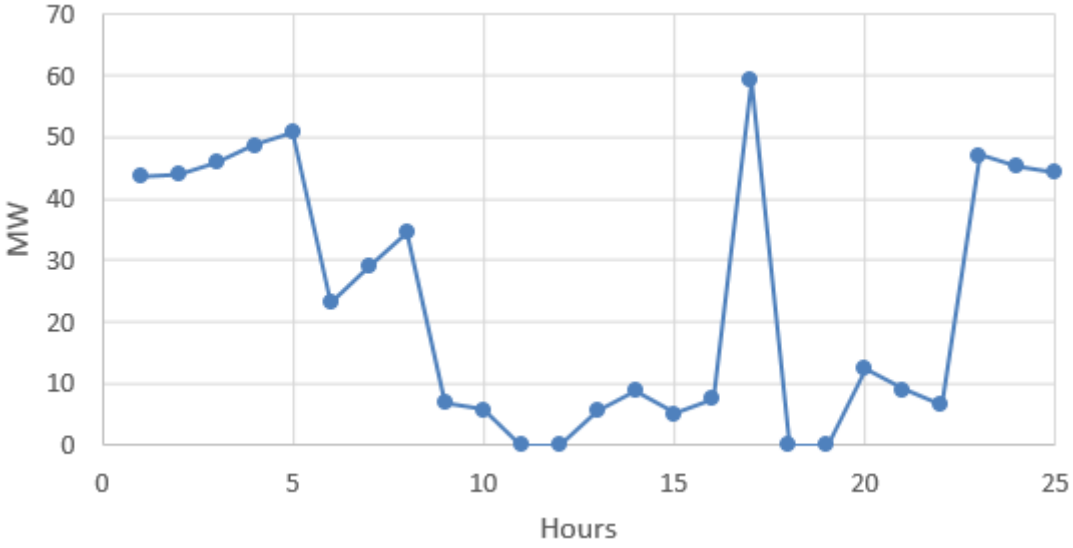

Figure 5.55: DUT 50% Daily Existing Cooling Production Profile

vi. **DUT 50% Daily New Cooling Production Profile**
Figure 5.56 represents the new cooling production plant profile during a day at DUT 50%. Similar to the DUT 100% profile, the graph shows that the new production plant was fully utilized during the day as it cost of operation for the new plant is cheaper than the existing plant and where it was utilized to charge the TES or to fulfill the cooling demand.

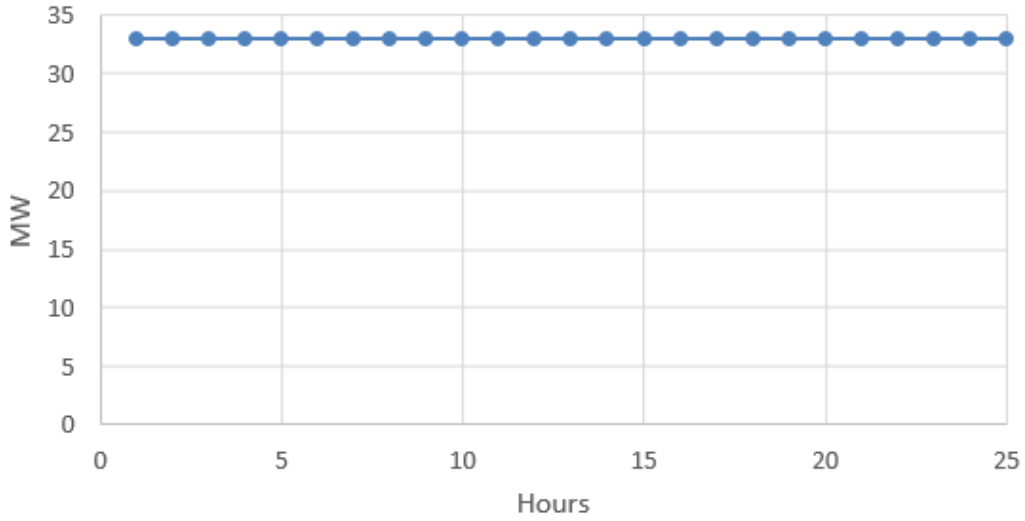

Figure 5.56: DUT 50% Daily New Cooling Production Profile

vii. **DUT 50% Daily TES Discharge Profile**
Figure 5.57 represents the TES discharge profile during a day at DUT 50%. Similar to DUT 100%, the graph shows only the daily discharge pattern from the TES and how the TES was utilized to fulfill the peak cooling demand hours. Where the tank starts discharging by 40 MW for each hour during daytime, between hours 9:00 until 15:00 when the peak load starts gradually to increase to reach its max at hour 14:00. It was also observed that during the hours 11:00 and 12:00 the required discharging capacity was around 30 MW instead of 40 MW. These are the same hours when the cooling demand has dropped during the daytime and the same when the existing plant stopped operation, which means that discharging a 30 MW from TES and full operation of the new plant was sufficient to fulfill the cooling demand at that certain hour. Later the TES was charged by 25 MW at hour 18:00 to re-discharge during the day to reduce the consumption of the electricity prices.

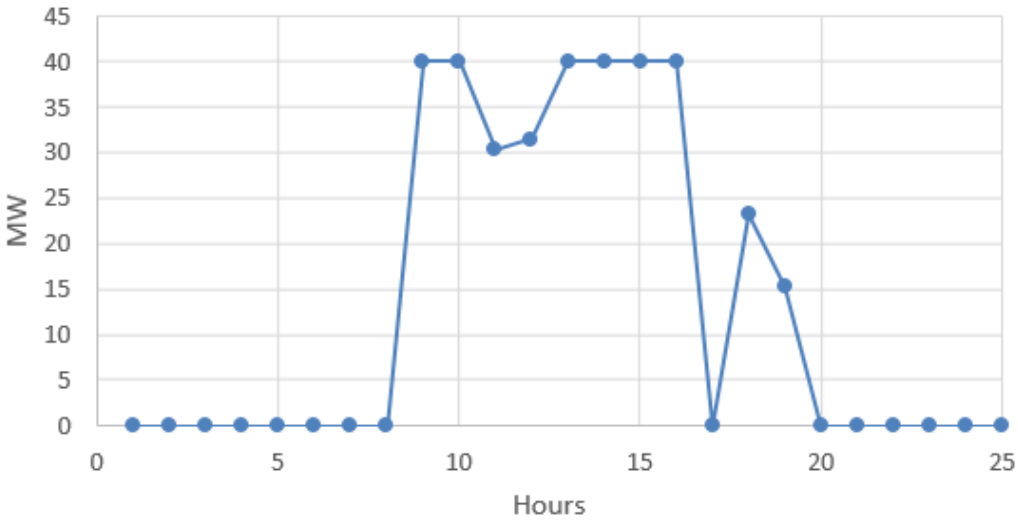

Figure 5.57: DUT 50% Daily TES Discharge Profile

viii. **DUT 50% Daily Cooling Demand and Production Profile**
Figure 5.58 represents the cooling production and demand profile during a day at DUT 75%. Similar to the DUT 100% profile, the graph shows the hours during the day where the new and the existing cooling production plant were operating above the cooling demand requirements and during the off-peak hours to charge the TES, which was utilized later to fulfill the demand at the peak hours between hour 8:00 until 15:00.

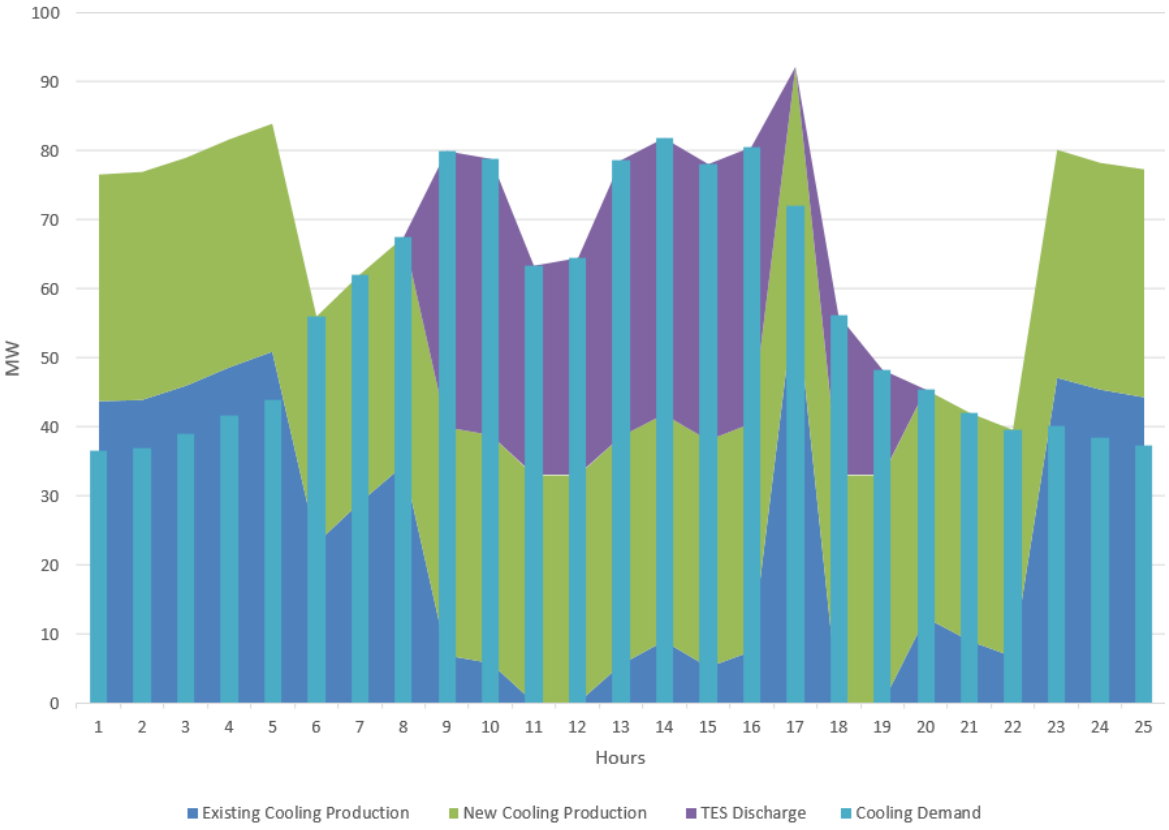

Figure 5.58: DUT 50% Daily Cooling Demand and Production Profile

(G) **Scenario 2-a outcomes**
Several inputs and constraints had played an essential role in deciding the outcomes of the optimized cost model, these inputs and constraints are such as the historical cooling demand data of 2020, the historical electricity prices data of 2020 and the Maximum Dis/Charge from the TES to name few. The outcome of the optimized cost model was the total annualized cost at 47.84 MSEK, considering a TES capacity of 320 MWh and the use of absorption chillers with a capacity of 33 MW for the new cooling production plant as a result to achieve the cheapest total annualized cost of for the system. Several other data can be seen as outcomes that concern the design such as the tank volume is 27,8 m^3, the tank diameter of 23.33 m when the tank height is 65 m, the total utilization factor is 27.2% for the TES during the year. In the next section, a further demonstrating of the sub-scenario 2a results and comparing it with other sub-scenario results will be presented.

5.2.3 Scenarios outcomes

(A) **Overall Scenario 1 outcomes**
Scenario 1 considers using compression chillers as a new cooling production plant with TES. Table 5.2 below summaries the results of each sub-scenario in scenario 1. It can be noticed that Scenario 1a has the cheapest optimization annualized cost with 58.59 M SEK compared with the other scenarios. It was noticed that the minimum accepted capacity of the new cooling production plant for scenarios 1a and 1b has been reached at 15 MW, and to accommodate the cooling demand of the cooling system, the tank size was required to be enlarged but even with this has been taken into consideration, scenario 1a was still the cheapest. A pattern from the results can be noticed as follow. The more the value of the maximum TES Dis/Charge was reduced or the more the discharge temperature was increased when the maximum flow rate is constant, then the more capacity from the new cooling production plant will be required and less capacity from the TES and the higher the total annualized cost for the system overall.

This can be elaborated as installing a larger TES capacity with more possibility to discharge from the tank per hour can play a significant role in reducing the overall cost of the system, compared to installing a larger capacity of the new cooling production plant.

Scenario 1 results						
Scenario name	Scenario 1a	Scenario 1b	Scenario 1c	Scenario 1d	Scenario 1e	Scenario 1f
Discharge Temperature (°C)	2	3	4	5	6	7
Maximum TES Dis/Charge (MW)	40	36.67	33.33	30	26.67	23.33
TES Capacity (MWh)	389	349	339	303	259	227
New production Plant (MW)	15	15	15	18	22	25
Total Annualized Cost (MSEK)	58.59	59.51	60.46	62.50	64.89	66.91
Tank Cost (SEK/MWh)	21.71	23.67	25.62	27.57	29.53	31.48
Tank Total Cost (MSEK)	3.70	3.62	3.80	3.66	3.35	3.13
Tank Volume (Thousand m^3)	33.79	33.35	35.99	36.19	35.36	36.15
Tank Height (m)	65.00	65.00	65.00	65.00	65.00	65.00
Tank Diameter (m)	25.73	25.56	26.55	26.63	26.32	26.61
Utilization factor per each Dis-/Charge	23.13%	23.48%	24.27%	24.67%	24.85%	25.16%
Hours per Day per each Discharge & Charge	5.55	5.63	5.82	5.92	5.96	6.03

Table 5.2: Scenario 1 results

Figure 5.59 demonstrates how reducing the TES capacity will require enlarging the capacity of the new cooling production plant to fulfill the cooling demand. and in both scenarios 1a and 1b the minimum capacity of the new production plant has been reached, it can be observed that due to the extra capacity of the production plant in both scenarios the required TES capacity was reduced from how originally would have been required if there was no limitation.

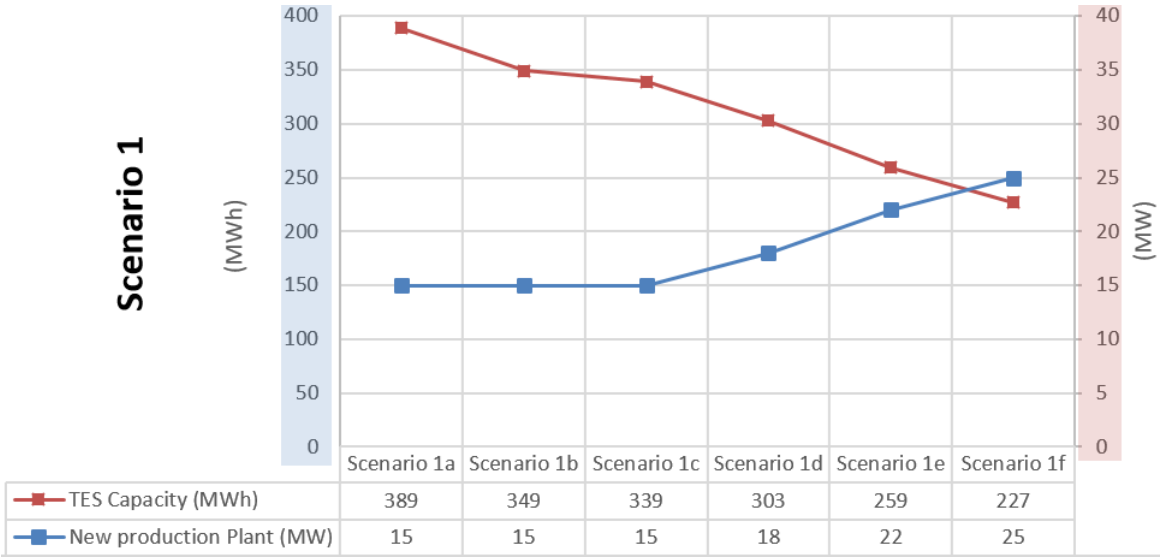

Figure 5.59: Scenario 1 - Sub-scenarios TES capacity and New Cooling Plant Capacity comparison

(B) **Overall Scenario 2 outcomes**

Scenario 2 considers using absorption chillers as a new cooling production plant with TES. Table 5.3 below summaries the results of each sub-scenario in scenario 2. it can be noticed that Scenario 2a has the cheapest optimization annualized cost with 47.84 M SEK compared with the other scenarios. Similar to the observation of scenario 1, a pattern from the results can be noticed as follow. The more the value of the maximum TES Dis/Charge was reduced or the more the discharge temperature was increased, then the more capacity from the new production plant will be required and less capacity from the TES and the higher the total annualized cost for the system overall. In the same, this can be elaborated as installing a larger TES capacity with more possibility to discharge from the tank per hour can play a big factor in reducing the overall cost of the system, compared to installing a larger capacity of the new cooling production plant.

Scenario 2 results						
Scenario name	Scenario 2a	Scenario 2b	Scenario 2c	Scenario 2d	Scenario 2e	Scenario 2f
Discharge Temperature (°C)	2	3	4	5	6	7
Maximum TES Dis/Charge (MW)	40	36.67	33.33	30	26.67	23.33
TES Capacity (MWh)	320	293	266	236	199	175
New production Plant (MW)	33	33	34	35	35	36
Total Annualized Cost (MSEK)	47.84	48.37	48.87	49.34	49.78	50.20
Tank Cost (SEK/MWh)	21.71	23.67	25.62	27.57	29.53	31.48
Tank Total Cost (MSEK)	3.04	3.04	2.98	2.85	2.57	2.41
Tank Volume (Thousand m^3)	27.80	28.00	28.24	28.19	27.17	27.87
Tank Height (m)	65	65	65	65	65	65
Tank Diameter (m)	23.33	23.42	23.52	23.50	23.07	23.37
Utilization factor per each Dis-/Charge	13.6%	14.2%	14.8%	15.5%	16.1%	17.2%
Hours per Day per each Discharge & Charge	3.27	3.41	3.56	3.72	3.86	4.12

Table 5.3: Scenario 2 results

Figure 5.60 demonstrates how reducing the TES capacity will require enlarging the capacity of the new cooling production plant in order to fulfill the cooling demand.

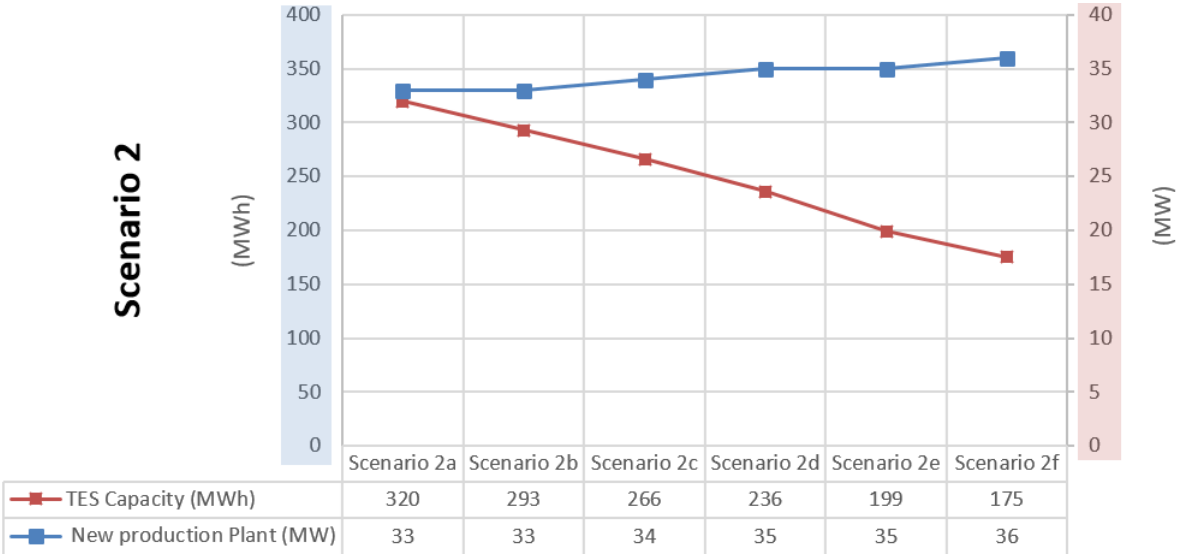

Figure 5.60: Scenario 2 - Sub-scenarios TES capacity and New Cooling Plant Capacity comparison

(C) **Overall Scenario 1 and 2 Total Annualized Cost outcomes**
Figure 5.61 shows scenarios 1 and 2 cases, it can be noticed that all scenario 2 sub-scenarios still have the cheapest total annualized cost compared with all sub-scenarios of scenario 1. It also shows that having a lower discharge temperature and a higher available discharge capacity from TES will always have the lowest cost compared with the other scenarios.

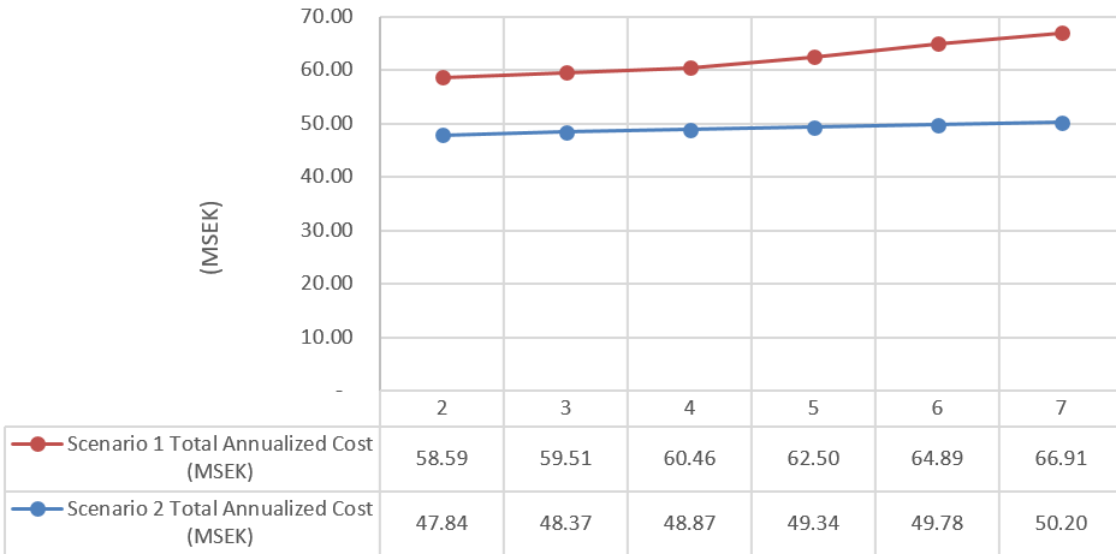

Figure 5.61: Scenario 2 - Sub-scenarios total annualized cost

5.2.4 Sensitivity Analysis Results

Sensitivity analysis was established for the best scenario which achieved the optimization cost goal, Scenario 2-a, the new absorption cooling production plant with TES, with discharging temperature of the chilled water at 2°C. The sub-scenario was made to test how the cost optimization will be impacted against the irregular pattern of the expected electricity prices and the cooling demand in the future, the year 2040.

(A) **Sensitivity Analysis Results - Historical electricity prices data**
Sensitivity analysis was done for historical data of electricity prices for the years 2021, 2019, 2018, and 2017 and comparing it with the electricity prices for the original model case as per the year 2020, to notice how this will impact the optimization cost model.

Table 5.4 below summarizes the results of the sensitivity analysis using different historical electricity prices data for the years 2021, 2022, 2019, 2018, and 2017.

Scenario 2-a - Cases					
Case name	Case 1	Case 2	Case 3	Case 4	Case 5
Historical data reference Year	2021	2020	2019	2018	2017
Discharge Temperature (°C)	2	2	2	2	2
Maximum TES Dis/Charge (MW)	40	40	40	40	40.00
TES Capacity (MWh)	227	320	147	100	127.00
New production Plant (MW)	25	33	33	38	35
Total Annualized Cost (MSEK)	37.28	47.84	38.88	44.22	41.25
Tank Cost (SEK/MWh)	21.71	21.71	21.71	21.71	21.71
Tank Total Cost (MSEK)	2.16	3.04	1.40	0.95	1.21
Tank Volume (Thousand m^3)	19.72	27.80	12.77	8.69	11.03
Tank Height (m)	65	65	65	65	65
Tank Diameter (m)	19.65	23.33	15.82	13.04	14.70
Utilization factor per each Dis/Charge	13.5%	13.6%	10.1%	8.7%	9.4%
Hours per Day per each Discharge & Charge	3.24	3.27	2.42	2.08	2.27

Table 5.4: Scenario 2-a - historical electricity prices data results

Figure 5.62 demonstrates the relationship between the TES capacity (MWh) and the capacity of the new cooling production plant (MW) for each sensitivity case of the historical electricity prices data. The data did not show a regular pattern for anticipating the future results of the TES and the new cooling production plant capacities to do a final decision based on. Instead, it presents that the original case, case 2 -2020, has the highest capacity for TES, 320 MWh, the value is higher by far compared with the other cases, where also the required capacity for the new production plant is considered high. This is a result of using the electricity prices of 2020 which had a high fluctuating in the electricity prices.

In addition to more possibility to invest in the new cooling production plant as its operating cost is lower than the existing cooling production plant. It can also be noticed that case 4 -2018, has the highest installed capacity of the new production plant and the lowest required installed capacity of TES. The higher the hourly electricity prices profile, the more need for a larger TES capacity followed by a sufficient capacity from the new production plant to charge the TES. In case 4 for example as the electricity prices had less fluctuation and the hourly electricity prices were low when the cooling demand was needed, this resulted that a small TES capacity will be required and count on using and enlarging the new production to fulfill the cooling demand.

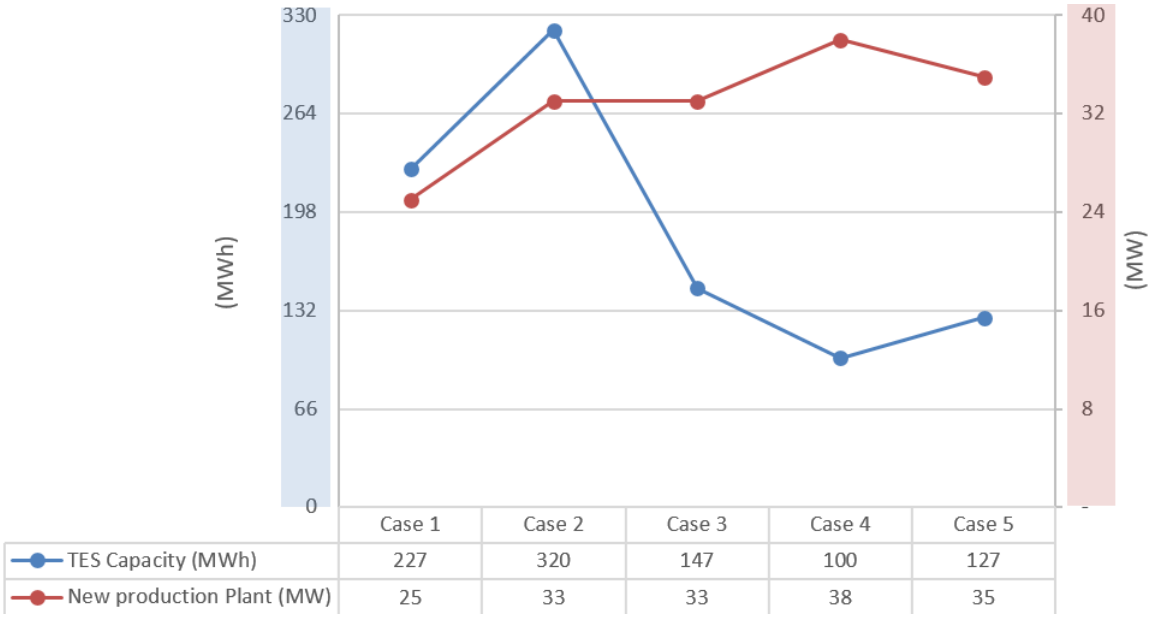

	Case 1	Case 2	Case 3	Case 4	Case 5
TES Capacity (MWh)	227	320	147	100	127
New production Plant (MW)	25	33	33	38	35

Figure 5.62: Scenario 2a - TES capacity and New Cooling Plant Capacity as per different historical electricity prices data

Figure 5.63 demonstrates the total annualized cost for each sensitivity case of the historical electricity prices data to find how the optimization will be impacted. The data do not show a regular pattern for anticipating the total annualized cost to do a final decision based on. It shows that the original case, case 2 - 2020, has the highest total annualized cost, 47.84 M SEK, followed by case 4, case 5, case 3, and case 1 respectively.

The electricity prices have a direct impact on the operational running cost of the cooling system, and by changing the electricity prices profile, the model starts calculating what would be the overall optimized cost model to fulfill the cooling demand while ensuring the lowest annualized cost. From the pattern, it can be noticed that the larger the capacity installed from the new production plant and the smallest installed capacity for the TES, the higher the overall annualized cost, and vice versa. In addition, it should be taken into consideration to have sufficient capacity of the new cooling production plant to charge

the TES with sufficient energy to discharge during the peak load hours.

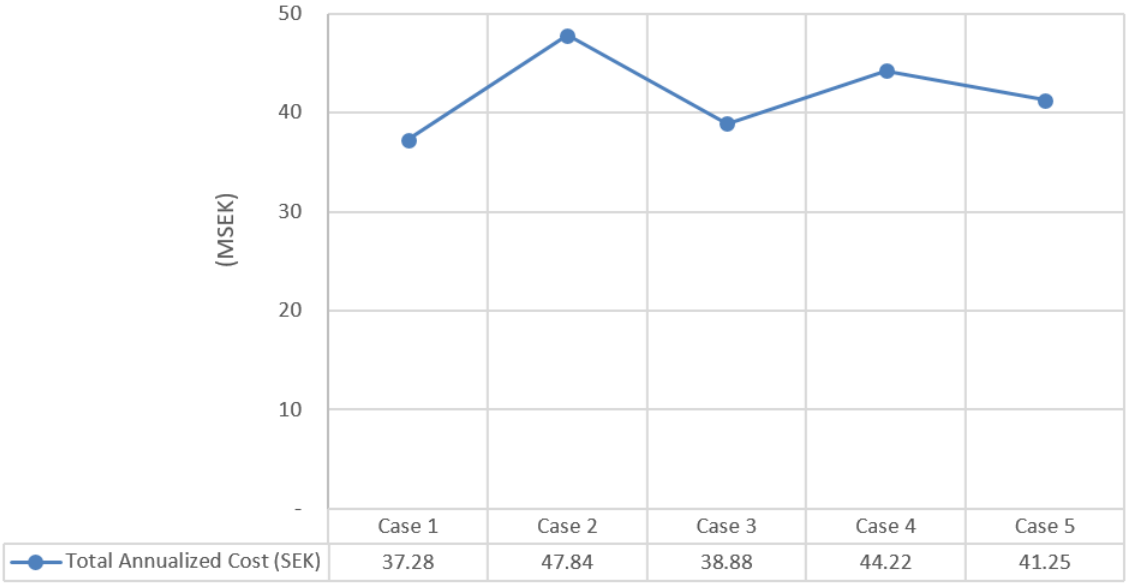

Figure 5.63: Scenario 2a - Total annualized cost as per different historical electricity prices data

(B) **Sensitivity Analysis Results - Historical cooling demand data**
Sensitivity analysis was done for historical data of cooling demand for the years 2019, 2018, and 2017 and compared it with the cooling demand for the original model case as per the year 2020, to notice how this will impact the optimization cost model.

Table 5.5 below summarizes the results of the sensitivity analysis using different historical cooling demand data for the years 2020, 2019, 2018, and 2017.

Scenario 2-a - Cases				
Case name	Case 1	Case 2	Case 3	Case 4
Historical data reference Year	2020	2019	2018	2017
Discharge Temperature (°C)	2	2	2	2
Maximum TES Dis/Charge (MW)	40	40	40	40
TES Capacity (MWh)	320	304	305	280
New production Plant (MW)	33	30	34	28
Total Annualized Cost (MSEK)	47.84	43.52	48.36	33.79
Tank Cost (SEK/MWh)	21.71	21.71	21.71	21.71
Tank Total Cost (MSEK)	3.04	2.89	2.90	2.66
Tank Volume (Thousand m3)	27.80	26.41	26.50	24.32
Tank Height (m)	65	65	65	65
Tank Diameter (m)	23.33	22.74	22.78	21.83
Utilization factor per each Dis/Charge	13.6%	14.1%	15.5%	13.7%
Hours per Day per each Discharge & Charge	3.27	3.37	3.72	3.29

Table 5.5: Scenario 2-a - historical cooling demand data results

Figure 5.64 demonstrates the relationship between the TES capacity (MWh) and the capacity of the new production plant (MW) for each case of the historical cooling demand data to identify how the optimization model will be impacted. The data do not show a regular pattern for anticipating the future results of the TES and the new cooling production plant capacities to do a final decision based on. It presents that the original case, case 1 -2020, has the highest capacity for TES, 320 MWh, where also the required capacity for the new production plant is considered high, this is a result of high cooling demand for several hours, which become beneficial to enlarge the tank to fulfill it.

It can also be noticed that the higher the cooling demand per hour, the more cooling production is required, even from TES or the new production plant. And as there was a limitation for the maximum discharge from the TES, 40 MW, then the new cooling production plant has to supply the additional cooling load requirements as its operational cost is cheaper than the existing one.

However, deciding the capacity of the new cooling production plant has been done considering a balance between the operational and the investment cost. In case 4 also, it can be observed that the cooling demand was not high compared with the other historical data and even did not achieve the maximum cooling demand of 163.7 MW in any hours, this has resulted in having a low capacity for both TES and the new production plant.

The additional increase in the new production plant for case 3 - 2018 compared to case 1 -2020, can be referred to that there were certain hours where the maximum discharging from TES, 40 MW, was not sufficient to fulfill the cooling demand which resulted in further increasing the capacity of the new cooling production plant.

The same can be observed from the percentage of TES Utilization factor, where a higher utilization factor means that the TES was required to operate with its maximum discharge capacity for more hours to fulfill the load. This also can mean that an additional capacity from the new cooling production plant is required also to fulfill the overall cooling demand as can be noticed in case 3 -2018.

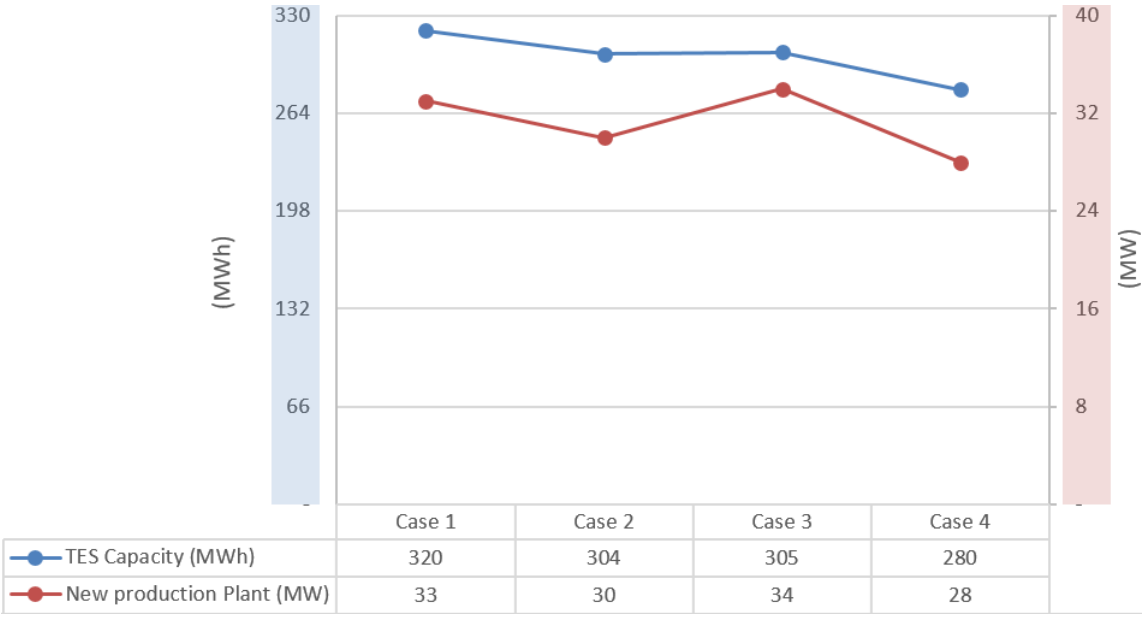

Figure 5.64: Scenario 2a - TES capacity and New Cooling Plant Capacity as per different historical cooling demand data

Figure 5.65 demonstrates the total annualized cost for each case of the historical cooling demand data to identify the impact on the optimization model. The data do not show a regular pattern for anticipating the total annualized cost to do a final decision based on. It shows that the original case, case 2 - 2020 does not have the highest total annualized cost, it was the second-highest, whereas the highest cost can be seen in case 3 -2018, 48.36 M SEK. The cooling demand has a direct impact on the required operating cooling capacity which defines the overall operational running cost of the cooling system. And by changing the cooling demand profile, the model starts calculating what would be the overall optimized cost model to achieve the cooling demand while ensuring the lowest annualized cost, this is done by considering the required balance between how much to invest and how much would be the cost of operation.

In addition, from the pattern, it can be noticed that having the largest new cooling production plant played a significant factor in increasing the overall annualized cost for the new installed cooling system (New cooling production plant and TES).

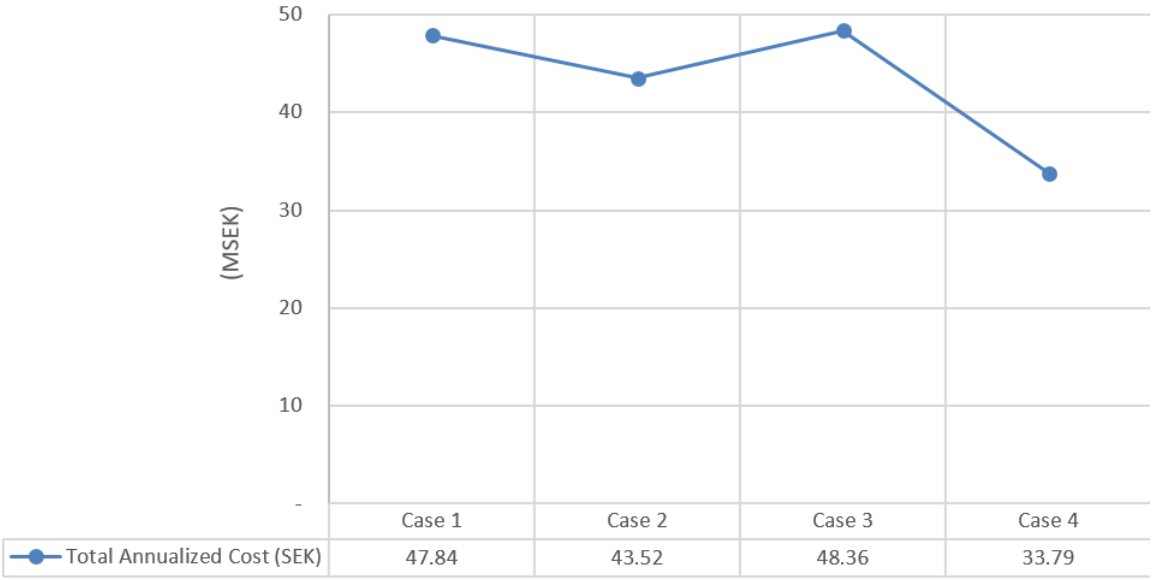

Figure 5.65: Scenario 2a - Total annualized cost as per different historical cooling demand data

5.2.5 Discussion

(A) **Long term storage vs Short term storage** From the optimization result, it is seen that TES is used for short-term storage rather than long-term storage. It mainly shifts daily peak hours to the off-peak hours by charging the tank during nighttime and discharging during daytime. For a city like Gothenburg, where free cooling is abundant in wintertime, long-term storage can be a good alternative to reduce the total cost of the district cooling system.

However, thermal energy storage is not a cost-effective option to serve this purpose due to its high investment cost per unit storage capacity. However, other storage alternatives such as cavern and borehole thermal energy storage can be cost-effective and can be looked further into.

(B) **Absorption chiller vs Compressor chiller**
An absorption chiller is a more cost-effective option in Gothenburg due to its high coefficient of performance and the free utilization of waste heat. Practically, if the waste heat is abundant and always available at any given time, it would always be more beneficial to install an absorption chiller than a compressor chiller.

(C) **Operational and Investment Cost**
From the investment cost perspective, investing in chillers is more expensive compared with the investment of TES. Therefore, the priority in making a decision goes to invest in TES first. However, to be able to utilize the TES and make the investment profitable, a sufficient cooling production from chillers

should be available to cover charging the TES and fulfilling the cooling demand.

In addition, when it is compared being absorption chillers or compression chillers, from an initial investing point of view, absorption chillers are more expensive and require a higher capital investment.

From the operational cost perspective, TES has the advantage as it uses cooling production plants to charge it with chilled water when the electricity prices in their lowest. To later discharge and supply, chilled water to fulfill the cooling demand when the electricity prices are high, and by considering this the operational cost of the overall cooling system will be reduced.

In addition, when it is compared using absorption chillers or compression chillers, from the operational cost point of view. Having an absorption chiller in the cooling system as the new cooling production plant has an advantage over considering the use of compression chillers for the new cooling production plant. This can be noticed as the considering a new cooling production plant using absorption chillers had ensured the lowest total annualized cost and its running with full capacity was prioritized over the existing cooling production plant, which used compression chillers. The reason is referred to the COP, for absorption chillers its 4 times higher than the compression chillers, which gave the absorption chillers to run first to charge the TES and fulfill the cooling demand and the remained cooling demand to be fulfilled by the existing cooling production plant.

This comes to a point that a where between the size of the investment of the TES and a new cooling production plant, the COP of the type of the chillers, the investment cost of the system, and the operational cost of the system are key factors to have an optimized model.

(D) **The impact of the hourly electricity prices**
In the historical data for 2021, and 2020, a high electricity prices fluctuation during the year can be noticed, especially in the summer hours when the cooling demand is required. Due to this, it can be observed that a high fluctuation in the electricity prices resulted in having a larger TES, with higher capacity (MWh) compared with the years 2019, 2018, and 2017 when a smaller TES was required. The same was noticed regarding the capacity of the new cooling production plant. Higher electricity prices fluctuating during the year resulted in to require for a larger capacity (MW) for the new cooling production plant (Absorption chillers) to charge the TES when the electricity prices are low and to prioritize fulfilling the demand in comparison with the existing cooling production plant (compression chillers) in both when the electricity prices are high and low.

It can be said that a higher fluctuating in electricity prices during the year

means that installing more capacity of TES becomes profitable as the TES can be charged during the low electricity prices hours to be later discharged during the high electricity prices hours. However, a larger TES will require a larger capacity of a new production plant (in case of using absorption chillers) to be able to fulfill the charging demand of TES and prioritize fulfilling the cooling demand. Where the use of a new cooling production plant comes before considering the use of the existing cooling production plant, which uses compression chillers with lower COP in comparison with the absorption chiller with high COP.

From another point of view, the factor which made the consideration of the historical data of the year 2021 present the cheapest total annualized cost is the installed capacity of the new cooling production plant, where the investment cost of the chiller is very high incomparable with the investment in the TES. Therefore, in the sensitivity analysis of the electricity prices, the year 2021 had shown the cheapest total annualized cost as it has the lowest installation of the new cooling production plant. Incomparable with the historical data for the year 2020 electricity prices, where show a high total annualized cost where both the capacity of TES and the new cooling production plant are high meaning that the required investment was high.

(E) **The impact of the hourly cooling demand**
Having an accurate prediction of future demand is very important. In the historical cooling demand profile data in the case of 2017, the demand had never reached the maximum of 163.7 MW in any hours compared with the other historical cooling demand data for 2020, 2019, and 2018. This means a less installment of the capacity will be required to fulfill the cooling demand and this will be translated that the cooling system has a cheaper total annualized cost as not much cooling demand is required.

To have an optimized cost model, then knowing the cooling demand is a necessary input, otherwise, the cooling production installation might be less or more than what is needed for the cooling demand. Where installing more production than the cooling demand requirements mean losing money and installing less production than the cooling demand means not achieving the cooling demand requirements.

However, predicting the future cooling demand is not as simple as it sounds, but a closer estimate can be made by having a future cooling demand-supply agreement with customers, or by considering a flexible cooling system design, which allows for future expansion. Allowing for flexibility for future expansion in the design can help in adding additional cooling production in every stage as the cooling demand increase with time. This can help to ensure that the equipment installed is fully utilized as much as possible, maximize the profit, and at the same time give the flexibility in the cooling system to further install more cooling production when the cooling demand increase.

6

Conclusion and Future work

6.1 Conclusion

For the computational fluid dynamics model, there is intensive mixing in the cold zone when water of 1 °C is charged to the tank with the presence of water of 4 °C. No thermocline can be developed in the cold zone to separate water of 1 and 4 °C. However, thermocline layer is formed between warm zone and cold zone with a volume corresponding to around 4-6% of the total volume of the tank at the end of the charging or discharging process, which enables efficient cooling energy storage. Moreover, thermocline layer develops during time due to the conduction and heat diffusion effect because of the temperature difference of water inside the tank. A high temperature gradient across the thin thermocline layer is ideal for storage. In addition, from the operational point of view, due to the limitation of the size of the new chiller, storing water down to 1 °C is unlikely as it requires much more time than the off-peak hours in a day. However, the storage temperature can be lowered down 2-3 °C, depending on the charging duration. This can bring down the investment cost by having a having a small tank and less pumping power. However, there are practical concerns for low-temperature water storage, including the risk of freezing with temperature close to 0 °C and accurate control of flow of water in and out of the tank.

Investing in TES is more cost-effective compared with chillers; it has lower investment and operational costs compared with mechanical chillers. The more capacity is available to discharge from the TES, the less capacity requirement for chillers and the lower the total annualized cost. However, more utilization of TES, can not be achieved without sufficient cooling production from chillers to charge the TES. In addition, several factors determined the preference for using absorption chillers over compression chillers in the new cooling production plant, mainly the availability of free heat. The advantage of using free heat has given the absorption chillers the advantage of lower operational cost. Mentioning the above, it can be said that a balance between the investment and the operational cost decides the optimum size for the TES and the new production plant to achieve the goal of finding the lowest total annualized cost.

Electricity prices play a role in determining the size of investment for both, TES and new cooling production plant, where high fluctuating in the electricity prices mean more possibility for TES installment resulting in cheaper total annualized

cost. Similarly, the cooling demand hourly profile also plays an important factor in determining the size of investment for both, TES and the new cooling production plant, where the higher the cooling demand in the future mean the higher installment would be required from the cooling production units (Chillers and TES).

Nevertheless, the electricity prices and the cooling demand profile are uncertain and not easy to predict in the future, this can be seen, as there is no consistent pattern in the historical data from the past years, making no conclusive decision for the optimum size for the TES and the new cooling production plant. By saying this, allowing for flexible cooling system design, and initiating risk assessment and operational strategy studies for future expansion can ensure to minimize the loss of money from installing higher capacity than required or not achieving the cooling demand due to not installing enough cooling capacity.

6.2 Future Work

Prototype experiment of CFD model
For validating the results of computational fluid dynamic model, an experimental prototype can be done to verify the results of the computational fluid dynamics model.

Investigation of long term storage
From the result obtained in the optimization model, tank thermal energy storage is appropriate only for short term storage. As abundant of cooling energy is available in the winter in Gothenburg, future study of long term cooling thermal energy storage can be done to investigate the feasibility and cost effectiveness to the system. A successful implementation of long term storage can be a more sustainable option for the system by utilizing cheap and clean energy at low cost. This will also decrease the need of short term thermal energy storage and the use of chillers, lowering down the overall cost.

Modelling with network constraints
A future study considering the network constraints, including the capacity pipelines, pressure and pumping constraints, can be taken into account in the investment analysis, which can give a more holistic view on how the system will operate.

Sector coupling of district heating with district cooling system
In this study, the operation of district heating system and district cooling system is completely independent and waste heat is assumed to be always available. A future study of combining district heating and cooling system can be done to investigate the potential economic benefits of the energy system as a whole. The use of waste heat from the industry, the reject heat from compressors, heat pumps, turbines and boilers can be coupled, so that an integrated energy system with optimized operation can be studied.

Sea temperature rise in 2040
In this study, the sea temperature profile of the river for the year 2040 was assumed similar to the year 2020 for simplicity. However, due to climate change, the sea temperature profile might rise or decrease differently during the year than what has been noticed in the year 2020. This will result in changing the amount and the percentage of the available free cooling load from the river during the year, and eventually affect the size of investment and the operational cost of the mechanical cooling system (Chillers and TES). Therefore, taking the change in sea temperature into account can give a more holistic view of how the system will operate.

Investment and maintenance cost
For this study, the cost of investment and maintenance was assumed as per previous studies and references. However, considering actual cost values from the Swedish market will ensure the results are more accurate.

Bibliography

[1] Alaa A Olama. *District cooling: Theory and practice*. CRC Press, 2016.

[2] Hafiz Muhammad Ali, Furqan Jamil, and Hamza Babar. *Thermal Energy Storage*. Springer, 2021.

[3] Refrigerating American Society of Heating and Inc. (ASHRAE) Air-Conditioning Engineers. American Society of Heating, Refrigerating and Air-Conditioning Engineers, Inc. (ASHRAE), 2019. ISBN 978-1-947192-15-7. URL https://app.knovel.com/hotlink/toc/id:kpDCGEOGB9/district-cooling-guide/district-cooling-guide.

[4] Wanruo Lou, Lingai Luo, Yuchao Hua, Yilin Fan, and Zhenyu Du. A review on the performance indicators and influencing factors for the thermocline thermal energy storage systems. *Energies*, 14(24):8384, 2021.

[5] A Jamil, A Benbassou, et al. Review on solar thermal stratified storage tanks (stsst): Insight on stratification studies and efficiency indicators. *Solar Energy*, 176:126–145, 2018.

[6] Nordpool. Historical market data, elspot prices. URL https://www.nordpoolgroup.com/en/historical-market-data/.

[7] Jason Glazer. *Design Guide for Cool Thermal Storage.*, volume Second edition. ASHRAE, 2019. ISBN 9781947192171. URL https://search.ebscohost.com/login.aspx?direct=true&AuthType=sso&db=nlebk&AN=2225738&site=ehost-live&scope=site&authtype=sso&custid=s3911979.

[8] Lucas B Hyman. *Sustainable thermal storage systems: planning, design, and operations*. McGraw-Hill Education, 2011.

[9] International Energy Agency. The future of cooling, . URL https://www.iea.org/reports/the-future-of-cooling.

[10] International Energy Agency. Cooling, . URL https://www.iea.org/reports/cooling.

[11] Sven Werner. District heating and cooling in sweden. *Energy*, 126:419–429, 2017.

[12] Nsilulu T Mbungu, Ramesh C Bansal, Raj M Naidoo, and Mukwanga W Siti. Analysis of a grid-connected battery energy storage based energy management

system. In *2020 First International Conference on Power, Control and Computing Technologies (ICPC2T)*, pages 1–5. IEEE, 2020.

[13] EMSD HK. Benefits of dcs. URL `https://www.emsd.gov.hk/energyland/en/building/district_cooling_sys/dcs_benefits.html`.

[14] Refrigerating American Society of Heating and Inc. Air-Conditioning Engineers. *District Cooling Guide*. American Society of Heating, Refrigerating and Air-Conditioning Engineers, Inc. (ASHRAE), 2013.

[15] INC. Delta Cooling Towers. Understanding wet bulb temperatures and how it affects cooling tower performance, 2021. URL `https://deltacooling.com/resources/news/understanding-wet-bulb-temperatures-and-how-it-affects\-cooling-tower-performance`.

[16] Rami M Saeed, Joshua P Schlegel, C Castano, and R Sawafta. Preparation and enhanced thermal performance of novel (solid to gel) form-stable eutectic pcm modified by nano-graphene platelets. *Journal of Energy Storage*, 15:91–102, 2018.

[17] Panel ASHRAE. Heating and cooling, ashrae handbook-hvac systems and equipment, si ed. *American Society of Heating Refrigerating and Air-Conditioning Engineers (ASHRAE) Atlanta, GA, US*, 2008.

[18] Gang Li. Sensible heat thermal storage energy and exergy performance evaluations. *Renewable and Sustainable Energy Reviews*, 53:897–923, 2016.

[19] Louise Jivan Shah and Simon Furbo. Entrance effects in solar storage tanks. *Solar energy*, 75(4):337–348, 2003.

[20] S Advaith, Dipti Ranjan Parida, KT Aswathi, Nikhil Dani, Utpal Kumar Chetia, Kamanio Chattopadhyay, and Saptarshi Basu. Experimental investigation on single-medium stratified thermal energy storage system. *Renewable Energy*, 164:146–155, 2021.

[21] Zilong Wang, Hua Zhang, Binlin Dou, Guanhua Zhang, Weidong Wu, and Liqiang Zhou. An experimental study for the enhancement of stratification in heat-storage tank by equalizer and pcm module. *Journal of Energy Storage*, 27:101010, 2020.

[22] Jose Fernandez-Seara, Francisco J Uhı, Jaime Sieres, et al. Experimental analysis of a domestic electric hot water storage tank. part ii: dynamic mode of operation. *Applied thermal engineering*, 27(1):137–144, 2007.

[23] Chee-Kong Yee and FC Lai. Effects of a porous manifold on thermal stratification in a liquid storage tank. *Solar Energy*, 71(4):241–254, 2001.

[24] HO Njoku, OV Ekechukwu, and SO Onyegegbu. Comparison of energy, exergy and entropy generation-based criteria for evaluating stratified thermal store performances. *Energy and Buildings*, 124:141–152, 2016.

[25] Scott M Flueckiger, Zhen Yang, and Suresh V Garimella. Review of molten-salt thermocline tank modeling for solar thermal energy storage. *Heat Transfer Engineering*, 34(10):787–800, 2013.

[26] Jean-Paul Rebert, Jean-René Donguy, Gérard Eldin, and K Wyrtki. Relations between sea level, thermocline depth, heat content, and dynamic height in the tropical pacific ocean. *Journal of Geophysical Research: Oceans*, 90(C6):11719–11725, 1985.

[27] N Ahmed, KE Elfeky, Lin Lu, and QW Wang. Thermal and economic evaluation of thermocline combined sensible-latent heat thermal energy storage system for medium temperature applications. *Energy Conversion and Management*, 189:14–23, 2019.

[28] Tobias Falke, Stefan Krengel, Ann-Kathrin Meinerzhagen, and Armin Schnettler. Multi-objective optimization and simulation model for the design of distributed energy systems. *Applied Energy*, 184:1508–1516, 2016.

[29] A Nottrott, Jan Kleissl, and Byron Washom. Energy dispatch schedule optimization and cost benefit analysis for grid-connected, photovoltaic-battery storage systems. *Renewable Energy*, 55:230–240, 2013.

[30] Marco Wirtz, Maria Hahn, Thomas Schreiber, and Dirk Müller. Design optimization of multi-energy systems using mixed-integer linear programming: Which model complexity and level of detail is sufficient? *Energy Conversion and Management*, 240:114249, 2021.

[31] Celine Weber and Nilay Shah. Optimisation based design of a district energy system for an eco-town in the united kingdom. *Energy*, 36(2):1292–1308, 2011.

[32] Pengfei Jie, Neng Zhu, and Deying Li. Operation optimization of existing district heating systems. *Applied Thermal Engineering*, 78:278–288, 2015.

[33] Torben Ommen, Wiebke Brix Markussen, and Brian Elmegaard. Comparison of linear, mixed integer and non-linear programming methods in energy system dispatch modelling. *Energy*, 74:109–118, 2014.

[34] Rocío Bayón, Esther Rivas, and Esther Rojas. Study of thermocline tank performance in dynamic processes and stand-by periods with an analytical function. *Energy Procedia*, 49:725–734, 2014.

[35] Azharul Karim, Ashley Burnett, and Sabrina Fawzia. Investigation of stratified thermal storage tank performance for heating and cooling applications. *Energies*, 11(5):1049, 2018.

[36] Jing Song, William P Bahnfleth, and John M Cimbala. Parametric study of single-pipe diffusers in stratified chilled water storage tanks (rp-1185). *HVAC&R Research*, 10(3):345–365, 2004.

[37] The Open University. The density of fresh water and seawater. URL `https://www.open.edu/openlearn/science-maths-technology/the-oceans/content-section-3.2`.

[38] Richard K Ellsworth. Capacity factor cost modeling for gas-fired power plants. *Construction Accounting & Taxation*, 19(1):31, 2009.

[39] Larry R Dysert. Sharpen your cost estimating skills. *Cost Engineering*, 45(6): 22, 2003.

[40] ELIXABET SARASKETA ZABALA. Technological and economic evaluation of district cooling with absorption cooling systems in gävle (sweden), 2009.

[41] Yamina Saheb, Sulejman Becirspahic, and Jérôme Simon. Effect of the certification on chillers energy efficiency. *IMPROVING ENERGY EFFICIENCY IN COMMERCIAL BUILDINGS*, page 137, 2006.

[42] Roger Hermansson. *Short term water heat storage: an experimental investigation of thermal stratification*. PhD thesis, Luleå tekniska universitet, 1989.

[43] Amy Musser and William P Bahnfleth. Parametric study of charging inlet diffuser performance in stratified chilled water storage tanks with radial diffusers: Part 1–model development and validation. *HVAC&R Research*, 7(1): 31–49, 2001.

[44] Joko Waluyo, M Amin A Majid, and M Amin. Temperature profile and thermocline thickness evaluation of a stratified thermal energy storage tank. *Int J Mech Mechatron Eng*, 1:7–12, 2010.

[45] Jian Sun, Jing Hua, Lin Fu, and Shigang Zhang. Experimental study of a large temperature difference thermal energy storage tank for centralized heating systems. *Thermal Science*, 22(1 Part B):613–621, 2018.

[46] Jae Dong Chung, Sung Hwan Cho, Choon Seob Tae, and Hoseon Yoo. The effect of diffuser configuration on thermal stratification in a rectangular storage tank. *Renewable Energy*, 33(10):2236–2245, 2008.

url

DEPARTMENT OF SOME SUBJECT OR TECHNOLOGY
CHALMERS UNIVERSITY OF TECHNOLOGY
Gothenburg, Sweden
www.chalmers.se

CHALMERS
UNIVERSITY OF TECHNOLOGY